TECHNISCHE UNIVERSITÄT MÜNCHEN

Lehrbereich Anorganische Chemie, Fachgruppe Analytische Chemie

Method Development of Extraction and Enrichment of Noble Metal Nanoparticles in Environmental Water Samples

Lingxiangyu Li

Vollständiger Abdruck der von der Fakultät für Chemie der Technischen Universität München zur Erlangung des akademischen Grades eines

Doktors der Naturwissenschaften

genehmigten Dissertation.

Vorsitzender: Univ. -Prof. Dr. Klaus Köhler

Prüfer der Dissertation:

1. Univ. -Prof. Dr. Michael Schuster
2. Univ. -Prof. Dr. Brigitte Helmreich

Die Dissertation wurde am 14.02.2013 bei der Technischen Universität München eingereicht und durch die Fakultät für Chemie am 02.07.2013 angenommen.

For My parents

and

My wife Zhenlan

Die vorliegende Arbeit wurde zwischen Juni 2010 und Juli 2013 in der Lehreinheit Anorganische Chemie der Technischen Universität München unter wissenschaftlicher Anleitung durch Prof. Michael Schuster angefertigt.

Ich erkläre hiermit an Eides statt, dass ich die vorliegende Arbeit ohne unzulässige Hilfe Dritter und ohne Benutzung anderer als der angegebenen Hilfsmittel angefertigt habe. Die aus anderen Quellen direkt oder indirekt übernommenen Daten und Konzepte sind unter Angabe des Literaturzitates gekennzeichnet.

ACKNOWLEDGEMENTS

I would like to start by thanking my supervisor Prof. Dr. Michael Schuster for his guidance and support for the last three years. He gave me the opportunity to do this PhD in his research group, even knowing the very poor chemical background i arrived with! He also gave me incredible freedom over the years to do what I wanted to do with my work. And I also would like to thank Prof. Dr. Kerstin Leopold for her great help during the first year in the lab, really!

A great thank goes to China Scholarship Council for giving me the opportunity to study in Germany. Also, a great thank goes to Consulate-General of the People's of China in Munich. And big thanks to Bavarian State Ministry of the Environment and Public Health for supporting some parts of this study. Thank you to Prof. Dr. Johann Plank (Group of Construction Chemistry, TUM), Prof. Dr. Johannes Buchner (Group of Biotechnology, TUM) and Prof. Dr. Fritz Kühn (Group of Inorganic Chemistry) for allowing me to use some experimental devices in your labs. Special thanks to Dr. Marianne Hanzlik from the Electron Microscopy Center (TUM) and Dr. Markus Döblinger from the Department of Chemistry and Center for NanoScience (University of Munich) for their kind help in analyzing morphology of nanoparticles. I would also like to thank Dr. Markus Drees who is a managing director of the faculty graduate center chemistry in TUM.

A big thanks to all of my past and present colleagues during my study in Prof. Schuster's group: Anna Kalinnik, Dr. Anja Zierhut, Dr. Heven Abdul-Jabbar, Georg Hartmann, Holger Sievers, Jessica Huber, Monika Stoiber, Nadine Feichtmeier, Roland Schindl, Sabrina Losert, Tobias Krammer and Vera Krekel. Also, Thomas Pavlitschek, Daniel Bülichen and Richard Beiderbeck spent time teaching me how to operate the DLS, TOC and Zeta Potential measurement and without them much of this work would not have been possible. I would also like to thank the support from nine wastewater treatment plants (Augsburg, Freising, Garching, Ingolstadt, Landshut, Moosburg, Munich, Regensburg and Ulm) in Germany.

My time at TUM would not have been the same without the past and present friends in Munich, especially Bo Wang, Bo Zhang, Dapeng Yang, Detian Yuan, Fengxiang Wang, Hai Bi, Haiyan He, Jian Jin, Jian Zheng, Ke Zhang, Mingxia Su, Nan Zou, Renfu Yin, Shaopeng Cui,

Shen Chi, Shengcai Han, Shenyu Lin, Shu Li, Xiaodong Yang, Xiaoming Cheng, Xiaopeng Ma, Yang Wang, Yawei Wang, Yonghong Bi, Yu Jin, Yuchen Xia, Yuchun Zhi, Yun Zhang, Zijian Zhao, Zhonghao Yu and every member of our football team. There are many other friends I met while living in Munich whom I will never forget and will always value their support and friendship.

Thanks to my parents. The most optimistic people I will probably ever meet. Thank you for all your support all these years, although there are thousands of miles between us. I have really missed you all these years.

Finally, and most importantly, I would like to thank my wife - Zhenlan. She has always been incredibly supportive of what I do and there is definitely no way I would have come this far in my life without her. I love you so much.

Publications and Poster

Publications

1. Ligand-assisted extraction for separation and pre-concentration of gold nanoparticles from waters, L. Li, K. Leopold, Analytical Chemistry 2012, 84, 4340.
2. Effective and selective extraction of noble metal nanoparticles from environmental water through a noncovalent reversible reaction on an ionic exchange resin, L. Li, K. Leopold, M. Schuster, Chemical Communication 2012, 48, 9165.
3. Comparative study of alkylthiols and alkylamines for the phase transfer of gold nanoparticles from an aqueous phase to n-hexane, L. Li, K. Leopold, M. Schuster, Journal of Colloid and Interface Science, 2013, 397, 199-205.
4. Quantification of nanoscale silver particles removal and release from municipal wastewater treatment plants in Germany, L. Li, G. Hartmann, M. Döblinger, M. Schuster, Environmental Science & Technology, 2013, 47, 7317-7323.

Poster

1. Effective and selective extraction of silver nanoparticles from environmental water by an ionic exchange resin, L. Li, K. Leopold, M. Schuster, Nanosafe 2012, 13-15. Nov. 2012, Grenoble, France.

List of Abbreviations and Acronyms

AFM	Atomic force microscopy
Ag-NPs	Silver nanoparticles
Ag_2S-NPs	Silver sulfide nanoparticles
Au-NPs	Gold nanoparticles
Aug	Augsburg
BET	Brunauer-emmett-teller
CNTs	Carbon nanotubes
CPE	Cloud point extraction
Cu-NPs	Copper nanoparticles
CuO-NPs	Copper oxide nanoparticles
DCHA	Dicyclohexylamine
DDA	Dodecylamine
DDT	1-Dodecanethiol
DLS	Dynamic light scattering
DOM	Dissolved organic matter
EDTA	Ethylenediaminetetraacetic acid
EDX	Energy dispersive x-ray
EELS	Electron energy loss spectroscopy
ENMs	Engineered nanomaterials
ENPs	Engineered nanoparticles
ESEM	Environmental scanning electron microscopy
ES-MS	Electrospray ionisation mass spectroscopy
FFF	Field-flow fractionation
FlFFF	Flow field flow fractionation
Fre	Freising
FTIR	Fourier transform infrared spectroscopy
Gar	Garching
GFAAS	Graphite furnace atomic absorption spectrometry

HA	Humic acid
HDC	Hydrodynamic chromatography
HR-TEM	High-resolution transmission electron microscopy
ICP-MS	Inductively coupled plasma-mass spectrometry
Ing	Ingolstadt
Lan	Landshut
LIBS	Laser-induced breakdown spectroscopy
LOD	Limit of detection
MNPs	Metal nanoparticles
Moo	Moosburg
MSA	Mercaptosuccinic acid
MUA	11-Mercaptoundecanoic acid
Mun	Munich
MWCNTs	Multi wall carbon nanotubes
n-Ag-Ps	Nanoscale silver particles including Ag-NPs and Ag_2S-NPs
NMNPs	Noble metal nanoparticles
NMs	Nanomaterials
NPs	Nanoparticles
ODA	Octadecylamine
ODT	1-Octadecanethiol
PAHs	Polynuclear aromatic hydrocarbons
Pd-NPs	Palladium nanoparticles
PEC	Predicted environmental concentration
PVP10	Polyvinylpyrrolidone average mol wt 10,000
PVP40	Polyvinylpyrrolidone average mol wt 40,000
QA	Quality assurance
QC	Quality control
Reg	Regensburg
RP-C18	Reversed phase C-18
SAED	Selected area electron diffraction

SEC	Size exclusion chromatography
SEM	Scanning electron microscope
SI	Supporting information
SiO_2-NPs	Silicon dioxide nanoparticles
SLS	Static light scattering
SWCNT	Single wall carbon nanotube
TBO	Toluidine blue O
TE	Transfer efficiency
TEM	Transmission electron microscopy
THGA	Transversally heated graphite atomizer
TI	Transfer index
TiO_2-NPs	Titanium dioxide nanoparticles
TOAB	Tetra-n-octylammonium bromide
TOC	Total organic carbon
Tween 20	Polyoxyethylene (20) sorbitan monolaurate
TX-114	Triton X-114
TXRF	Total reflection x-ray fluorescence
UPW	Ultrapure water
WSEM	Wet scanning electron microscopy
WSTEM	Wet scanning transmission electron microscopy
WWTPs	Wastewater treatment plants
XRD	X-ray diffraction
ZnO-NPs	Zinc oxide nanoparticles

Abstract

The increasing use of noble metal nanoparticles (NMNPs) in industrial and household applications has led to the release of NMNPs into the environment. Consequently, it is essential to understand their distribution and effects in environmental matrices. Moreover, quantitative analytical methods are also required to determine their environmental concentrations. However, practically nothing is known about their concentration, shape and size under environmental conditions due to the lack of analytical or pre-treatment methods for NMNPs in real environmental samples.

In the present work, ligand-assisted liquid-liquid extraction method was investigated to extract and concentrate gold nanoparticles (Au-NPs). The 1-Dodecanethiol (DDT) was found the most efficient ligand for extraction of Au-NPs from water to n-hexane among four ligands namely DDT, 1-Octadecanethiol (ODT), dodecylamine (DDA) and octadecylamine (ODA). However, this ligand-assisted liquid-liquid extraction method was not applicable to extract Au-NPs at low concentration (< 100 µg/L). Hence, ligand-assisted solid-liquid extraction methods were developed.

Two solid-liquid extraction methods using reversed-phase C18 (RP-C18) and ionic exchange resin (IRN-78) as adsorbent respectively were optimized to efficiently and selectively extract NMNPs (Au-NPs, Ag-NPs and Pd-NPs). Based on the optimized procedures, the extraction efficiencies and recoveries of NMNPs spiked into real environmental water samples were investigated, which demonstrated that both of the ligand-assisted solid-liquid extraction methods are applicable to extract NMNPs even at ng/L levels. Moreover, transmission electron microscopy (TEM) analysis confirmed that the size and shape of NMNPs could be preserved by these extraction methods.

Finally, the solid(IRN-78)-liquid extraction method was used to extract nanoscale silver particles (n-Ag-Ps) from effluents of nine municipal wastewater treatment plants (WWTPs) in Germany. It shows that the concentrations of n-Ag-Ps in the field-collected effluents of WWTPs range from 2.2 to 9.4 ng/L. Moreover, based on the actual concentrations, we estimated that the daily n-Ag-Ps load entering water environment through effluent discharge (e.g., a WWTP with 520000 t/d treatment capacity) equates to about 4.4 g/d.

Inhaltsübersicht

Der zunehmende Einsatz von Edelmetallnanopartikeln (NMNPs) im industriellen Umfeld und in Konsumprodukten hat zwangsläufig zu deren Freisetzung in die Umwelt geführt. Als Konsequenz daraus ist es unabdingbar, die Verteilung dieser Partikel in der Umwelt zu erfassen und die dort ausgelösten Effekte zu verstehen. Das erfordert neue analytische Methoden zur Anreicherung und Vorkonzentrierung der Partikel aus realen Matrices, die bisher aber nicht existieren. Aus diesem Grund ist praktisch nichts über die realen Konzentrationen von NMNPs sowie deren Größe und Form in der Umwelt bekannt.

In der vorliegenden Arbeit wurde eine ligandunterstützte Flüssig-Flüssig-Extraktionsmethode untersucht, um Goldnanopartikel (Au-NPs) zu extrahieren und aufzukonzentrieren. Von den vier Liganden 1-Dodekanthiol (DDT), 1-Oktadekanthiol (ODT), Dodecylamin (DDA) und Oktadecylamin (ODA) war DDT der effizienteste Ligand für die Extraktion von Au-NPs aus wäßrigen Lösungen in n-Hexan. Jedoch kann diese Methode nicht für Au-NPs-Konzentrationen unter 100 µg/L angewandt werden. Infolgedessen wurden ligandunterstützte Fest-Flüssig-Extraktionsmethoden entwickelt.

Zwei Fest-Flüssig-Extraktionsmethoden mit einer C18 Umkehrphase (RP-18) und einem Ionenaustauscherharz (IRN-78) als Adsorbens wurden jeweils optimiert, um NMNPs (Au-NPs, Ag-NPs und Pd-NPs) effizient und selektiv zu extrahieren. Mit den optimierten Verfahren wurden die Extraktionseffizienz und die Wiederfindung von NMNPs in Realwasserproben untersucht. Dabei zeigte sich, dass es beide Fest-Flüssig-Extraktionsmethoden ermöglichen, NMNPs im ng/L-Bereich zu extrahieren. Außerdem konnte durch Transmissionselektronenmikroskopie ermittelt werden, dass die Größen und die Form der Teilchen durch die Extraktion nicht verändert werden.

Die Fest-Flüssig-Extraktion mit IRN-78 wurde schließlich verwendet, um Ag-NPs in den Ausläufen von neun Klärwerken in Deutschland zu bestimmen. Die Konzentrationen der Ag-NPs lagen dabei im Bereich von 2.2 bis 9.4 ng/L. Darüber hinaus wurden die täglichen Ag-NPs-Einträge in die Hydrosphäre durch Klärwasserabflüsse (z. B. eine Kläranlage mit 520000 t/d Behandlungskapazität) auf ungefähr 4.4 g/d abgeschätzt.

Contents

List of Figures

List of Tables

1 Introduction

1.1 What is Nanotechnology and Nanoparticles?

The US National Nanotechnology Initiative (www.nano.gov/nni2.htm) says: Nanotechnology is concerned with materials and systems whose structures and components exhibit novel and significantly improved physical, chemical and biological properties, phenomena and processes due to their nanoscale size. The goal is to exploit these properties by gaining control of structures and devices at atomic, molecular and supramolecular levels and to learn to efficiently manufacture and use these devices [1,2]. In short, nanotechnology, encompassing the design, production, characterization, and application of structures and systems at the nanometre scale, opens up a tremendous field of new applications beneficial to human being and the environment. The total global investment in the nanotechnology was around $10 billion in 2005 and it is estimated that the annual value for all nanotechnology-related products will be $1 trillion by 2011-2015 [3].

Nanoparticles (NPs) are considered to be the building blocks for nanotechnology, and are referred to particles having at least one dimension in the nanoscale (ca. 1-100 nm) and that have been specifically engineered for applications [4,5]. Figure 1 shows how the NPs fit into other size-dependent categories that have been used for many decades [6]. Particles in these size ranges have been used by several industries and humankind for thousands of years [7,8]; however, there has been a recent resurgence as a result of the ability to synthesize and manipulate such nanomaterials (NMs). The extremely small sizes of NPs results in a high percentage of surface atoms which can give rise to novel properties and reactivity compared to their bulk counterparts. For example, bulk gold is typically inert but becomes catalytic as the size of particles decreases to a few nanometres [9-11]. Silver in its bulk form has long been known to be bactericidal and has therefore been used for disinfection purposed long before the invention of antibiotics. In a NP format silver can serve as a versatile bactericide with a wide range of uses such as in water filters, filtration membranes, fabrics and surgical instruments [12-16]. Moreover, silver nanoparticles (Ag-NPs) exhibit properties that are attractive for use in highly sensitive optical sensors, conductive inks for electronic applications, and as colloidal catalysts for organic

oxidation [17-19].

Over the past decade, an increasing number of NPs have been incorporated into products and manufacturing processes due to the rapid innovation and commercialization in the field of nanotechnology. The Project on Emerging Nanotechnologies of Woodrow Wilson International Center for Scholars maintains an online database designed to track the role of nanotechnologies and NMs in the production of consumer products [20]. A research of this database in February 2008 yielded 606 nanotechnology-based consumer products [21]. A subsequent statistic research in September 2009 reported that the number of nanotechnology-based consumer products had nearly doubled, increasing to 1020 [20]. Recently, the number of nanotechnology-based consumer products or product lines has reached 1317 available on the market in March 2011 [20].

Of the NMs currently in use, noble metal nanoparticles (NMNPs) like above-mentioned gold nanoparticles (Au-NPs) and Ag-NPs in particular are one of the most widely used, given their unique optical, electronic, and chemical properties. To our knowledge, NMNPs have been used in a variety of applications including as stabilizing agents in personal care products like sunscreens and cosmetics, as a delivery tool in nanomedicine, and as a photocatalyst for remediation and industrial applications [22-24]. Totally, thousands of tonnes of such NMNPs are produced annually for commercial purposes or as by-products of human activity.

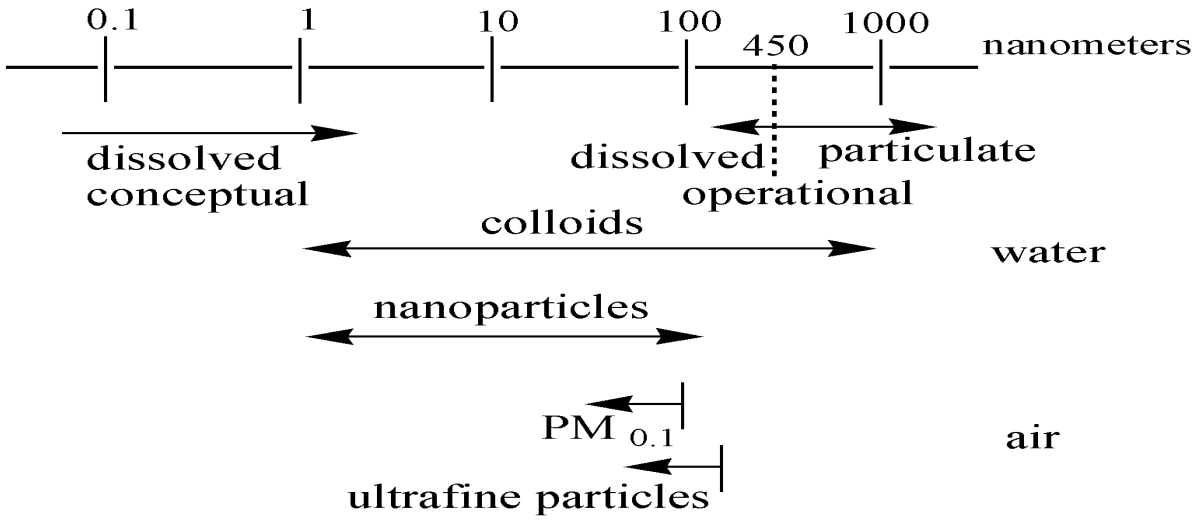

Figure 1. Definitions of different size classes relevant for NPs [6]

1.2 Sources of NPs

1.2.1 Natural Sources of NPs

NPs can be divided into natural and anthropogenic particles. Normally, NPs are abundant in nature, since they are produced in many natural processes, including volcanic eruptions, forest fires, simple erosion, and photochemical reactions, and by animals, plants and microbes [6,25-30]. Scientists in the last two decades have shown that NPs are quite literally everywhere in natural environments. They exist in nearly all components of the Earth, including the atmosphere, oceans and subsurface. Table 1 classifies NPs according to origin and composition; as can be seen, many are of natural origin [6,25]. For example, although we usually associate air pollution with human activities like cars, industry, and charcoal burning, natural events such as volcanic eruptions, forest fires and dust storms can produce such vast quantifies of nanoscale matter that they profoundly affect air quality worldwide [31]. When a volcano erupts, ash and gases containing particulate matter ranging from the nanoscale to microns, are propelled high into the atmosphere. Normally, the quantity of particles released into the atmosphere is enormous; a single volcanic eruption can eject up to 30 million tons of ash [31,32]. Taylor [33] found that the aerosols generated by human activities are estimated to be only about 10% of the total, the remaining 90% having a natural origin.

In addition, even natural NPs can be further separated based on their chemical composition into carbon-containing and inorganic NPs (Table 1). The C-containing natural NPs are divided into biogenic, geogenic, atmospheric and pyrogenic NPs, and the inorganic natural NPs are divided into biogenic, geogenic and atmospheric NPs. For the C-containing natural NPs, natural NPs are fullerenes and CNT of geogenic or pyrogenic origin, biogenic organic colloids or atmospheric aerosols like humic acids and organic acids. For the inorganic NPs, biogenic oxide NPs are sometimes formed directly by the organism as a metabolic requirement (e.g., magnetite, Fe_3O_4, produced intracellularly by magnetotactic bacteria is required for mobility) [29]. In addition, biogenic metal NPs like Ag-NPs and Au-NPs, Yin et al. [34] observed that the dissolved organic matter (DOM) in natural water can reduce Ag^+ and $AuCl_4^-$ to their elemental NPs under sunlight. Moreover, Glover et al. [35] also found that metal NPs like Ag-

Table 1. Classification of NPs in environment [6,25]

Formation				Examples
Natural	C-containing	Biogenic	Organic colloids	Humic, fulvic acids
			Organisms	Viruses
		Geogenic	Soot	Fullerenes
		Atmospheric	Aerosols	Organic acids
		Pyrogenic	Soot	CNT
				Fullerenes
				Nanoglobules, onion-shaped nanospheres
	Inorganic	Biogenic	Oxides	Magnetite
			Metals	Ag, Au
		Geogenic	Oxides	Fe-oxides
			Clays	Allophane
		Atmospheric	Aerosols	Sea salt
Anthropogenic (Manufactured/ Engineered)	C-containing	By-product	Combustion by-products	CNT
				Nanoglobules, onion-shaped nanospheres
				Carbon Black
		Engineered	Soot	Fullerenes
				Functionalized CNT, fullerenes
			Polymeric NP	Polyethyleneglycol (PEG) NP
	Inorganic	By-product	Combustion by-products	Platinum group metals
		Engineered	Oxides	TiO_2, SiO_2
			Metals	Ag, iron
			Salts	Metal-phosphates
			Aluminosilicates	Zeolites, clays, ceramics

NPs and Cu-NPs had been present as incidental NMs and in contact with human being for several thousand years due to the formation of Ag-NPs and Cu-NPs under common

environmental conditions. In total, naturally occurring nanoscale particles like colloidal minerals and oxides are ubiquitous in the biosphere, comprising the very building blocks of life and likely playing a very important role in ecosystem dynamics.

1.2.2 Anthropogenic Sources of NPs

Humans have created NMs for millennia, as they are by-products of simple combustion (with sizes down to several nm) and food cooking, and more recently, chemical manufacturing, welding, ore refining and smelting, combustion in vehicle and airplane engines, combustion of coal and fuel oil for power generation, and combustion of treated pulverized sewage sludge (Table 1) [31,36-38]. On the other hand, different kinds of engineered nanoparticles (ENPs) like single wall carbon nanotube (SWCNT), multi wall carbon nanotubes (MWCNTs), fullerenes, Au-NPs, palladium nanoparticles (Pd-NPs), Ag-NPs, titanium dioxide nanoparticles (Ti_2O-NPs) and et al. are now being manufactured in ever increasing quantities. These ENPs are used in a wide range of products and sectors including medicines, cosmetics, clothing, engineering, electronics, and environmental protection [39,40]. The intentional or accidental releases of these ENPs to environment is hence largely unavoidable. Kaegi et al. [41] investigated the release of Ag-NPs from paints used for outdoor application, which reported that more than 30% of Ag-NPs with size < 15 nm were released to the environment. In addition, Hsu and Chein [42] evaluated the NPs emission for TiO_2 nanopowder coating materials, which proclaimed UV radiation is able to increase the release of TiO_2 particles below 200 nm from TiO_2 coating products.

On the other hand, numerous studies also showed that ENPs like TiO_2-NPs and Ag-NPs in consumer products would be likely released into sewer systems [43-47]. Municipal wastewater treatment plants (WWTPs) therefore act as the ‘gateways’ controlling release of these ENPs from domestic or industrial sources to aquatic environment. The quantity of anthropogenic NPs ranges from well-established multi-ton per year production of TiO_2-NPs (for cosmetics) to microgram quantities of fluorescent quantum dots (markers in biological imaging) [31,35,48-50]. Mueller and Nowack [51] quantified the ENPs such as Ag-NPs and TiO_2-NPs and carbon nanotubes (CNTs) released into the environment in Switzerland by using a substance flow analysis, which showed that the predicted environmental concentrations of Ag-NPs, TiO_2-NPs and CNTs in water are 0.03, 0.7 and 0.0005 μg/L respectively due to the wide application of these NMs.

Totally, given an increasing number of manufactured NMs, ENPs can be released intentionally and/or accidentally into natural systems like environmental waters during the manufacturing process, transport, or use.

1.3 Impact of NPs

1.3.1 Impact of NPs on Microbes

Nanotechnology has great potential in improving air, water, and soil quality in the environment. For example, it can improve detection and sensing of pollutants and help in the development of new technologies for remediation [52-54]. However, because of the large-scale production and application of NMs, it will inevitably give rise to their accumulation in the environment, which has a possibility that organisms and ecosystems may be exposed to new levels and qualities of substances with unknown consequences [55,56]. In particular, particles in the nanoscale range fall in the transitional zone between individual atoms or molecules and the corresponding bulk material, which can modify the physicochemical properties of the material, leading to generate adverse biological effects in living cells. Therefore, the potential effects on ecosystems and human health are very important aspects that should be considered (Figure 2).

Many NMs have already been reported to have anti-microbial properties and thus directly affect microbes; the NPs can change microbial viability, damage cell wall/membranes, and affect growth performance and metabolism [57-59]. For example, C60 fullerene is a hydrophobic, carbon NM capable to adsorb various organic and inorganic compounds like amino acid and minerals. Inhibitory effect of fullerene on the bacterial growth under pure culture conditions has been well documented [60,61]. Lyon et al. [62] found that C60 exhibited relatively strong antibacterial activity ranging from 0.09 to 0.7 mg/L. Ag-NPs, a broad-spectrum antimicrobial agent, have been proved to be a powerful nanoweapon against multidrug-resistant bacteria in recent years [57,63]. ZnO-NPs also have been shown that both gram-negative and gram-positive bactericidal cells can be damaged after ZnO-NPs exposure [64]. In addition, iron and copper based NPs could be presumed to react with peroxides present in the environment generating free radicals which are known to be highly toxic to microbes [65]. Among all, Ag-NPs and ZnO-NPs have proved to be the most effective antimicrobial agents against bacteria, viruses and eukaryotic

micro-organisms. Therefore, they are currently widely used in biomedical applications, personal care products and food package.

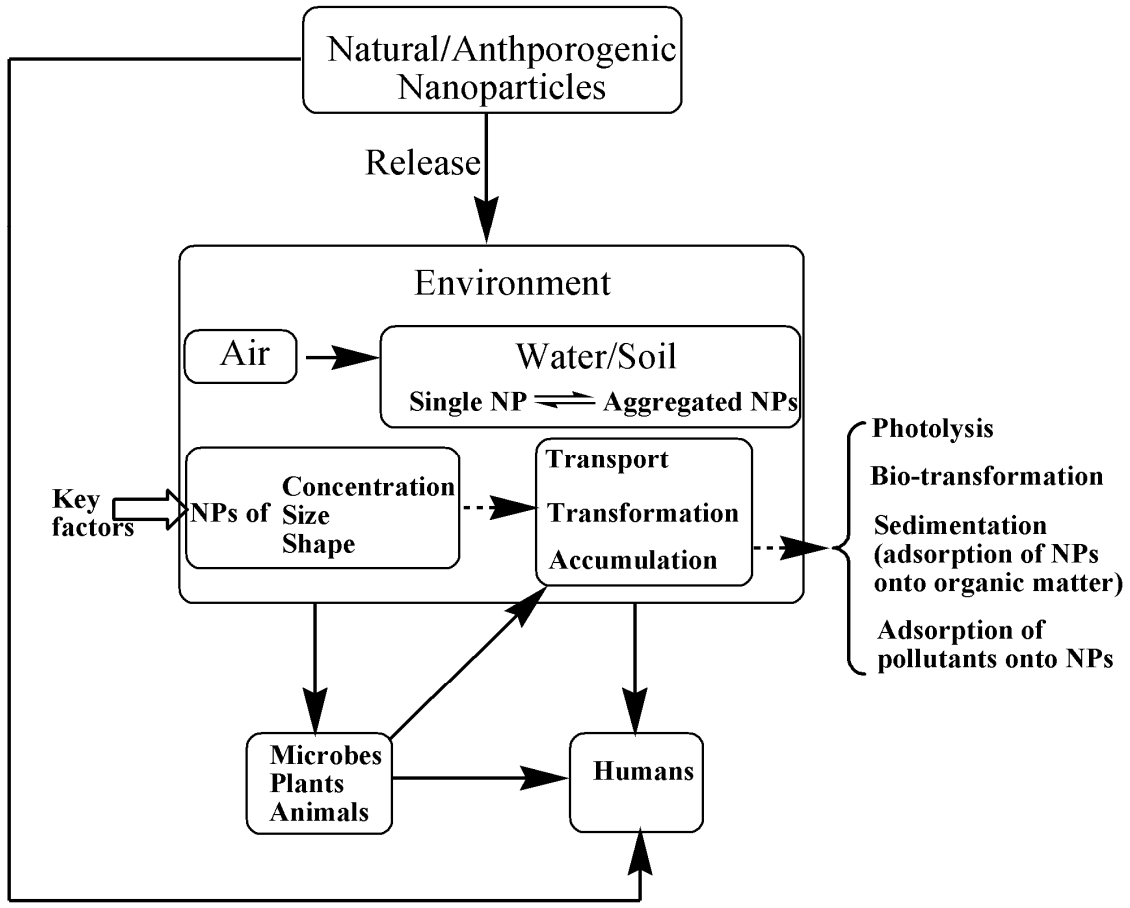

Figure 2. Potential pathways and impact of NPs in the environment on ecosystems

Although numerous studies have established the microbial effect of NPs (including metal NPs like Ag-NPs, metal oxide NPs like ZnO-NPs and C-containing NMs like C60 and SWCNT), the basic mechanisms of the underlying biological and chemical processes that affect the microbes are different [57,63-66]. Normally, the toxicity of metal NPs and metal oxide NPs is attributed to the release of corresponding metal ions from these NPs. Xiu et al. [67] investigated the toxicity mechanism of Ag-NPs using dose-response model under anaerobic conditions, confirming that antibacterial activity could be controlled by modulating Ag^{+} release, possible through manipulation of oxygen availability, particle size, shape, and/or type of coating. Dimkpa et al. [68] found that the impact of ZnO-NPs on bacterial cells was also dependent on the amount of Zn^{2+} released from ZnO-NPs. However, some researchers believe that the bactericidal effect of Ag-NPs leads to increased cell permeability and cell death [69]. For the C-containing NMs, how

they affect living cells remains unknown, although some studies found that SWCNT limit cell growth via a concentration-dependent model [66]. Totally, various nanoscale particles have been demonstrated to have negative impact on microbes, which possibly provides new opportunities to control the drug-resistant bacteria's spread and their impact on human health.

1.3.2 Impact of NPs on Plants

Soil and sediments are the ultimate sinks of NPs and, whether directly or indirectly released (e.g., via sewage treatment plants, waste handling, and aerial deposition), NPs will end up in soil or sediments [70]. Therefore, soil system may present the most important exposure avenue for assessing NPs' environmental risk. Being soil one of the main sinks, it raises concern about the entry of NPs into food webs and human access to contaminated agriculture. Hence, it is of importance to investigate the impact of NPs on plants.

Soil system contains a lot of natural NPs like clays, iron oxides, organic matter, and other minerals that play a very important role in biogeochemical processes. However, the introduction of ENPs to soil system may change the profile of the natural NPs and therefore interfere with soil behaviour. Recently, Atha et al. [71] tested the impact of copper oxide nanoparticles (CuO-NPs) between 1 and 100 nm in size on three different plants (*radish, perennial ryegrass* and *annual ryegrass*), which reported that CuO-NPs can enter plant root cells and generate many mutagenic DNA base lesions. Shen et al. [72] investigated the toxicological impact of SWCNT on rice leaves, which showed that SWCNT has an adverse effect on protoplasts and leaves through oxidative stress, leading to a certain amount of programmed cell death. Also, Lee et al. [73] found that the seedling growth of plants was adversely affected by exposure to Ag-NPs. In addition, Ag-NPs inhibited seed germination at lower concentrations (10 mg/L), but showed no clear size-dependant effects, and never completely impeded germination [74].

Although the toxic effect of ENPs on plants have been widely investigated, very few references describe the biotransformation of NPs in food crops and/or the possible biomagnification or bioaccumulation of NPs in the food chain. Zhu et al. [75] found that pumpkin plants can take up Fe_3O_4-NPs through their roots and that the particles are transported around the plant and accumulated by the pumpkin. On the other hand, Starnes et al. [76] compared the capacity of accumulating Au-NPs among six different plants including alfalfa,

cucumber, red clover, ryegrass, sunflower and oregano. Significant variations were detected in the uptake of Au-NPs in their roots ranging from 500 mg/kg (*ryegrass*) to 2500 mg/kg (*alfalfa*), and temporal analysis revealed that most of the Au-NPs accumulated within 6 h of treatment. Lee et al. [77] investigated the uptake and translocation of copper nanoparticles (Cu-NPs) in mungbean (*Phaseolus radiata*) and wheat (*Triticum aestivum*) in agar growth medium. The study showed that the Cu-NPs can cross the cell membrane and agglomerate in the cells. And meanwhile, the bioaccumulation Cu-NPs concentrations of mungbean and wheat plants exposed to 1000 mg/L Cu-NPs were 8 and 32 mg/L, respectively. Moreover, a responsive relationship between the bioaccumulated NPs in plant tissues and growth media was observed. Totally, the probability of plant exposure to ENPs has increased to a greater extent with the ongoing increasing production and use of ENPs in a variety of products, indicating much more studies on the impact of NPs on plants should be performed.

1.3.3 Impact of NPs on Animals

Given the bioaccumulation of ENPs in plants and the predatorprey relationship between plants and animals, impact of ENPs on animals has received considerable attention. Once ENPs are discharged into the soil system as well as the aquatic environment, one part of the ENPs will be bioaccumulated by plants via their roots and the other part of ENPs will be bioaccumulated by animals such as earthworms and fish [78-80]. Golobic et al. [80] used a test system with terrestrial isopods (*Porcellio scaber*) fed with food spiked with Cu-NPs for 14 days, which reported that about 99% of accumulated Cu^{2+} ions are dissolved from ingested Cu-NPs in the digestive system of isopods. On the other hand, even though the concentration of ENPs in aquatic environment may be low, the low degradability combined with feeding traits and habits of many invertebrates like earthworms (filter feeders, shredders, sediment dwelling) still can accumulate high level of ENPs [81].

Besides the accumulation of NPs by these animals, numerous studies also showed that the ENPs had toxic effects on the animals. For example, Van der Ploeg et al. [82] reported that C60 exposure (154 mg/kg) has a significant effect on earthworm (*Lumbricus rubellus*) cocoon production, juvenile growth rate and mortality. In addition, a dose-related increase in mortality was observed in earthworms (*Eisenia fetida*) exposed in agar with almost 100% mortality after

96 h exposure to the 1000 mg/kg of ZnO-NPs in soil [83]. Hu et al. [79] further investigated the mechanism of high percentage of mortality caused by high concentration (1000 mg/kg) of ZnO-NPs in soil, which reported that ZnO-NPs could induce significant damage of antioxidant system and DNA in earthworms when doses were close to 1000 mg/kg.

1.3.4 Impact of NPs on Humans

Nanotechnology and the respective NMs are contained in many commercially available products, which means that the general public is currently being exposed to various kinds of NMs. Normally, the impact of ENPs on humans can be divided into two parts (Figure 2); first, direct exposure to the ENPs, second, indirect uptake of the microbes/plants/animals with ENPs.

ENPs can be taken up into the human body via a variety of different pathways like the lung, the gastro-intestinal tract and the skin. Under practical conditions the most important pathways of uptake for ENPs are inhalation (via lung) or oral uptake (via gastro-intestinal tract). The lung is the most common way for NPs uptake; a number of studies have reported that free ENPs, due to their small size, can penetrate into the finest lung structures by breathing, can cause inflammatory reactions, and subsequently can enter the bloodstream. Diesel and automobile exhaust are the primary source of atmospheric nano- and microparticles in urban areas; most particles from vehicle exhaust are in the size of 20-130 nm for diesel engines and 20-60 nm for gasoline engines [31,84-86]. Knox [87] found that childhood cancers are strongly determined by prenatal or early postnatal exposure to oil-based combustion gases, primarily engine exhaust. In addition, epidemiological studies conducted on diesel locomotive drivers showed a correlation between occupational exposures to diesel engine exhaust and incidence of lung cancer in the workers [88]. Moreover, given the construct characteristics of NPs, they can adsorb other toxic chemicals which will enhance the adverse impact of NPs on humans. For example, diesel exhaust is known to be very toxic as it contains ENPs with high levels of polynuclear aromatic hydrocarbons (PAHs) [89].

On the other hand, NPs like TiO_2-NP, ZnO-NPs and Ag-NPs come in direct contact with skin as they are widely used in various cosmetics and personal care products. Pan et al. [90] reported that the dermal exposure to TiO_2-NPs decreases cell area, cell proliferation, mobility, and ability to contract collagen. Moreover, Liu et al. [91] further found that the EC50 values of human cell

(A549, SGC-7901, HepG2 and MCF-7) are size-dependent of NPs, and smaller NPs enter cells more easily than larger ones. Besides the direct inhalation uptake of the NPs through lung, the oral uptake of NPs via food chain (gastro-intestinal tract) is another potential pathway. A recent study showed that ENPs transported through an aquatic food chain from algae, through zooplankton to fish, affect lipid metabolism and behaviour of the top consumer [92]. According to this finding, ENPs can affect food chains and, ultimately, too human health.

1.4 Analysis and Characterization of NPs in Environmental Samples

The increasing use of NMs in industrial and household applications has led to the release of NPs into the environment. Moreover, the uncertain effects resulting from the novel properties and reactivity exhibited by NPs need assess the risk of NMs on ecosystems and/or human health. Assessing the risks of these NPs in the environment requires an understanding of their fate, transport and transformation, in particular the characterization (shape and size) of the NPs in the environmental matrix (Figure 2). Furthermore, quantitative analytical methods are also required to determine their environmental concentrations. However, practically nothing is known about their concentration, shape and size under environmental conditions due to the lack of analytical methods for NPs in real environmental samples.

To date, a variety of methods such as filtration [93], centrifugation [94,95], size exclusion chromatography [96,97], flow field flow fractionation [98-100], gel electrophoresis [101], and capillary electrophoresis [102] have been developed for extraction and pre-concentration of NPs from aqueous phase. Among these methods, flow field flow fractionation has become a popular method for the characterization of NPs. Unlike conventional filtration methods, flow field flow fractionation provides a continuous and high-resolution separation of NPs as a function of their diffusion coefficient, hence the interest for use in determining particle size distribution. In addition, when coupled to other detectors such as inductively coupled plasma-mass spectroscopy (ICP-MS), UV-absorbance, light scattering, fluorescence, transmission electron microscopy (TEM), flow field flow fractionation (FlFFF) can provide a wealth of data on particles properties like size, shape and chemical composition [103,104]. In recent, gel electrophoresis also has been used to separate the NPs according to size and shape [101]. Unfortunately, many of these approaches suffer from disadvantages, such as application of only small sample volumes,

Table 2. Specifications of methods for analysis and characterization of NPs [105]

Method	Approximate size range (nm)	Limit of detection[a]	Level of sample perturbation
AFM	0.5 to > 1000	ppb-ppm	Medium
BET	1 to > 1000	Dry powder	High
Centrifugation	10 to > 1000	Detection dependant	Low
Dialysis	0.5 – 100	Detection dependant	Low
DLS	3 to > 1000	ppm	Minimum
Electrophoresis	3 to > 1000	ppm	Minimum
EM-EELS/-EDX	Analysis spot size: ≈ 1 nm	ppm in single particle	High
ESEM	40 to > 1000	ppb-ppm	Medium
ES-MS	< 3	ppb	Medium
FFF	Flow FFF: 1 – 1000 Sed FFF: 50 – 1000	Detection dependant; UV: ppm Fluo&ICP-MS: ppb	Low
HDC	5 – 1200	Detection dependant	Low
ICP-MS	Depends on fractionation	ppt-ppb	-
LIBS	5 to > 1000	ppt	Minimum
Microfiltration	100 to > 1000	Detection dependant	Low-medium
SEC	0.5 – 10	Detection dependant	Medium
SEM	10 to > 1000	ppb-ppm	High
SLS	50 to > 1000	-	Minimum
TEM/HR-TEM	1 to > 1000	ppb-ppm	High
TEM-SAED	Analysis spot size: 1 nm	-	High
Turbidimetry nephelometr	50 to > 1000	ppb-ppm	Minimum
Ultrafiltration	1 – 30	Detection dependant	Medium
WSEM	50 to > 1000	ppm	Low
WSTEM	-	ppm	Low
XRD	0.5 to > 1000	Dry powder	High

[a] For comparison mass concentration limit of detection for 100 nm particle are estimated

providing non-sufficient enrichment, risking agglomeration of NPs, etc. Moreover, established analytical tools for NPs characterisation and quantification have focused so far on synthetic products and are in the most cases not suitable for complex mixtures, like environmental or biological samples, nor are they able to detect very low concentrations (in the low range between µg/L and pg/L). As shown in Table 2, [105] each method has its limitations in applicable size and concentration ranges. For example, although dynamic light scattering (DLS) can analyze the NPs with size from 3 to 1000 nm, its limit of detection must be at mg/L level which is far higher than the actual concentration (pg/L - ng/L) of NPs in environmental samples.

1.5 Motivation, Scope and Outline

1.5.1 Motivation

A tremendous increase in the applications of metal nanoparticles (MNPs) in various products has occurred (**chapters 1.1 and 1.2.2**). This rise obviously results in an increased potential for their widespread release into the environment (**chapter 1.2.2**). In this context, ongoing research evaluates the impact of MNPs on ecosystems and humans and numerous exposure studies suggest their uptake in microbes, plants, fish, earthworms, humans and other organisms causing different adverse effects (**chapter 1.3**). To ensure sustainable development of nanotechnology, it is essential to assess the risk of MNPs introduced from various applications. Conventionally, assessing the risks of these MNPs in the environment requires an understanding of their fate, transport and transformation, in particular the characterization (shape and size) as well as the actual concentration of the MNPs in environmental matrices (Figure 2). However, established analytical methods/tools for MNPs characterisation and quantification had focused so far on synthetic products and are in the most cases not suitable for complex mixtures, like environmental samples, nor are they able to detect very low concentrations (**chapter 1.4**). In other words, there are two special challenges for studies of MNPs in environmental samples; first, for environmentally relevant concentrations (pg/L - ng/L), the detection limits for most established methods are not sufficiently low, second, environmental samples are a complex matrix with a high background of natural and unintentionally produced impurities. Hence, as a first step sample preparation, i.e. separation and enrichment of MNPs from matrices is required.

In this context, development of methods to efficiently and selectively extract, separate and concentrate MNPs in environmental water samples is necessary. Moreover, in order to gain the original morphology of the MNPs in environmental water samples, the novel pre-treatment methods should preserve their shape and size after the extraction and enrichment. On the other hand, to examine the feasibility of the novel methods, they were applied to extract and concentrate spiked MNPs in real environmental samples. In addition, one of the optimized methods was applied to extract and concentrate nanoscale silver particles (n-Ag-Ps) in the effluent of WWTPs.

1.5.2 Scope and Outline

The ligand-assisted liquid-liquid extraction method, which was tested for four different ligands namely 1-dodecanethiol (DDT), 1-octadecanethiol (ODT), dodecylamine (DDA) and octadecylamine (ODA), was investigated in **chapter 2**. The ODT was found to be the most efficient ligand. However, the ligand-assisted liquid-liquid extraction method was not applicable to extract the NPs once the concentration of NPs was lower than 100 μg/L.

Consequently, the DDT-assisted solid-liquid extraction method was developed, which is presented in **chapter 3**. Au-NPs were loaded onto a reversed phase C-18 (RP-C18) column and then DDT-assisted extraction into chloroform was performed. Hence, the work investigated the development and optimisation of the ligand-assisted solid(RP-C18)-liquid extraction procedure in regard to sample volumes, organic solvent, concentration and nature of the ligand, ultrasonication time, and pH of the sample. The influences of Au-NPs size as well as of different coating of the NPs were examined. Moreover, potential interferences of the method from other M-NPs or dissolved organic carbon were studied. Finally, extraction efficiencies for Au-NPs and recoveries in model and real water samples were investigated.

Chapter 4 describes another solid-liquid extraction method, where an anionic exchange resin (Amberlite IRN-78) was used to adsorb the mercaptosuccinic acid (MSA) modified NMNPs (e.g., Au-NPs, Ag-NPs and Pd-NPs) via the electrostatic interaction of the positively charged amino group from the resin with the negatively charged carboxylic acid groups from the MSA ligands. The reaction mechanism is presented in chapter 4. The adsorbed NMNPs were eluted by a mixture of formic acid and methanol. Moreover, three real water samples were tested by the

proposed method.

Chapter 5 presents applications of the solid(IRN-78)-liquid extraction method to extract, concentrate and quantify n-Ag-Ps in effluents of nine municipal WWTPs in Germany. Special emphasis was placed on (1) optimizing the IER method for quantifying n-Ag-Ps in aqueous samples; (2) investigating whether and to what extent mechanical treatment plays a role in the n-Ag-Ps removal; (3) quantifying the n-Ag-Ps in field-collected wastewater effluent through IER and CPE methods respectively, and further determining the relative contribution of biological treatment to n-Ag-Ps removal compared to mechanical treatment; (4) finally, estimating the daily n-Ag-Ps load entering water environment through effluent discharge.

Chapter 6 summarizes the main findings on the basis of these studies.

Chapter 7 is appendix presenting the materials, methods, instrumentation, and all other important information used in this study.

Chapter 8 represents all the references cited by this thesis.

2 Ligand-Assisted Liquid-Liquid Extraction of Au-NPs

2.1 Liquid-Liquid Extraction of NMNPs

NMNPs have been extensively studied over the last decade due to their unique physical and chemical properties as compared to their bulk metal equivalents [106-108]. Consequently, a tremendous increase in the application of NMNPs in various fields has occurred. This rise obviously results in an increased potential for their widespread release into the environment.

In this context, it is essential to assess the risks of these NMNPs in the environment, which requires an understanding of their fate, transport and transformation, in particular the characterization (shape and size) as well as the actual concentration of the NMNPs in environmental matrices (Figure 2). Liquid-liquid extraction is a very common method by which a compound is pulled from solvent A to solvent B where solvents A and B are not miscible [109]. To our knowledge, NPs can be extracted from aqueous solutions to organic solvents because of varying their surfaces from hydrophilicity to hydrophobicity using surfactant modification [110]. So far, many types of NMNPs have been extracted from an aqueous phase to an organic phase with the assistance of alkylamine or alkylthiol compounds [111-116]. For example, Yang et al. [111] extracted alkylamine-stabilized NMNPs (< 7 nm) from an aqueous layer to toluene. McMahon and Emory [117] developed a method to extract large Au-NPs (d > 45 nm) from aqueous solutions to chloroform with dicyclohexylamine (DCHA). In addition, Sekiguchi et al. [118] also developed an octanethiol-assisted method for extracting small Au-NPs (5 nm) from an aqueous phase to chloroform.

Consequently, a liquid-liquid extraction method was applied to extract the Au-NPs with an average diameter of 10 nm from an aqueous phase to organic phase (n-hexane). The whole extraction process can be completed within only 1 min. Four different ligands namely 1-dodecanethiol (DDT), dodecyl amine (DDA), 1-octadecanethiol (ODT) and octadecylamine (ODA) were tested, and the transfer efficiency (TE) as a function of ligand concentration in the n-hexane (or the molar ratio of ligand to Au-NPs) was investigated. Moreover, the transfer index (TI) was calculated to confirm the TE. Finally, the extracted Au-NPs were characterized by UV-vis spectroscopy and TEM to evaluate their shape and size after the extraction.

2.2 Comparative Study of Alkylthiols and Alkylamines for the Liquid-Liquid Extraction of Au-NPs

2.2.1 Effect of Ligands on the Extraction of Au-NPs from Water to n-Hexane

To our knowledge, the extraction of NPs strongly depends on both the chemical affinity between the ligand and the NPs and the solubility of the ligand-NPs-complex compounds in the solvent. The four ligands investigated in this study have a strong binding affinity to Au-NPs due to their thiol or amine groups [119-122]. Moreover, they are long-chained hydrophobic molecules which are well dissolved in solvents like n-hexane. However, it was found that they have different capacities of extracting the Au-NPs from the aqueous phase to n-hexane. When DDT containing n-hexane is mixed with an Au-NPs solution, DDT can immediately bind to the surface of the Au-NPs through the thiol groups [123,124], resulting in a remarkably fast movement (within 1 min) of the Au-NPs to the n-hexane phase (Figure 3a). In the case of ODT and DDA, the Au-NPs containing aqueous phase also immediately turned from wine red to colorless (Figures 3b and 3c) after shaking the biphasic mixture, which indicates a complete extraction of Au-NPs. We speculate that the DDT, ODT and DDA molecules serve two functions: they bring the Au-NPs into contact with the immiscible n-hexane by emulsification and also engulf the Au-NPs via surfactant modification allowing them to transfer the phase. Therefore, the Au-NPs were easily extracted from the aqueous layer to n-hexane because the hydrophobic groups of DDT, ODT and DDA are exposed to the n-hexane solvent.

However, for ODA, vigorous shaking of the biphasic mixture resulted in a foam like n-hexane layer (Figure 3d), and only sparse Au-NPs transfer to the n-hexane phase was observed. This result may be attributed to the poor contact between ODA and Au-NPs when shaking the mixture. Based on this consideration, ethanol, which is water miscible and a good solvent for the contact between ODA and Au-NPs, was used as a modifier for the extraction. However, the Au-NPs still could not be extracted from aqueous solution to n-hexane under the ethanol abundant conditions. Obviously, the ODA-assisted extraction does not work under the described conditions. On the contrary, Wang et al. [125] reported that the ODA with ethanol is a highly efficient chemical inducer to extract Au-NPs in aqueous solution. We speculate that the differences may be

attributed to the different size of Au-NPs. In our study, the size of Au-NPs is between 5 and 25 nm, whereas Wang et al. [125] used Au-NPs with an average size of 106 nm.

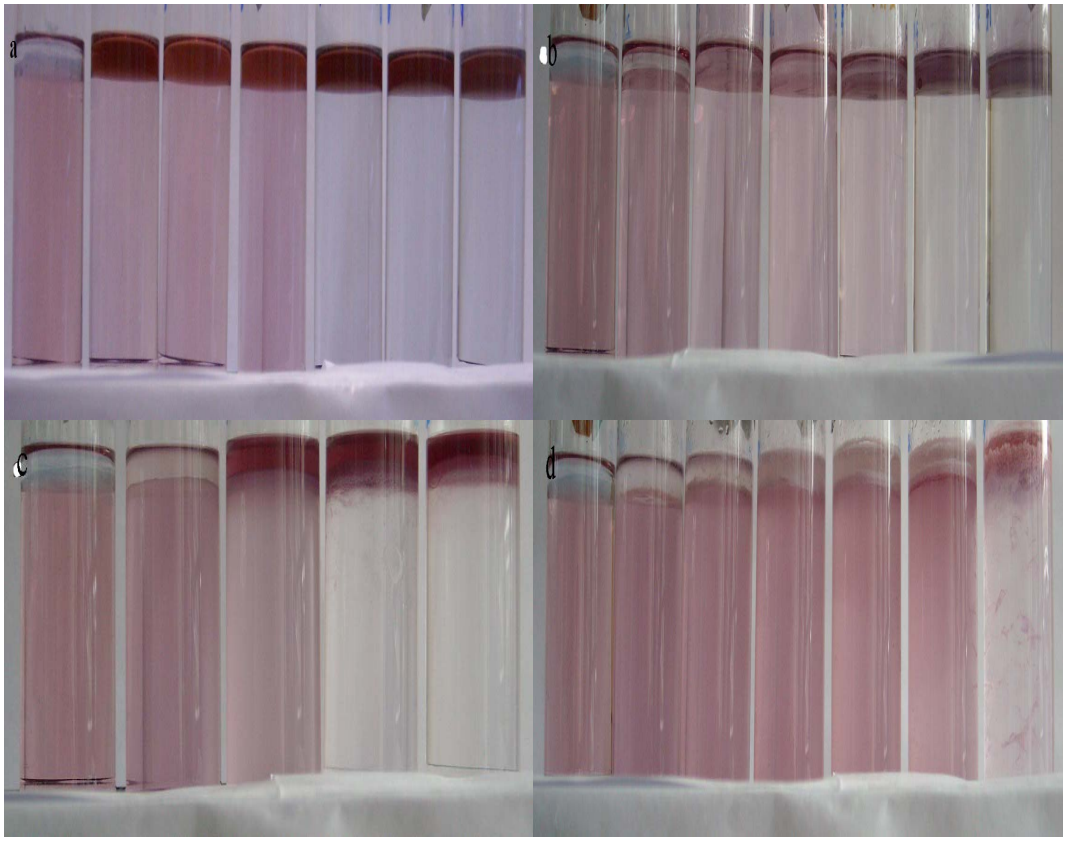

Figure 3. Photos for extraction of Au-NPs (0.05 mmol/L) from water to n-hexane using different concentrations of ligand. a) DDT. b) ODT. c) DDA. d) ODA

2.2.2 Effect of DDT Concentration in n-Hexane on Extraction of Au-NPs

Usually, surfactant modification is carried out by mass action; an excesses of several orders of magnitude of ligand is used to drive the reaction [126,127]. For example, Woehrle et al. [128] found that the molar ratio of ligand to Au-NPs (or the concentration of ligand) has strong influence on the extraction of Au-NPs. Figure 4a shows that the TE increases with the DDT concentration in n-hexane and reaches a plateau after about 210 mmol/L (corresponding molar ratio of DDT to Au-NPs: 270) with a final TE in a range from 92% to 98%. Additionally, the DDT-assisted liquid-liquid extraction was also applicable to extract low concentration (0.005 mmol/L) of Au-NPs from aqueous to n-hexane phase (Figure 5a). As shown in Figure 5b, the TE increases sharply when the DDT concentration in n-hexane increases from 0 to 14 mmol/L

(corresponding molar ratio of DDT to Au-NPs: 310) followed by a slight decrease when the concentration of DDT increases from 14 to 21 mmol/L, and afterwards, the TE reaches a plateau with a final efficiency of 92%.

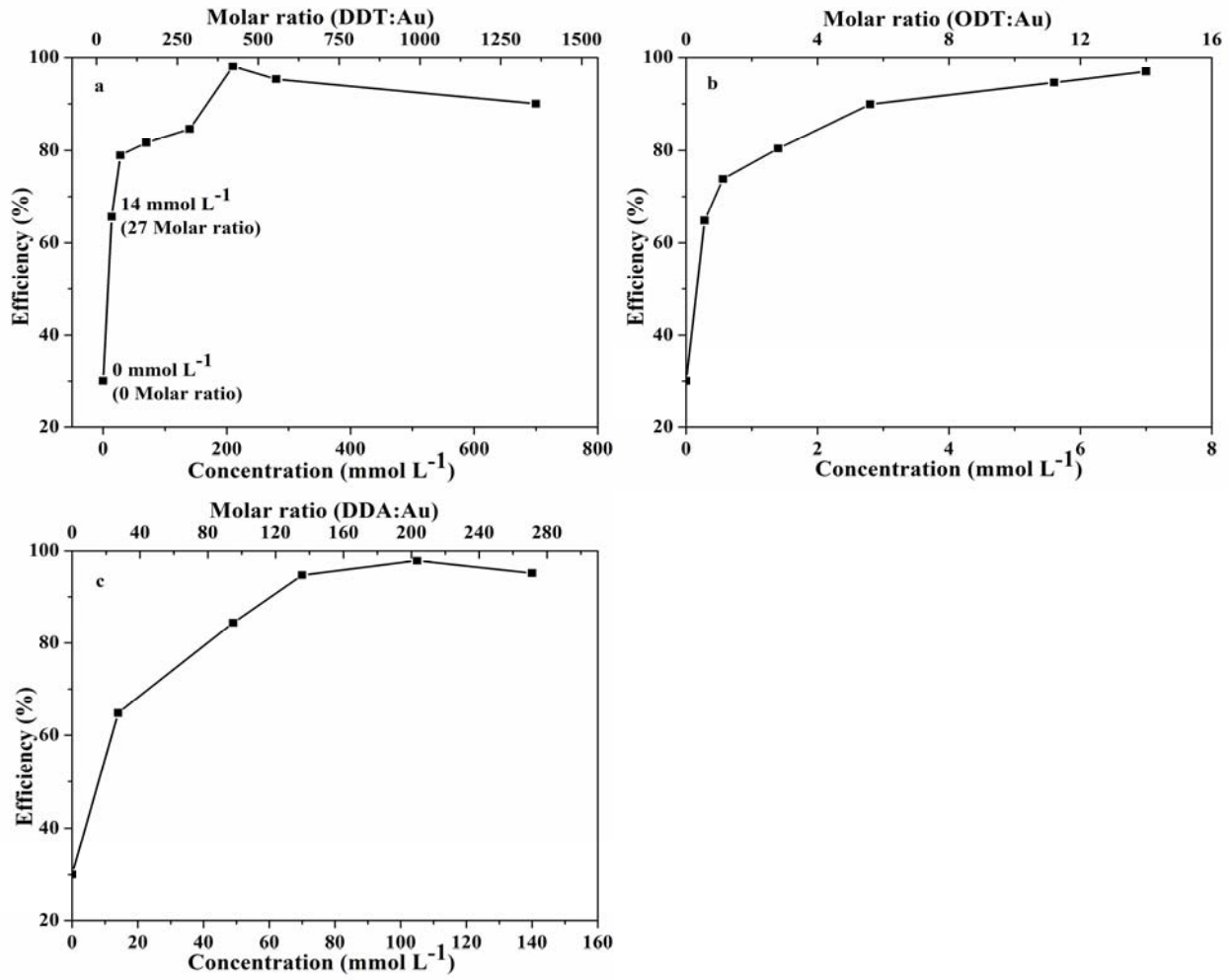

Figure 4. Effect of the ligand concentration in n-hexane on the transfer efficiency of Au-NPs. a) DDT. b) ODT. c) DDA

In combination, we found that the TE kept a plateau with > 96% when the molar ratio of DDT to Au-NPs was in a range from 270 to 310. Under these conditions, the citrate molecules are easily displaced upon shaking at room temperature in presence of excess DDT, since the thiol bond formed between the DDT and the Au-NPs surface is much stronger than the bond formed with the initial citrate molecules [124]. On the basis of these results, the PVP 10- and PVP 40-stabilized Au-NPs were also tested. It was found that the DDT-assisted liquid-liquid extraction was applicable to these Au-NPs under the optimized conditions.

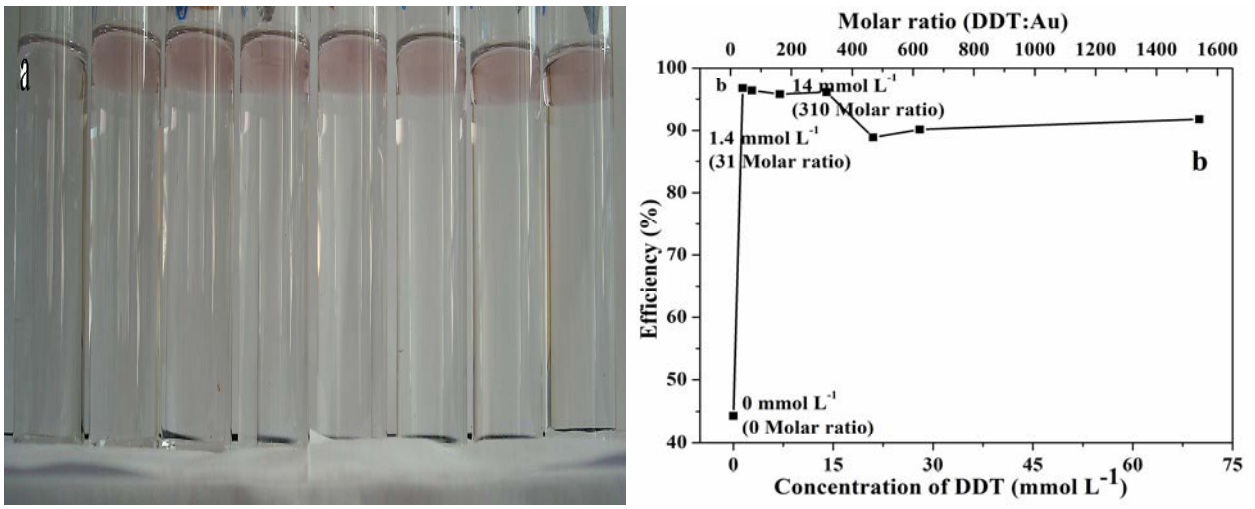

Figure 5. a) A photo for Au-NPs (0.005 mmol/L) extraction using different concentrations of DDT. b) Effect of DDT concentration in n-hexane on the extraction of Au-NPs (0.005 mmol/L)

2.2.3 Effect of ODT Concentration in n-Hexane on Extraction of Au-NPs

As for the ODT, the TE of Au-NPs also increased with ODT concentration in n-hexane and reached the maximum value (97%) at 7 mmol/L of ODT (Figure 4b). Obviously, the consumption of ODT for maximum efficiency only accounts for 3.3% that of DDT used in the liquid-liquid extraction. However, the color varied from wine red to pale purple in the n-hexane phase if high concentrations (> 3 mmol/L) of ODT are used (Figure 3b), implying the potential aggregation or coagulation of Au-NPs in the n-hexane phase after the ODT-assisted extraction. Similar color changes from red to purple to blue were observed during the coalescence of Au-NPs [129-131].

The implication was confirmed by UV-vis spectra, since NPs aggregation gives rise to a red-shift and broadening of the plasmon band absorption [132-135]. As shown in Figure 6a, a 56-nm red-shift in the wavelength of the surface plasmon band peak maximum is observed after the liquid-liquid extraction (water to n-hexane), indicating that the ODT-assisted extraction of Au-NPs causes aggregation of the particles in the n-hexane phase. In addition, while the TE was high (up to 97%), the extracted Au-NPs assembled at the interface of aqueous phase and organic solvent (Figure 3b). Obviously, TE is not a sufficient criterion to evaluate a ligand-assisted extraction method for MNPs. Hence, the TI analysis was further conducted according to equation 2 (chapter 7.8.2).

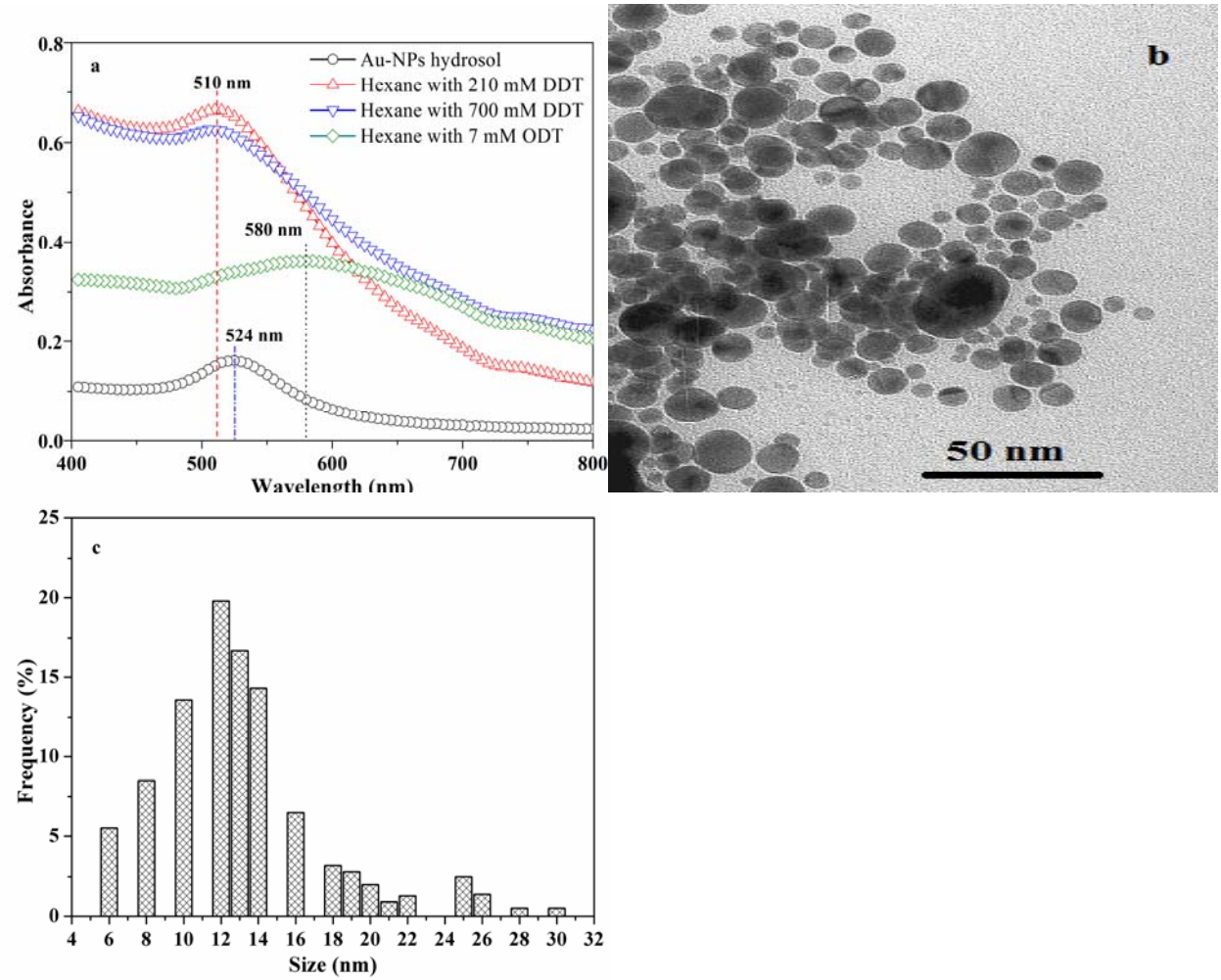

Figure 6. a) UV-vis spectra of Au-NPs before and after liquid-liquid extraction assisted by different ligands. b) TEM micrograph of the extracted Au-NPs in n-hexane with 210 mmol/L DDT, the scale bar corresponds to 50 nm. c) Size distribution of 305 of the extracted Au-NPs with an average diameter of 13.2 ± 0.8 nm

As shown in Figure 7a, the TIs are far lower than 1, indicating that the Au-NPs extracted by an ODT-assisted process are poorly dispersed in n-hexane. For example, the TE for ODT-assisted extraction was about 97% under the optimized conditions, whereas the corresponding TI was only 0.38 (Figure 7b). On the contrary, all the TIs of DDT-assisted extraction were close to 1 (Figure 7b and Figure 8). Totally, although the Au-NPs could be extracted from aqueous solution to n-hexane by the ODT-assisted liquid-liquid extraction, the extracted Au-NPs were not stable in the n-hexane phase.

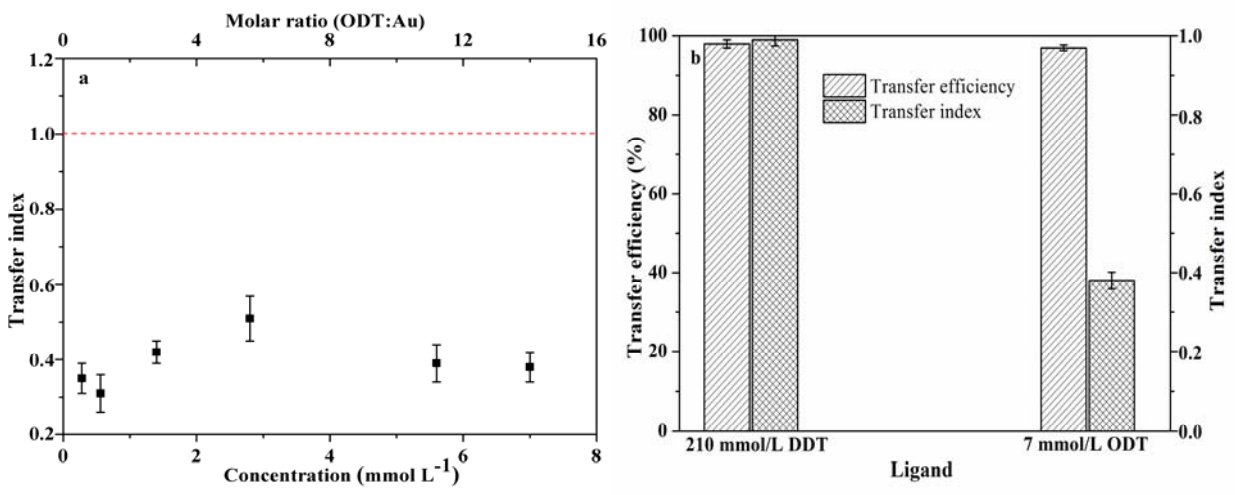

Figure 7. a) Effect of the ODT concentration in n-hexane on the transfer index of Au-NPs. b) Comparison between transfer efficiency and transfer index of Au-NPs under optimized conditions

2.2.4 Effect of DDA Concentration in n-Hexane on Extraction of Au-NPs

Figure 4c shows that the TE increases with the DDA concentration in n-hexane and reaches a plateau after about 105 mmol/L (corresponding molar ratio of DDA to Au-NPs: 202) with a final efficiency of 98%. Yang et al. [136] also reported that the efficiency of the DDA-assisted liquid-liquid extraction was nearly 100%. Moreover, they found the extracted Au-NPs could be well dispersed in toluene. However, in this study, the extracted Au-NPs were not stable; most of the particles precipitated at the interface of aqueous layer and n-hexane, what can be observed with the bare eye.

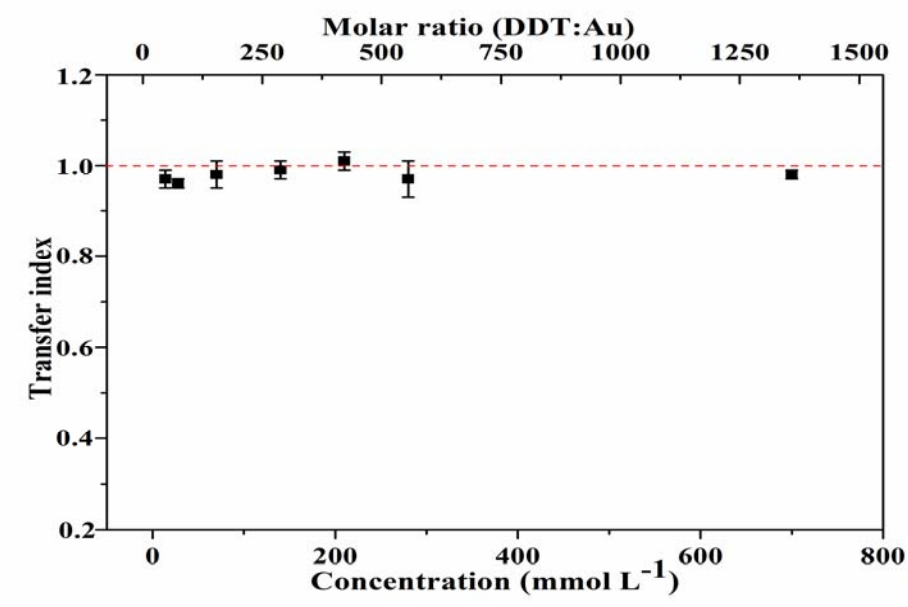

Figure 8. a) Effect of the DDT concentration in n-hexane on the transfer index of Au-NPs

2.3 Preservation of Size and Shape of Au-NPs via the DDT-Assisted Liquid-Liquid Extraction

Beside efficient extraction of the Au-NPs from an aqueous solution to n-hexane by the ligand-assisted liquid-liquid extraction, the most important issue for the method is the preservation of size and shape of the Au-NPs. On the basis of above-mentioned TE and TI analyses, DDT was the best suited ligand for extraction of Au-NPs from an aqueous solution to n-hexane. Therefore, the preservation of the size and shape of Au-NPs during DDT-assisted extraction was further investigated. A first indication of similar size of the Au-NPs before and after the extraction gives the UV-vis spectra shown in Figure 6a. Here, a slight blue-shift of 14-nm in the wavelength of the surface plasmon band peak maximum is observed in the organosol (n-hexane with 210 mmol/L or 700 mmol/L DDT) in comparison to the Au-NPs hydrosol. This shift may arise from the change in refractive index of the solvent medium (from 1.446 in water to 1.375 in n-hexane). Additionally, for the n-hexane with 210 mmol/L DDT, the plasmon peak remained narrow in its band width. This indicates the Au-NPs are well dispersed in the n-hexane, which is in good agreement with the TI analysis (Figure 8). Furthermore, the TEM investigation proved that the Au-NPs did not aggregate after they were extracted to n-hexane with 210 mmol/L DDT (Figure 6b). Meanwhile, as shown in Figure 6c, there is no change in the size distribution of the Au-NPs extracted to n-hexane with 210 mmol/L DDT. Totally, the obtained results confirm no change in particle size (with average diameter of 13.2 ± 0.8 nm) and shape.

2.4 Conclusions

On the basis of a comparative study, we developed an efficient ligand-assisted liquid-liquid extraction method which can extract Au-NPs (d: 5-25 nm) from an aqueous solution to n-hexane. In this study, the molar ratio of DDT to Au-NPs is a critical factor affecting the TE, and 270 - 310 is found to be the optimum range, under which the TE of this method is > 96%. Moreover, the proposed method can preserve the shape and size of the Au-NPs, which was confirmed by UV-vis spectra and TEM analysis. Meanwhile, the extracted Au-NPs can well disperse in the n-hexane and kept stable for some weeks, which appears reasonable when compared to available

literatures [118,125].

It is interesting to note that this study provides a possibility to efficiently collect and recover the Au-NPs from aqueous solution through a simple to perform and rapid method. Moreover, this method may aid in removing the Au-NPs in industrial wastewater, which is of importance to protect the environment [137]. Hence, application of this method to remove the Au-NPs as well as other MNPs in wastewater will be undertaken in future.

3 Ligand-Assisted Solid(RP-C18)-Liquid Extraction for Separation and Pre-concentration of Au-NPs from Water

3.1 Ligand-Assisted Solid(RP-C18)-Liquid Extraction of Au-NPs from Water

To date, a variety of approaches such as filtration [93], centrifugation [94,95], size exclusion chromatography [96,97], flow field flow fractionation (FlFFF) [98-100], gel electrophoresis [101], and capillary electrophoresis [102] have been developed for extraction and concentration of NPs from aqueous phase. Unfortunately, many of these approaches suffer from disadvantages, such as application of only small sample volumes, providing non-sufficient enrichment, risking agglomeration of NPs, etc. Moreover, methods that meet the requirements of separation and pre-concentration of NPs from environmental matrixes and at the same time preserve the size and shape of the NPs are sparsely reported. Quite recently, Liu et al. [138,139] reported an elegant method for Ag-NPs separation and concentration by cloud point extraction with Triton X-114. Nevertheless, there is an urgent need for methodologies to separate and pre-concentrate NPs from complex matrices, preserve their size and shape and thereby overcome limitations of existing analytical techniques for size fractionation, characterisation, and quantification of MNPs in environmental samples.

Consequently, we focussed on Au-NPs as a representative for the group of NMNPs. Studies on the presence and/or concentration level of Au-NPs in environmental samples are due to the lack of suitable analytical methodology not published. In this work a two-step selective extraction procedure was developed. Separation of the Au-NPs from the water samples was performed by application of reversed phase C-18 (RP-C18) material. Re-extraction from the solid phase into a small volume of organic solvent was assisted by a suitable organic ligand. In this study, DDT, the most efficient ligand reported in chapter 2, serves as an important surfactant and stabilizer for Au-NPs re-extraction from RP-C18. Hence, the work presented here describes the development and optimisation of the two-step extraction procedure in regard to sample volumes, organic solvent, concentration and nature of the ligand, ultrasonication time, and pH of the sample. The influences of Au-NPs size as well as of different coating of the NPs were examined. Moreover,

potential interferences of the method from other MNPs or dissolved organic carbon were studied. Extraction efficiencies for Au-NPs and recoveries in model and real water samples were investigated.

3.2 Optimization of the Extraction Method for Separation and Pre-concentration of Au-NPs from Water

3.2.1 General Procedure for the Two-Step Extraction

Figure 9a shows a scheme of the general procedure proposed for the separation and pre-concentration of Au-NPs from aqueous samples. In a first step, a defined volume (10 - 500 mL) of the Au-NPs containing sample is passed over a micro column filled with RP-C18 providing quantitative adsorption of the Au-NPs (1^{st} step). At this point, RP-C18 turns wine red in colour when the initial concentration of the Au-NPs sample was high enough (higher than 1 mg/L). The interaction of the nonpolar adsorption material (RP-C18) with the NPs is very strong and leads to quantitative retention of the Au-NPs. Elution by organic solvents or aqueous solutions in a pH range between 2 and 10 does not release considerable amounts of the NPs. Even the use of ligand-containing organic solvents for elution does not lead to quantitative release. Moreover, the specific interaction between RP-C18 and citrate-coated Au-NPs was confirmed by an experiment in which the RP-C18 was replaced by silica gel of the same particle size. With this column retention of Au-NPs was irreproducible varying from 31.1% to 77.6 %. Therefore, the RP-C18 loaded with Au-NPs is dried by application of vacuum and removed from the column. Then, Au-NPs are extracted into chloroform by assistance of DDT and ultrasonic treatment at about 0 °C (2^{nd} step). The chloroform began to turn pink in colour after 30 min of ultrasonication, indicating the extraction of the Au-NPs from the adsorption material to chloroform. After centrifugation at 2000 rpm for 3 min the chloroform supernatant phase (in the following referred to as Au-NPs organosol) was collected and checked for Au concentration.

Figure 9b presents the UV spectra of the Au-NPs aqueous sample (referred to as Au-NPs hydrosol) in comparison to that of the resulting organosol indicating quantitative extraction of the Au-NPs. In addition Figure 9b shows the resulting UV spectra after performing the described two-step procedure omitting addition of DDT (dashed red line) or ultrasonication (dotted blue

line), respectively. Minor recoveries of Au-NPs in the chloroform phase were observed, confirming that both, the ultrasonic treatment and the addition of DDT in chloroform are essential for quantitative extraction of Au-NPs. By varying the volume and initial concentration of the Au-NPs samples, enrichment factors of up to 250 were obtained. However, higher ratios of sample to extractant volume were not checked, it is assumed that even higher enrichment factors could be reached by this approach. Moreover, the extracted Au-NPs organosol turned out to be stable within months in regard to the NPs size, which was confirmed by UV-vis spectra (Figure 10). However, the concentration of Au-NPs may slightly decrease probably due to loss of NPs attached to the vessel wall. Thus, beside separation and efficient pre-concentration of Au-NPs from water samples the novel approach also allowed effective stabilization of Au-NPs' size.

Here, we speculate that the adsorption of DDT on the surface of Au-NPs leads to the positive stabilization. In this regard, Figure 9c provides significant evidence that the DDT molecules ($CH_3(CH_2)_{11}SH$) bind to the surface of the Au-NPs through their thiol group. The S-H stretching vibration of free alkanethiols is typically found at 2560 cm^{-1}, [140] which we observed in the solution of DDT in chloroform (Figure 9c, inset, dotted blue line). Therefore, the absence of this peak in the Au-NPs organosol (Figure 9c, inset, red line) indicates that the SH bond of the DDT is broken upon binding to the Au-NPs surface. This observation is consistent with the reported cleavage of the S-H bond for alkanethiols adsorbed onto Au-NPs in surface-enhanced Raman spectroscopy [117,140]. Furthermore, the IR spectrogram of the Au-NPs organosol shows in comparison to the solution of DDT in chloroform three additional peaks at 2923 cm^{-1}, 2850 cm^{-1}, and 1096 cm^{-1}. The additional IR peaks at 2923 and 2850 cm^{-1} correspond to C-H stretching modes, whereas the peak at 1096 cm^{-1} relates to stretching modes of C-C, which are typically found between 950 and 1150 cm^{-1}. Such bands were also observed by Bryant and Pemberton [140] in surface-enhanced Raman spectroscopy used for analysis of alkanethiols and alkanethiolate monolayers.

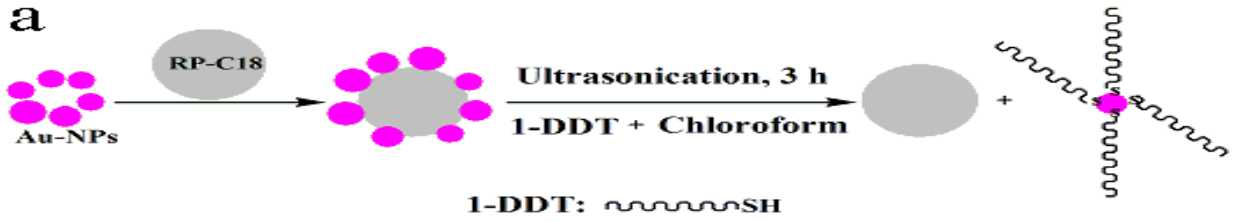

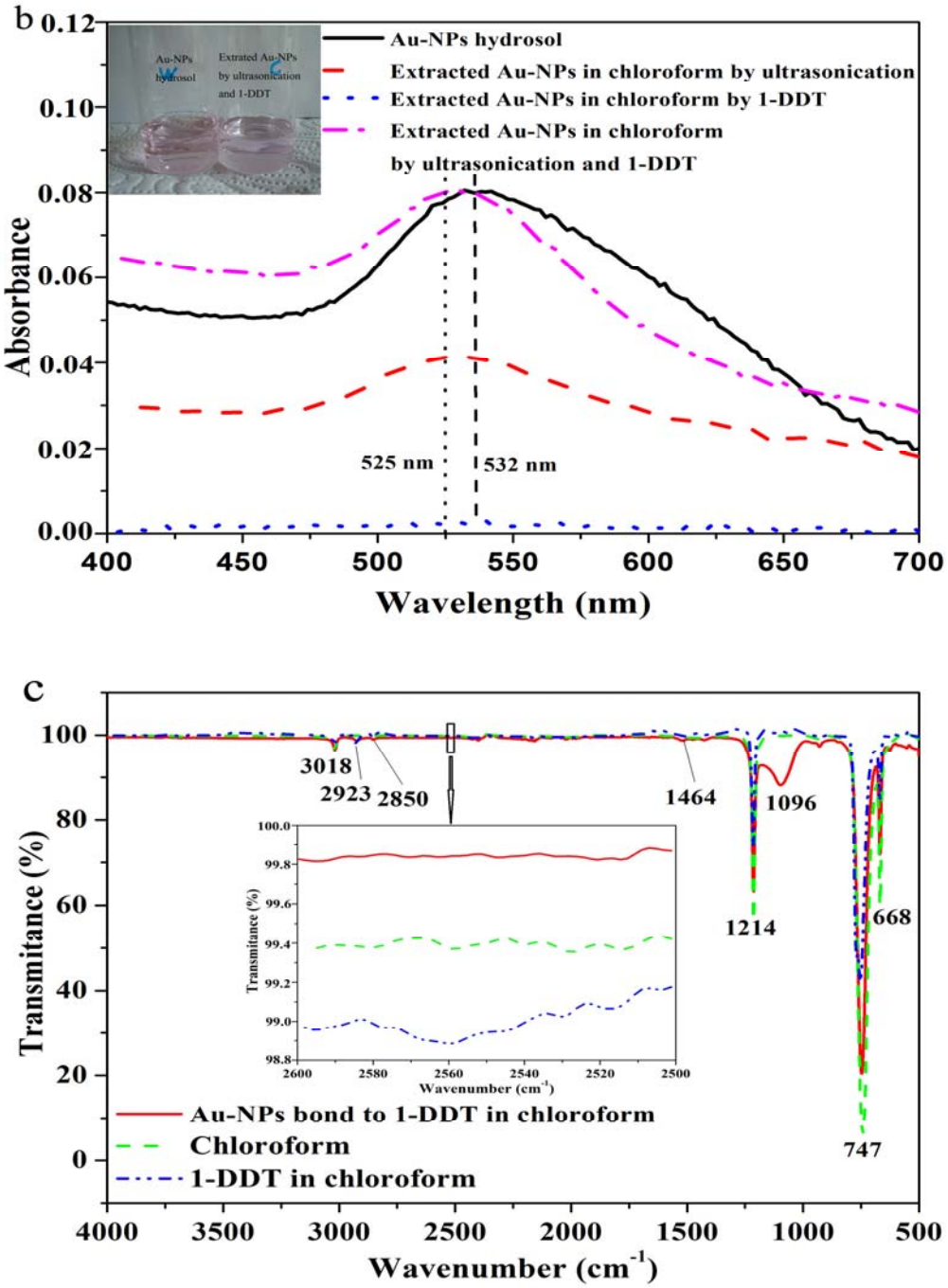

Figure 9. a) Schematic illustration of the strategy for separation and concentration of Au-NPs from waters by two-step extraction. b) UV-vis absorbance spectra of the Au-NPs hydrosol and organosols demonstrating that both (extraction efficiency: 99.5%), ultrasonic treatment (extraction efficiency: 66.1%) and addition of DDT (extraction efficiency: 5.0%), are essential for quantitative extraction of Au-NPs; Inset: visual appearance of Au-NPs hydrosol and extracted Au-NPs using ultrasonication and DDT. c) IR spectra of pure chloroform, chloroform with 5 mmol/L DDT and Au-NPs bond to DDT in chloroform extracted from hydrosol source, respectively. The inset shows the FT-IR spectra from 2500 to 2600 cm^{-1}

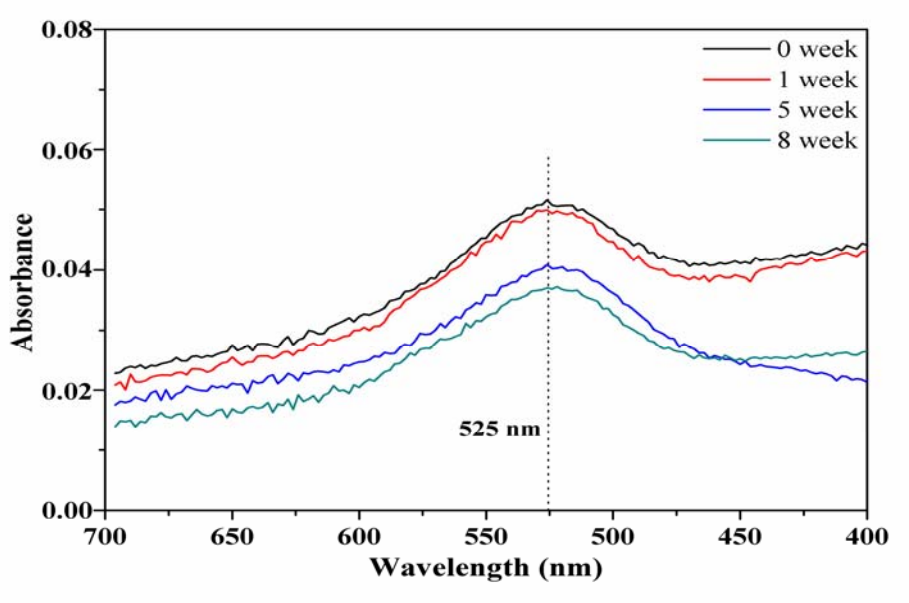

Figure 10. UV-vis spectra of extracted Au-NPs in chloroform at different time

3.2.2 Optimization of the Extraction Parameters

Parameters that affect the two-step extraction procedure of Au-NPs from aqueous phase into organic phase, such as the flow rate of the sample passing the column, the organic extractant, the nature and concentration of the ligand in the organic extractant, the ultrasonication time, the centrifugation speed, and the pH of the Au-NPs hydrosol source were studied.

3.2.2.1 Flow Rate of the Sample

The maximum flow rate of the samples passing the column that provides quantitative extraction efficiency was 3 mL/min. At higher flow rates, such as 6 or 9 mL/min, minor recoveries of 75% or 30%, respectively, were observed.

3.2.2.2 Extractants

Five different organic solvents namely chloroform, ethanol, methanol, n-hexane, and ethyl acetate, as well as mixtures of these solvents were tested for ligand-assisted extraction of Au-NPs from the RP-C18 material. For these experiments all other parameters were kept constant, i.e. concentration of DDT was 10 mmol/L, ultrasonication time 3 h, volume ratio of source to extractant was 1:1. Figure 11a presents UV-vis spectra of the resulting Au-NPs organosols in

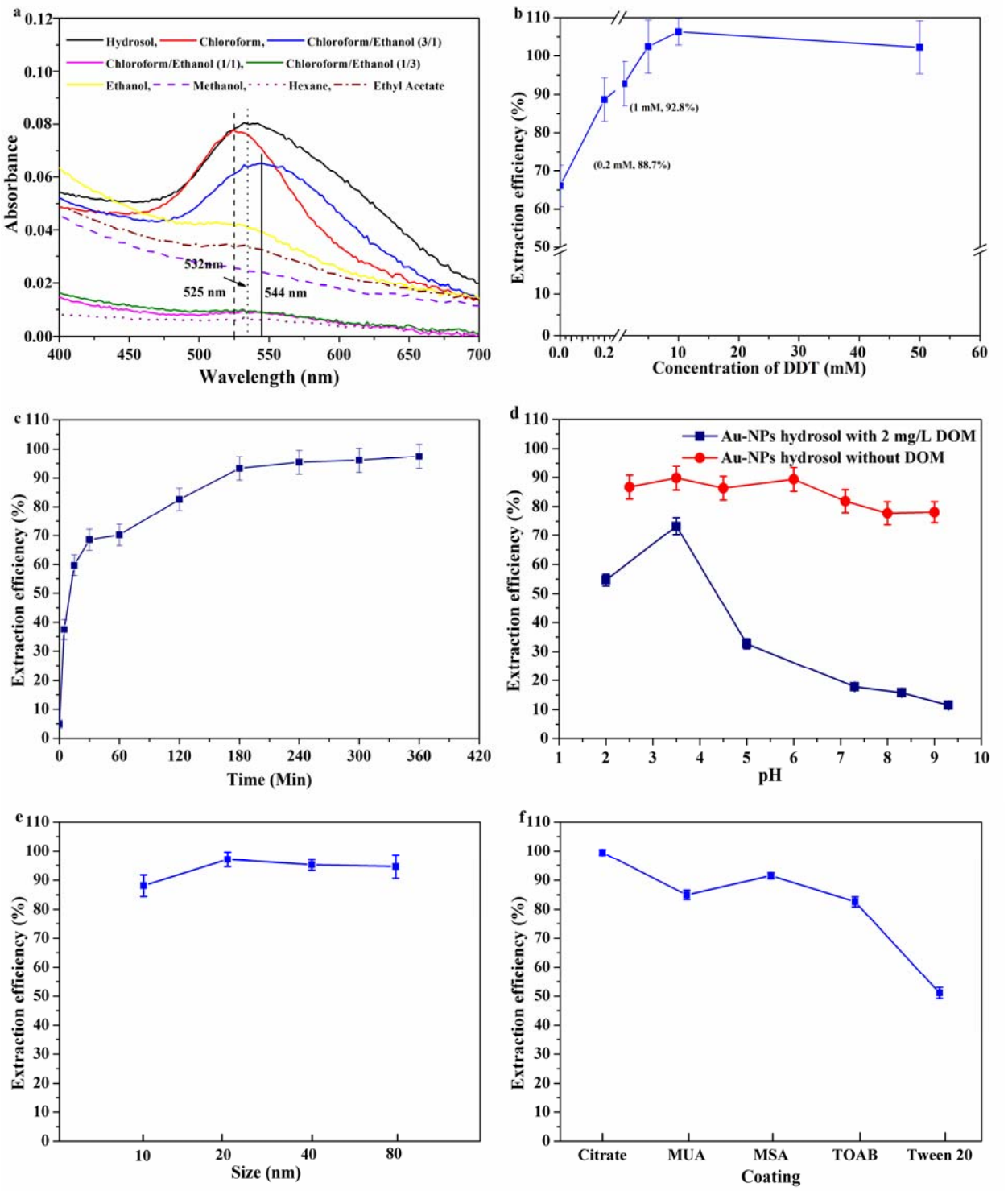

Figure 11. Parameters affecting the extraction efficiency of Au-NPs from hydrosol source. a) UV-vis spectra of extracted Au-NPs in different organic solvents and Au-NPs hydrosol. b) Effect of DDT concentration in chloroform on the extraction of Au-NPs. c) Effect of ultrasonication time on the extraction of Au-NPs. d) Effect of pH of Au-NPs hydrosol without and with DOM on the extraction of Au-NPs. e) Effect of Au-NPs' size on their extraction efficiency. f) Effect of Au-NPs' coating on their extraction efficiency

comparison to the Au-NPs hydrosol source. The most similar spectrum in regard to intensity and wavelength of the maximum is obtained by application of pure chloroform. No absorbance peak was observed after application of ethanol, methanol, n-hexane, ethyl acetate, 1:1 chloroform/ethanol, and 1:3 chloroform/ethanol mixtures. The spectrum of a 3:1 mixture of chloroform/ethanol shows a surface plasmon band peak maximum, however 12-nm red-shifted (Figure 11a). Apparently, addition of ethanol led to destabilization of the Au-NPs by aggregation, which has been observed for MNPs before [141]. Thus, among the tested organic solvents pure chloroform is the only effective extractant, capable of extracting and stabilizing Au-NPs. Notably, the Au-NPs chloroform organosol was observed to be stable for at least 2 months at 4 °C with little or no change in the extinction band position.

3.2.2.3 Nature and Concentration of Ligand

The efficiency of three different ligands, DDT, DDA, and ODT for extraction into chloroform was investigated. Best results were obtained by application of the sulfur-containing ligand DDT, followed by the results achieved with ODT, where application of about 10 times higher concentrations in the extractant was necessary to ensure efficient extraction; application of DDA requires about 200 times higher concentrations and causes Au-NPs aggregation. Hence, DDT was selected as ligand in all further extraction experiments. Figure 11b shows the extraction efficiency of Au-NPs depending on DDT concentration in chloroform. The presented efficiencies derive from the comparison of the concentration of Au-NPs in the initial source to that of the organosol determined by graphite furnace atomic absorption spectrometry (GFAAS). The efficiency clearly increases with higher DDT concentrations reaching quantitative transfer at a concentration of 5 mmol/L. In addition, UV-vis spectra of the resulting Au-NPs organosols all exhibit a peak at 524 nm (Figure 12), the intensity of which increases in a concentration-dependent and linear manner.

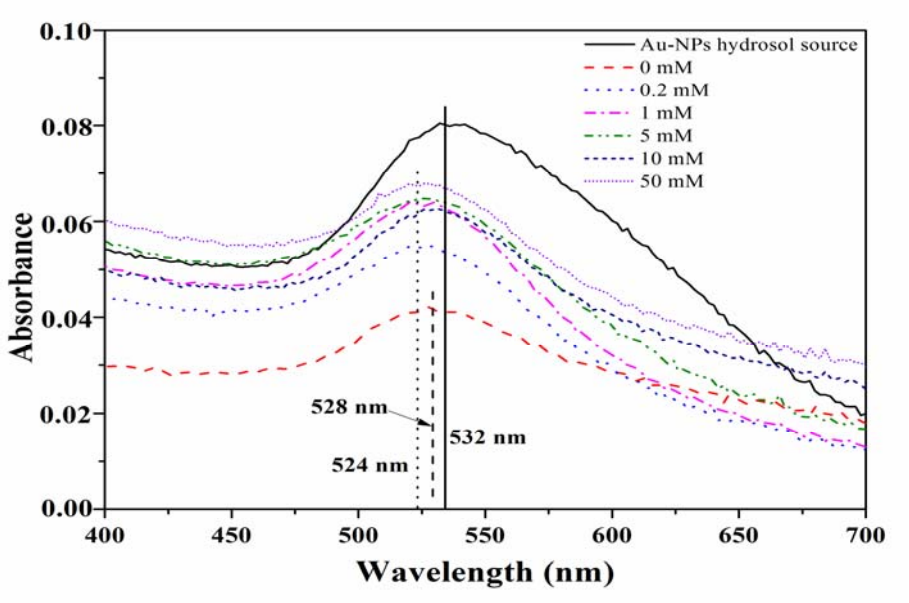

Figure 12. UV-vis spectra of Au-NPs (black solid line) in hydrosol source and (coloured dotted lines) in organosol after extraction, i.e. in chloroform with different concentrations of DDT

3.2.2.4 Ultrasonication Time and pH

Other factors taken into account for the optimization are the ultrasonication time and pH of the Au-NP hydrosol source. The effect of ultrasonication time was studied in the range of 0 to 360 min. As shown in Figure 11c, the extraction efficiency increases with time up to ultrasonication duration of 180 min. This result indicates that the extraction reaches equilibrium within 180 min, and more importantly, quantitative extraction is assured.

As shown in Figure 11d the pH of Au-NPs hydrosol has less effect on the extraction efficiency. Extraction rates all higher than 86% were achieved in a pH range from 2.5 to 6.0. In addition, lower efficiency was reached in a range of 7.1 to 9.0 (81% to 77%). pH values below 2.5 and above 9.0 were not tested in order not to exceed the limits of resistance for the RP-C18 material. In presence of dissolved organic matter (DOM) in the Au-NPs hydrosol, pH shows in contrast a significant effect on the extraction efficiency. The highest extraction efficiency was achieved at a pH of 3.5 (Figure 11d). Therefore, effects of DOM were studied in more detail and the results are presented in Figure 13 and are discussed below.

3.2.2.5 Centrifugation Speed

Separation of RP-C18 material from the Au-NPs organosol after ultrasonication was accelerated by centrifugation. However, potential losses of Au-NPs by agglomeration and sedimentation at high speed have to be avoided. Centrifugation speeds ranging from 1500 to 3500 rpm were tested. Quantitative Au-NPs recovery was obtained at maximum 2000 rpm.

In conclusion, the optimal conditions for the extraction and pre-concentration of Au-NPs from aqueous samples are summarised in Table 3.

Table 3. Optimal parameters and figures of merit for the two-step procedure for extraction and pre-concentration of Au-NPs from aqueous samples

Parameter	Set-up
Sample pretreatment [a]	Addition of 3% (v/v) H_2O_2 for 24 h
pH adjustment of sample [b]	4.5
Flow rate of the sample passing the column	3 mL/min
Organic extractant	Chloroform
1-DDT concentration in chloroform	5 mM
Ultrasonication time	180 min
Speed of centrifugation	2000 rpm
Initial sample volume	10 to 500 mL
Enrichment factor	1 to 250
Extraction efficiency	68.4 to 103.2%

[a] Only in samples with dissolved organic carbon concentrations >1 mg/L; [b] pH adjustment was achieved by stepwise addition of HCl or NaOH solution (0.5 mol/L), respectively.

3.2.3 Studying Effects of Sample Parameters on the Extraction Efficiency

In order to evaluate the robustness and limitations of the proposed method for Au-NPs separation and pre-concentration from environmental water samples the effects of the following sample parameters were studied: Size and coating of the Au-NPs in the hydrosol source, presence of other MNPs (Ag- and Pd-NPs), and presence of DOM.

3.2.3.1 Size and Coating of Au-NPs

In environmental samples a broad range of NPs' sizes are to be expected. Therefore, in addition to the self-prepared Au-NPs with an average diameter of 10.0 ± 0.6 nm the proposed method was tested using commercially available Au-NPs with four different sizes, i.e. 10, 20, 40, and 80 nm. In Figure 11e the extraction efficiencies for Au-NPs with different sizes are presented showing no significant differences and recoveries all higher than 88.1%. Hence, Au-NPs' size in a range from 10 to 80 nm does not have an influence on the proposed extraction method.

As a matter of fact, the nature of the coating of Au-NPs emitted to the environment depends on their initial application. Therefore, we have studied the extraction efficiency of Au-NPs modified with different surfactants, namely citrate, MUA, MSA, TOAB, and Tween 20, respectively. As shown in Figure 11f, the proposed method can extract and pre-concentrate citrate-coated Au-NPs with an efficiency of 99.5 ± 1.0%; MUA-, MSA-, and TOAB-coated Au-NPs are pre-concentrated in similarly high rates varying from 82.6 ± 1.7% to 91.5 ± 1.0%. A significantly lower efficiency of 51.1 ± 1.9% was observed with Au-NPs stabilised by Tween-20. This minor recovery resulted from inferior adsorption onto the RP-C18 material (1st step of the procedure); more than 46% of the Au-NPs were found in the run-off of the column.

3.2.3.2 Effect of Ag- and Pd-NPs in Au-NPs Hydrosol Source

Potential interferences from other MNPs in the recovery of Au-NPs and the applicability of the proposed method for separation and pre-concentration of these MNPs were studied. Here, Ag-NPs as the most commonly used MNPs in consumer products and Pd-NPs (emitted e.g. from car catalytic converters) as very thiophilic MNPs were exemplarily selected. Firstly, extraction efficiencies of Au-NPs in suspensions with a 1:1 mixture of Au- / Pd-NPs, Au- / Ag-NPs, and Au- / Ag- / Pd-NPs (1:1:1) were all higher than 92.6% (92.7 ± 0.9%, 91.8 ± 2.0%, 93.2 ± 1.3%, respectively, see Table 4). Secondly, the proposed procedure is also capable of separating and pre-concentrating Pd- and Ag-NPs from these mixtures with high efficiencies (Pd-NPs recoveries >92.0%, Ag-NPs recoveries >81.1%, see also Table 4). In conclusion, these results indicate the high potential of the proposed method for separation and pre-concentration of anthropogenic MNPs from waters.

Table 4. Recovery of MNPs from different mixtures [a]

Initial [MNPs] in the mixture (μg/L)			MNPs recovery (%)		
Au-NPs	Ag-NPs	Pd-NPs	Au-NPs	Ag-NPs	Pd-NPs
880	910	880	93.2 ± 1.3	85.9 ± 0.6	92.0 ± 1.7
980	1010	-	91.8 ± 2.0	81.1 ± 1.2	-
4050	-	4900	92.7 ± 0.9	-	94.9 ± 0.9

[a] Given uncertainties represent ± one standard deviation with n=3, P=95%.

3.2.3.3 Effect of Dissolved Organic Matter in Au-NPs Hydrosol Source

In environmental waters Au-NPs will be stabilised by interaction with natural ligands, such as DOM [142-144]. In this respect, the presence of DOM in the Au-NPs hydrosol source might be critical for the proposed extraction procedure. Hence, we studied the potential effect of DOM in an environmental relevant concentration range from 0 to 16 mg/L. As shown in Figure 13 increasing DOM concentration in the hydrosol significantly lowers the recovery of Au-NPs (dotted red line). Hence, as expected, DOM strongly interacts with the Au-NPs by surface adsorption blocking apparently DDT adsorption sites. Decreasing pH and/or increasing concentration of DDT is not effective enough to overcome this problem. However, as shown in Figure 13 (solid black line), the extraction efficiency was increased significantly when the DOM-containing Au-NPs hydrosol source was pre-treated by addition of 3% H_2O_2 at room temperature for 24 h. Obviously, no complete degradation of DOM can be achieved by this procedure, however, Au recoveries higher than 92.6 ± 5.1% were obtained up to a DOM concentration of 3.4 mg/L.

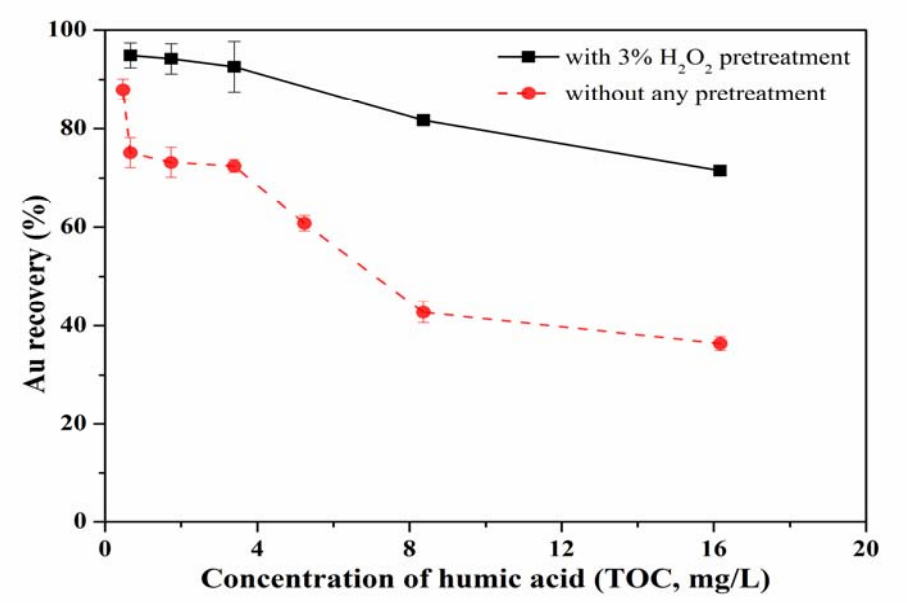

Figure 13. The effect of dissolved organic matter in Au-NPs hydrosol source on the recovery of Au-NPs: Dotted red line: without pre-treatment; Solid black line: After pre-treatment with 3% H_2O_2

3.3 Selectivity of Separation and Efficiency of Pre-concentration

In order to provide a method for pre-concentration of MNPs from natural aqueous samples especially separation from metal ions is required. Only then element selective detection methods are applicable for the quantification of metals present as MNPs. Hence, the two-step procedure was tested by application of an aqueous solution of $HAuCl_4$ instead of Au-NPs. After the first step more than 90% of the Au(III) ions were found in the run-off of the column. Furthermore, less than 3.5% of the adsorbed ions were extracted into DDT containing chloroform under ultrasonication in the 2nd step. Collectively, less than 0.35% of the total Au ions were transferred from the aqueous phase into chloroform by this approach. In other words, the proposed method has the potential to selectively extract and pre-concentrate Au-NPs even from an aqueous mixture containing Au ions.

As described above, comparison of the absorbance intensity in the UV-vis spectra of the Au-NPs hydrosol source and resulting Au-NPs organosol indicate quantitative extraction of the NPs (Figure 9b). However, the exact Au concentrations before and after the two-step extraction procedure were determined by GFAAS. The results obtained for different initial concentrations of Au-NPs are given in Table 5, confirming quantitative extraction rates of higher than 99.5% in all cases.

Table 5. Extraction efficiency of the two-step procedure and size of Au-NPs [a]

Spiked [Au-NPs] [b] (μg/L)	Enrichment factor	Detected [Au] (μg/L)	Recovery (%)	Extracted Au-NPs size [c] (nm)
4513.3 ± 12.6	1	4473.8 ± 44.5	99.5 ± 1.0	12.1 ± 0.8
9.7 ± 0.8	10	98.6 ± 2.9	101.6 ± 3.0	11.5 ± 0.8
0.15 ± 0.01	250	38.7 ± 1.4	103.2 ± 3.7	10.9 ± 0.9

[a] Given uncertainties represent ± one standard deviation with n = 3, P = 95%; [b] The size of Au-NPs spiked is 10.0 ± 0.6 nm; [c] The size of Au-NPs was calculated from several TEM images (n = 80).

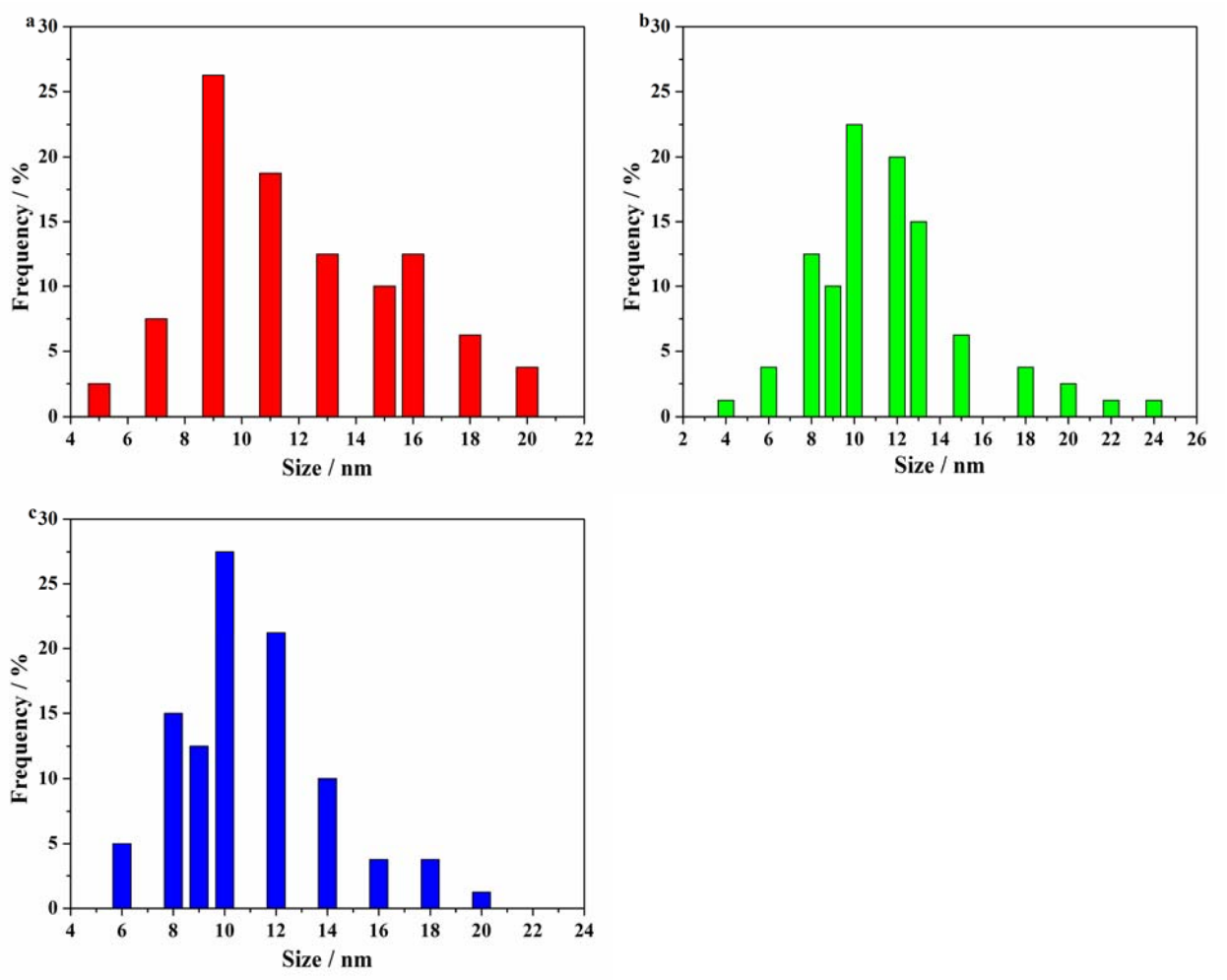

Figure 14. Size distribution of extracted Au-NPs in chloroform after two-step extraction (n = 80). a) The initial concentration of Au-NPs hydrosol is 4513 μg/L; b) The initial concentration of Au-NPs hydrosol is 9.7 μg/L; c) The initial concentration of Au-NPs hydrosol is 0.15 μg/L

Table 6. Investigation of real water samples spiked with Au-NPs

Sample [a]	Spiked [Au-NPs] (μg/L)	Enrichment factor	Detected [Au-NPs] [b] (μg/L)	Recovery (%)
	5100	1	4503.2 ± 43.0	88.3 ± 1.0
Tap water	10.20	10	101.3 ± 2.3	99.4 ± 2.6
filtered (0.45μm)	1.02	50	48.7 ± 0.6	95.5 ± 2.3
	0.15	250	35.1 ± 1.1	93.6 ± 2.9
	5100	1	4625.8 ± 88.2	90.7 ± 2.1
Tap water	10.2	10	100.7 ± 0.9	98.8 ± 1.0
unfiltered	1.02	50	46.6 ± 0.7	91.5 ± 1.2
	4500	1	4410.0 ± 34.9	98.0 ± 0.8
River water	8.22	10	65.8 ± 0.9	80.1 ± 0.9
filtered (0.45μm)	0.19	250	41.2 ± 1.5	86.7 ± 2.7
	4500	1	4419.0 ± 42.4	98.2 ± 1.0
River water	9.08	10	74.2 ± 1.1	81.7 ± 1.1
unfiltered	0.94	50	39.1 ± 0.2	83.2 ± 1.8
Lake water	8.81	10	74.9 ± 1.5	85.0 ± 1.6
filtered (0.45μm)	0.90	50	35.5 ± 1.0	78.8 ± 2.1
Lake water	8.80	10	71.7 ± 1.9	81.6 ± 2.2
unfiltered	0.90	50	36.5 ± 0.7	81.0 ± 1.4
Brook water	9.10	10	72.6 ± 2.4	79.9 ± 2.6
filtered (0.45μm)	0.83	50	29.0 ± 1.6	70.1 ± 3.7
Brook water	9.10	10	71.0 ± 1.1	78.2 ± 1.2
unfiltered	0.83	50	29.3 ± 0.8	70.8 ± 1.9
WWTP effluent	4.70	10	34.7 ± 1.4	74.0 ± 3.0
filtered (0.45μm)	0.94	50	33.8 ± 1.0	72.1 ± 2.2
WWTP effluent	4.70	10	32.9 ± 1.1	70.1 ± 2.4
unfiltered	0.94	50	32.1 ± 1.1	68.4 ± 2.3

[a] Characteristics of real samples are shown in the Table S3; [b] Given uncertainties represent ± one standard deviation with n=3, P=95%).

3.4 Preserving Size and Shape of the Au-NPs

Beside selective separation and efficient pre-concentration the most important issue for the procedure is the preservation of size and shape of the Au-NPs. Particle aggregation would lead to a red-shift and broadening of the plasmon band absorption [133,145]. Hence, a first indication of similar size of the NPs before and after the two-step extraction procedure gives the UV-vis spectra shown in Figure 9b. Here, a slight blue-shift of 7 nm in the wavelength of the surface plasmon band peak maximum is observed in the organosol in comparison to the hydrosol source. This shift may arise from the combined effect of the change in refractive index of the solvent medium [133] (from 1.446 in water to 1.334 in chloroform) and adsorption of DDT onto Au-NPs surface, as confirmed by IR spectroscopy (Figure 9c). This conclusion is further supported by TEM investigation of the Au-NPs before and after extraction. The obtained results confirm no change in particle size and shape, i.e. spheres of 10 to 15 nm in size were observed (see Table 5, Figures 14 and 24c).

3.5 Application to Real Water Samples

The feasibility of the proposed approach was evaluated by application of the optimized procedure to five real water samples, namely tap, river, lake, and brook water, as well as to an effluent of a WWTP, spiked with Au-NPs in a concentration range from 0.15 - 5100 µg/L. Models predicting Au-NPs concentrations in environmental waters estimate contents of 0.14 µg/L to be found within the next 10 years due to their broad application in electronics and medical diagnosis [146]. Hence, spiking of the samples was performed within a reasonable concentration range. All samples were investigated without and after filtration through a 0.45 µm filter in order to check whether naturally occurring particles might interfere with the procedure.
Table 6 summarises the Au-NPs recoveries obtained for 5 real water samples ranging from 68.4 ± 2.3% to 99.4 ± 2.6%. No significant differences between recoveries for filtered and unfiltered samples were observed, which seems reasonable since all investigated water samples had very low particulate matter content (<1 mg/L). Interferences from naturally occurring dissolved compounds in the real waters were observed in the effluent from the WWTP leading to significantly lower recoveries ranging from 68.4 to 74.0%. This water has obviously the most

complex matrix among the studied samples. Totally, the results suggest that the proposed method is capable of quantitatively extracting and pre-concentrating Au-NPs from natural water samples.

3.6 Conclusions

This work demonstrates the successful extraction and concentration of Au-NPs in a size range from 10 to 80 nm from water samples by means of solid phase extraction followed by ligand-assisted liquid extraction. The two-step procedure uses RP-C18 as solid phase and 5 mmol/L of DDT in chloroform for most effective re-extraction. An enrichment factor as high as 250 was obtained and recovery studies in model solutions (recoveries: 99.5 - 103.2%) as well as in real waters (recoveries: 68.4 - 99.4%) confirm the feasibility of this approach. Selectivity in regard to chemical species was given, since separation from ionic gold species was provided. The presence of other MNPs, namely Ag- and Pd-NPs, did not interfere the proposed procedure. Moreover, Ag- and Pd-NPs were also separated from aqueous suspensions in high yields, which indicates a high potential for application of the approach to other MNPs. Interferences occurring in presence of dissolved organic matter up to a concentration of 3.4 mg/L can be overcome by pre-treatment with hydrogen peroxide, which does not affect the extraction procedure. Moreover, preservation of size and shape of the Au-NPs after application of the novel approach was proved by UV-vis and TEM analysis of the NPs suspension. Effects resulting from different coatings of the original Au-NPs were observed with Tween-20, a non-ionic dendritic surfactant with a high molecular weight. Here, non-quantitative adsorption onto the RP-C18 was observed leading to minor recoveries from the spiked water sample. Future investigation will have to further enlighten the role of different initial NPs' coatings and their stability under environmental conditions, i.e. their relevance to proposed analytical procedures. Thereby also natural "coating" by e.g. DOM will have to be considered in more detail. Hence, application and optimisation of this approach to a broader variety of water matrices and for extraction and concentration of other MNPs from environmental waters are currently undertaken.

4 Ligand-Assisted Solid(IRN-78)-Liquid Extraction of NMNPs for Separation and Pre-concentration of NMNPs from Water

4.1 General Procedure for the Ligand-Assisted Solid(IRN-78)-Liquid Extraction

In this work, we developed another novel ligand-assisted solid-liquid extraction method for separation and pre-concentration of NMNPs from water samples. An anionic exchange resin, Amberlite IRN-78, was used in the present study. This resin contains positively charged ammonium groups. As illustrated in Figure 15, mercaptosuccinic acid (MSA) (molecular formula: $C_4H_6O_4S$, pK_{COOH}: 3.30 and 4.94), a bifunctional ligand, was used to bind to the surface of the NMNPs through its thiol group, with its two carboxylic acid groups exposed to the medium. Previous studies have shown that the carboxyl group tends to be deprotonated (negatively charged) in a basic environment (pH > 7) [147]. The MSA-modified NMNPs therefore were loaded onto the resin directly due to the electrostatic interaction of the positively charged amino groups from the resin with the negatively charged carboxylic acid groups from the MSA ligands (steps 1, 2 and 3 in Figure 15). The successfully adsorbed NMNPs were then completely extracted using a solution of 8% (v/v) formic acid in methanol with gentle shaking at room temperature (step 4). The resin can be reused after consecutive conditioning with 5% (v/v) hydrochloric acid and 5% (v/v) sodium hydroxide solution (step 5).

4.2 Mechanism of Ligand-Assisted Solid(IRN-78)-Liquid Extraction

Once the MSA-modified NMNPs are loaded onto the resin, they can not be eluted from the resin using sodium hydroxide (0.75 mol/L), sodium bicarbonate (1.0 mol/L) and even hydrochloride acid (0.75 mol/L) solutions. Moreover, some of the eluting agents facilitate subsequent aggregation of NMNPs in the effluent and hence were not used. Only the organic weak acid formic acid in methanol can elute the NMNPs from the resin. Moreover, the quantitative extraction was performed under gentle shaking at room temperature.

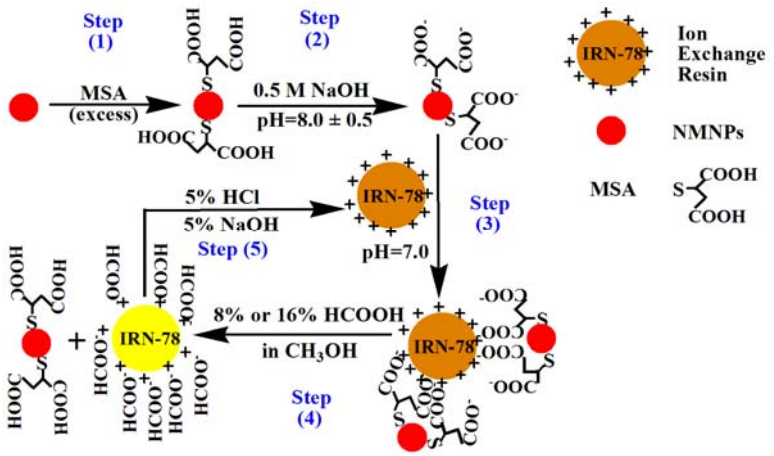

Figure 15. Effective separation and extraction of NMNPs by a noncovalent reversible reaction on an ionic exchange resin. Separation: steps (1), (2) and (3); Extraction: step (4); Regeneration: step (5)

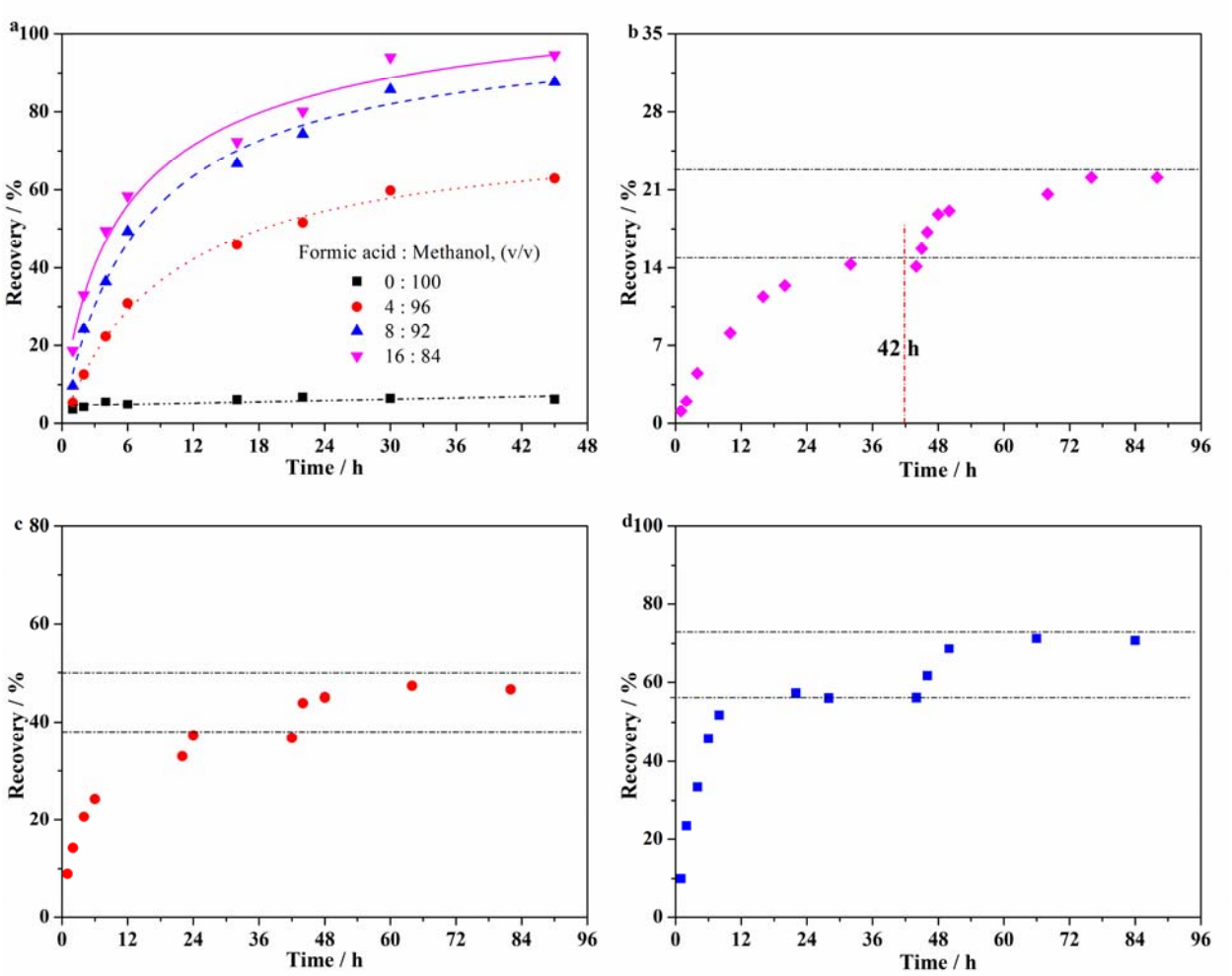

Figure 16. a) Time progress of cleavage reactions of adsorbed MSA-modified Pd-NPs with different concentrations of formic acid. The initial concentration of Pd-NPs hydrosol is lower than 100 μg/L. b-d) Chemical cleavage reaction of adsorbed MSA-modified NMNPs by 8% formic acid in methanol. The initial concentration of NMNPs is 1 mg/L. After 42 h, a second equivalent of 8% formic acid in methanol was added. b) Pd-NPs. c) Au-NPs. d) Ag-NPs

Figure 16a presents the time progress of cleavage reactions of adsorbed MSA-modified Pd-NPs with formic acid, where the formic acid/methanol (v/v) ratio ranges from 0:100 to 16:84. The cleavage reaction proceeds in a progressive manner over 45 h, and reaches a maximum depending on the formic acid/methanol ratio. This result indicates that the H^+ plays a key role in extracting NPs from the resin. In addition to that, Figure 16b provides additional evidence that the extent of extraction depends on the amount of acid used for the reaction. When studying the extraction step, we observed that addition of a second equivalent of formic acid to a reaction whose conversion had already reached a limiting value results in additional conversion. Similar results were also obtained for Ag- and Pd-NPs (Figure 16c and 16d). Totally, for the quantitative extraction of Pd-NPs, 16% of formic acid in methanol was required, whereas for Au- and Ag-NPs 8% formic acid in methanol was applicable. This can be explained by the different sizes of NPs; Pd-NPs (6.5 ± 1.2 nm) are significantly smaller, providing more surface area at similar concentrations than the Au-NPs (10.0 ± 0.5 nm) and Ag-NPs (17.2 ± 0.5 nm). Hence more MSA molecules are bound to the Pd-NPs.

Although the H^+ concentration plays a key role in extracting NMNPs from the resin, the exact mechanism for extraction of MSA-modified NMNPs is still intriguing at this stage. Consequently, the composition of the extracted NMNPs was analyzed by energy dispersive x-ray fluorescence (EDX) and infrared (IR) spectroscopy. The EDX of extracted Ag-NPs suspension in Figure 17a reveals the presence of sulphur from MSA ligand, which indicates the MSA might still bind onto the surface of the Ag-NPs through their SH group. Furthermore, the IR spectrogram of the extracted Ag-NPs suspension shows in comparison to the formic acid an additional peak at 1466 cm^{-1} corresponding to CH_2 bond (Figure 17b), which confirms the finding from EDX analysis. In addition, as shown in Figure 17c and 17d, the toluidine blue O (TBO) adsorption peak at about 633 nm was observed in the UV-vis spectra of the extracted NPs, indicating the presence of carboxylic group of MSA on the surface of extracted NPs.

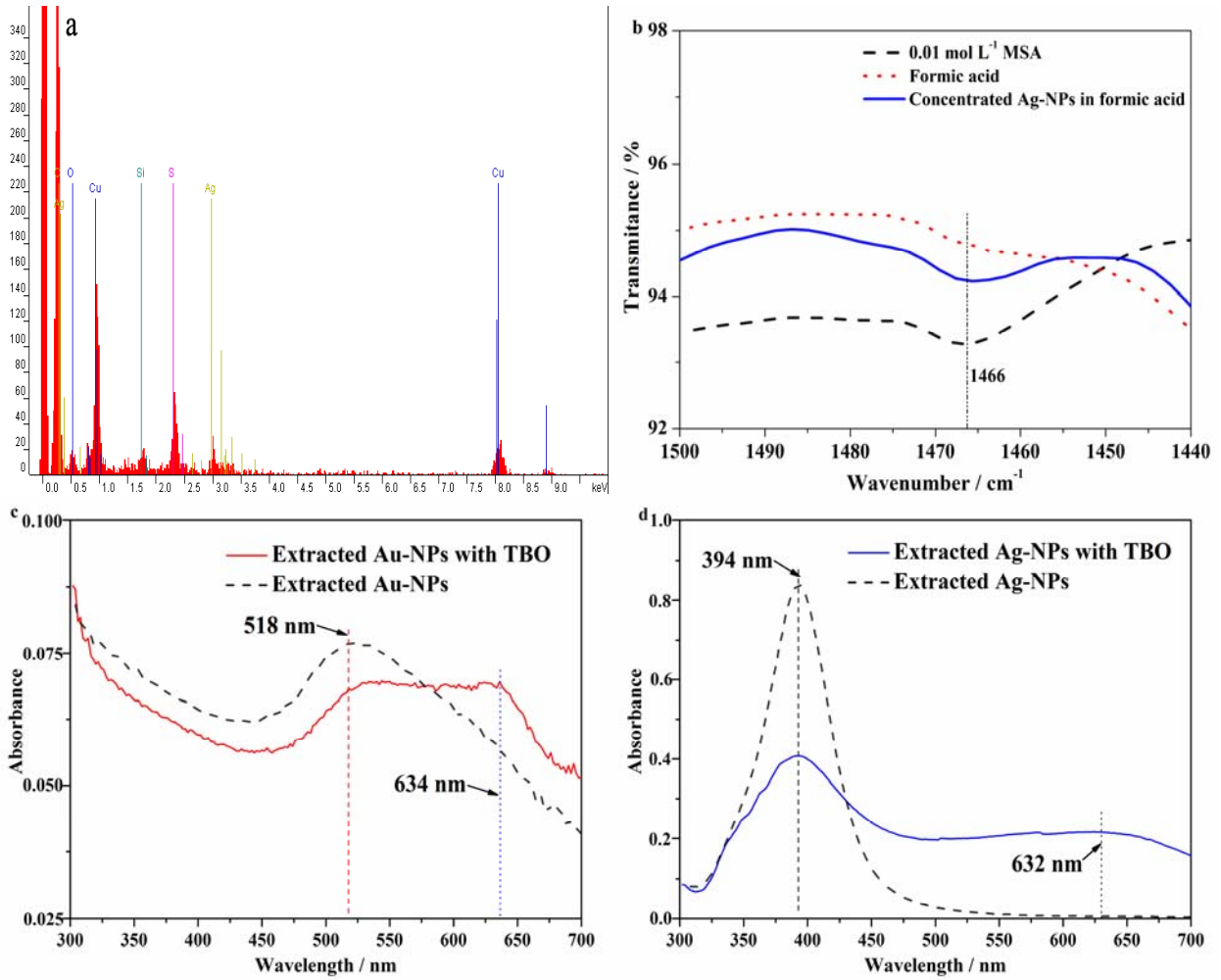

Figure 17. a) EDX spectrum of the extracted Ag-NPs. b) IR spectrogram of the extracted Ag-NPs. c) and d) UV-vis spectra of extracted Au-NPs and Ag-NPs without and with TBO analysis

4.3 Optimization of the Extraction Method for Separation and Pre-concentration of NMNPs from Water

Before the extraction of NMNPs at environmental levels (*i.e.*, in ng/L range) was examined, the feasibility of this procedure was investigated at high concentrations (*i.e.*, in mg/L and µg/L range). As shown in Figure 18, the UV-vis absorbance of NMNPs (2 mg/L) solution is decreased considerably after passing through the column filled with resin. Moreover, the concentrations of NMNPs in the run-off of the column were measured by GFAAS, where typically traces of Au, Ag and Pd were found, respectively. Meanwhile, the increase of pH and decrease of zeta potential are observed in the run-off in comparison to the initial NPs solution (Table 7). These indicate the effective adsorption of MSA-modified NMNPs from water onto the resin due to the

electrostatic interaction between carboxyl and amino groups. In addition to that, we found a clear trend of increasing separation efficiency with decreasing flow rate; in the case of Au-NPs, the average separation rate increased from 70 to 97% with the flow rate decreasing from 2.5 to 1.5 mL/min. Similar results were also obtained for Ag-NPs and Pd-NPs; the separation efficiencies of Ag-NPs and Pd-NPs reached 93 and 87% respectively when the flow rate was 1.5 mL/min. Therefore, a flow rate of 1.5 mL/min was selected for further studies.

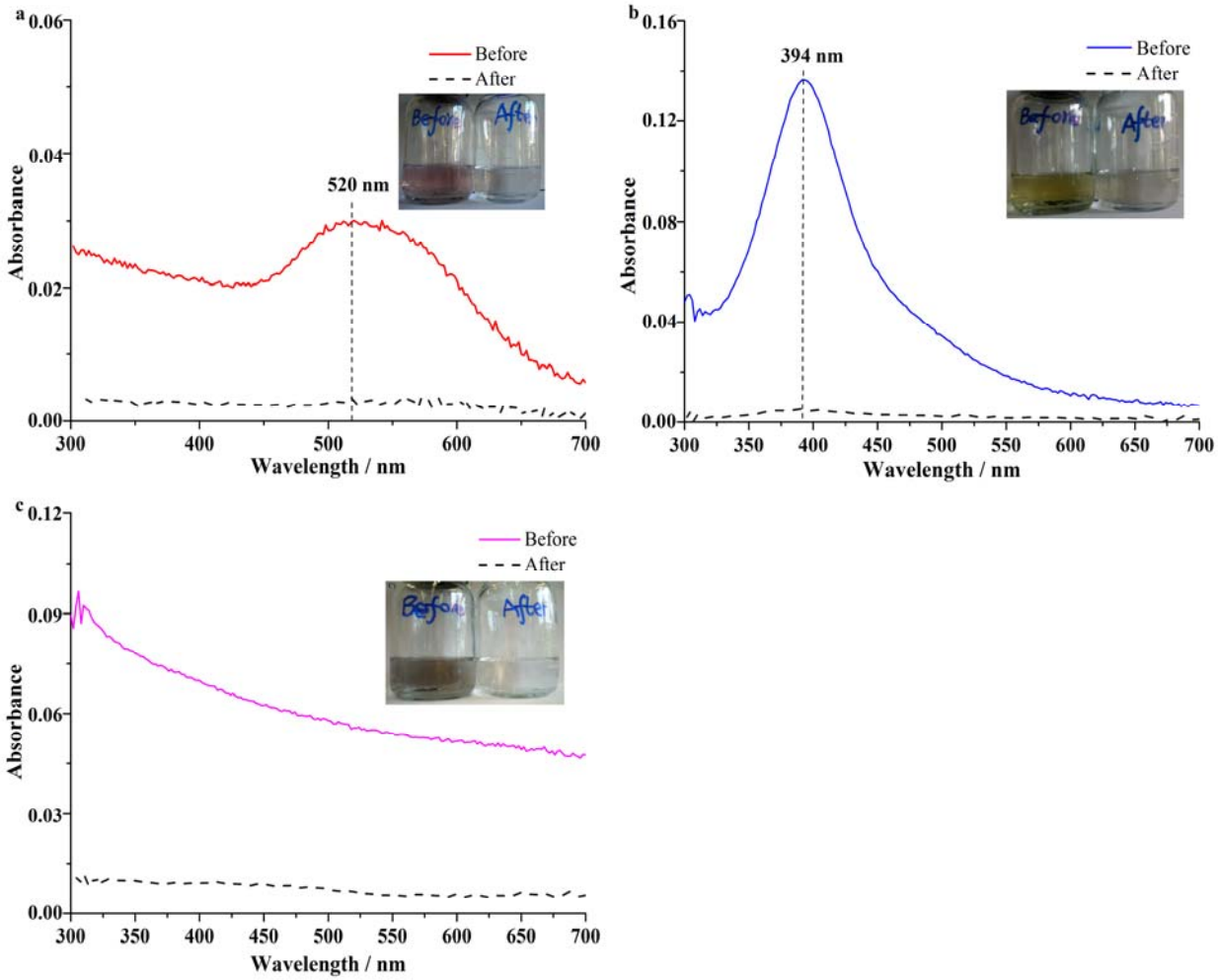

Figure 18. UV-vis spectra of the MSA-modified NMNPs aqueous solution measured before and after adsorption of NPs onto the resin. Inset: visual appearance of samples before and after adsorption. a) Au-NPs, b) Ag-NPs, and c) Pd-NPs

Table 7. The changes in pH and Zeta potential before and after NPs passing through the column with resin

NPs	pH			Zeta potential (mV)		
	Initial hydrosol	Before loading	After loading	Initial hydrosol	Before loading	After loading
Au	2.50 ± 0.20		11.46 ± 0.16	-22.8 ± 0.8	-33.3 ± 3.4	-37.2± 0.8
Ag	7.60 ± 0.02	8.00 ± 0.50	11.72 ± 0.05	-21.5 ± 0.9	-23.8 ± 1.5	-27.3 ± 2.1
Pd	8.21 ± 0.04		11.87 ± 0.09	-16.0 ± 1.5	-29.0 ± 2.7	-35.1 ± 2.5

With the proposed procedure an enrichment factor of up to 232 was obtained when the initial concentration of NPs was as low as 100 ng/L (Table 8). However, in environmental waters, NPs will be stabilized by interaction with natural ligands, such as DOM. In this respect, the presence of DOM in the NPs solution might be critical for the proposed extraction procedure. The DOM at a concentration of 2 mg/L in the initial NPs hydrosol has no effect on the separation and concentration of NPs. As a matter of fact, the nature of the coating of NPs emitted to environment depends on their initial application. Therefore, we also studied the extraction of NMNPs stabilized with citrate, PVP10, PVP40 and TOAB, respectively. As shown in Table 9, this method can extract citrate-stabilized NPs with an efficiency of 105.0 ± 2.4%, and PVP10- and TOAB-stabilized NMNPs are extracted in similarly high rates varying from 85.0 ± 1.6% to 103.7 ± 1.8%. However, a significantly lower efficiency was observed with NMNPs stabilized by PVP40 (< 36.3 ± 1.7%).

Table 8. Extraction of NMNPs through the proposed method

NP	Initial NPs (μg/L)	Separation efficiency (%)	Concentrated NPs (μg/L)	Recovery (%)	Enrichment
Au	41.0	97.6 ± 1.1	8487.5 ± 88.4	105.0 ± 2.4	207 ± 2
	0.1	>97	23.2 ± 0.9	94.7 ± 3.9	232 ± 9
Ag	43	93.0 ± 1.5	8680 ± 184	107.4 ± 4.0	202 ± 4
	0.1	>93	22.9 ± 1.1	97.5 ± 4.1	229 ± 11
Pd	83.6	87.1 ± 1.4	15690 ± 303	106.6 ± 3.5	188 ± 4
	0.11	>87	21.7 ± 1.1	89.8 ± 3.8	197 ± 10

In order to provide a method for extraction of NMNPs from natural aqueous samples, especially separation from metal ions is required. Only then, element selective detection methods are applicable for the quantification of metals present as NPs. As shown in Table 10, the recoveries of NPs are more than 96.4 ± 2.2%, while less than 10% of the corresponding metal ions are recovered, indicating that this method has the potential to selectively extract and concentrate NMNPs even from a mixture containing the NMNPs and corresponding metal ions.

Table 9. Effect of different coatings on the proposed method

NMNPs	Coating	Separation efficiency (%)		Recovery (%)	
		Without MSA	With MSA	Without MSA	With MSA
Au	Citrate	41.5 ± 2.9	97.6 ± 1.1	29.7 ± 4.5	105.0 ± 2.4
	PVP10	35.9 ± 1.7	98.3 ± 0.8	32.5 ± 2.7	95.5 ± 1.1
	PVP40	29.2 ± 0.9	90.2 ± 2.1	33.2 ± 5.2	36.3 ± 1.7
	TOAB	42.5 ± 1.3	99.5 ± 1.5	40.5 ± 2.8	88.6 ± 2.0
Ag	Citrate	35.7 ± 2.5	93.0 ± 1.5	31.2 ± 3.9	107.4 ± 4.0
	PVP10	37.9 ± 2.0	95.0 ± 0.9	38.7 ± 1.7	103.7 ± 1.8
	PVP40	30.1 ± 1.9	97.1 ± 0.8	32.8 ± 2.9	15.4 ± 2.5
	TOAB	38.6 ± 3.1	89.9 ± 1.3	40.2 ± 3.1	85.0 ± 1.6
Pd	Citrate	32.7 ± 2.1	87.1 ± 1.4	36.9 ± 0.8	106.6 ± 3.5
	PVP10	40.5 ± 2.9	86.6 ± 2.7	36.8 ± 3.0	92.4 ± 3.5
	PVP40	26.8 ± 5.7	89.1 ± 1.1	31.5 ± 4.1	15.3 ± 2.9
	TOAB	37.8 ± 2.4	90.3 ± 2.1	38.9 ± 2.9	88.6 ± 4.1

Table 10. Recovery of NMNPs in comparison to corresponding ions using the proposed method

Element	Concentration (µg/L)		Concentration (µg/L)		Recovery (%)	
	Spiked NPs	Spiked ions	Extracted NPs	Extracted ions	NPs	Ions
Au	80	10	77.1 ± 1.8	< 1.0 [a]	96.4 ± 2.2	< 10
Ag	80	10	81.4 ± 1.0	< 0.5 [b]	101.8 ± 1.3	< 5
Pd	80	10	81.6 ± 2.0	< 0.5 [c]	102.0 ± 2.5	< 5

4.4 Regeneration of the Ion Exchange Resin

For regeneration of the ion exchange resin the $HCOO^-$ ions were exchanged with Cl^- and then replaced by OH^- without any significant change of the resin by reaction with aqueous HCl and NaOH solution sequentially. Figure 19 shows scanning electron microscopy (SEM) images of the resins surface at the different stages. Therefore, the present results show that the resin can be used repeatedly. Good reusability of resin had also been demonstrated by the second time extraction; the regenerated resin yielded good performance with separation efficiencies of NMNPs > 80%, as well as recoveries > 70%.

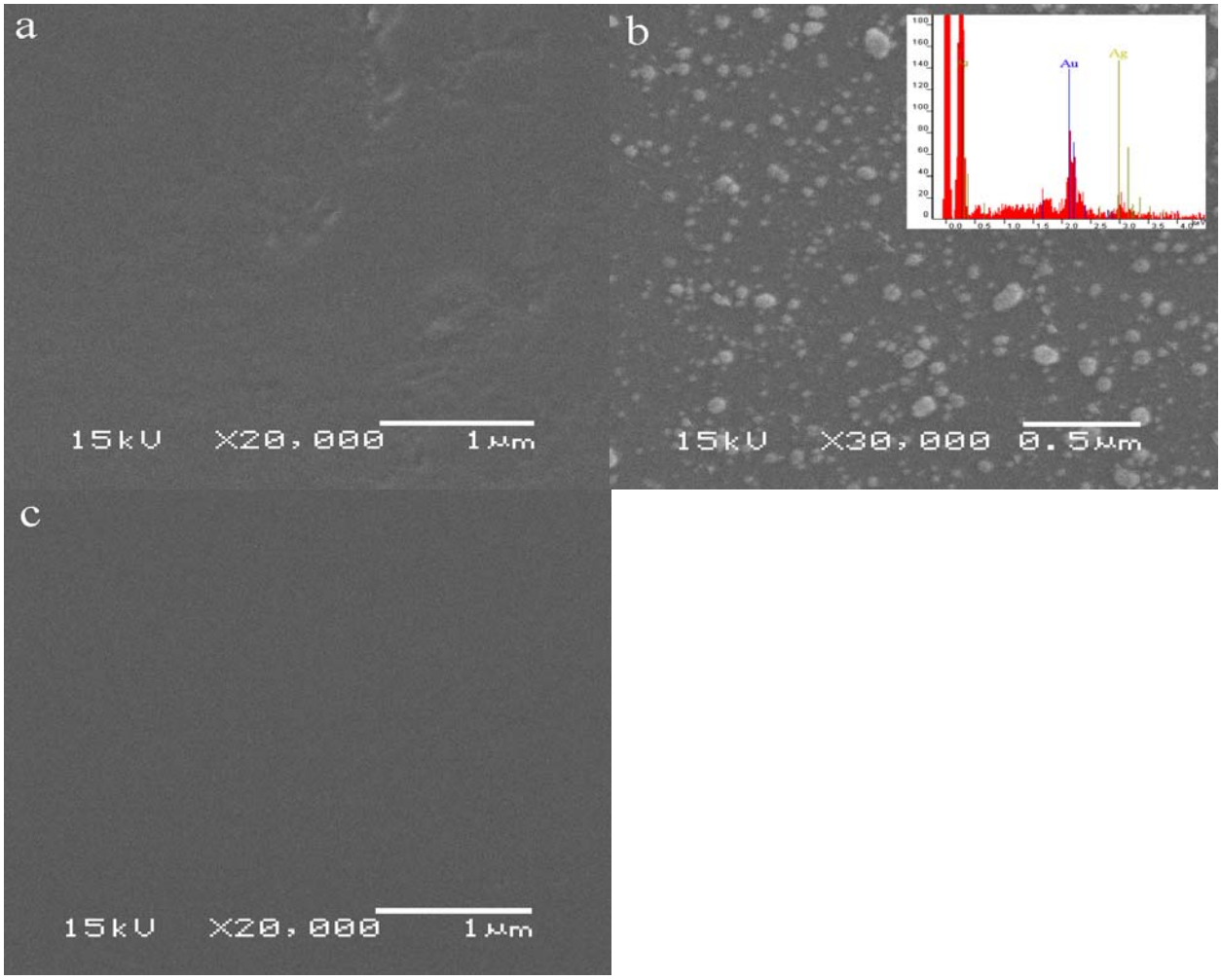

Figure 19. SEM images of the resin's surface. a) New resin, b) MSA-modified Ag-NPs adsorbed onto resin, Inset: EDX spectrum, and c) Regenerated resin's surface

4.5 Preserving Size and Shape of the NMNPs

It is well known that NPs aggregate very easily by coagulation due to their high surface reactivity and large surface area. Consequently, to preserve their original size and shape throughout separation and pre-concentration is an important issue. The TEM measurements to characterise the size distribution of the NPs (250-600 particles per metal) before and after the proposed procedure was performed. The results are presented in Figure 20 confirming that no significant changes in particle size and shape occur.

4.6 Application to Real Water Samples

To further evaluate the applicability of the proposed method to real natural waters, three different real environmental water samples (Donau river, Starnberger lake, and brook; Characteristics are shown in chapter 7 Table 20) were tested by spiking 90, 80 and 130 ng/L Au-, Ag-, and Pd-NPs, respectively. As shown in Figure 21, the obtained recoveries of Au-, Ag- and Pd-NPs are all higher than 65.6 ± 3.7%, 69.1 ± 2.3% and 81.0 ± 1.3% respectively, which is satisfactory with regard to the low spiking level. Moreover, the corresponding enrichment factors of Au-NPs, Ag-NPs and Pd-NPs can reach 132, 138 and 163, respectively.

4.7 Conclusions

In this study, we present a new method to effectively and selectively extract Au-, Ag- and Pd-NPs at ng/L level from real environmental water (river/lake/brook) through the noncovalent reversible adsorption onto an ionic exchange resin. In addition, preservation of size and shape of these NPs after application of the method was proved by TEM analysis of the concentrated NPs suspension. The electrostatic adsorption onto resin is reversible so that the resin can be reused for the extraction of NPs.

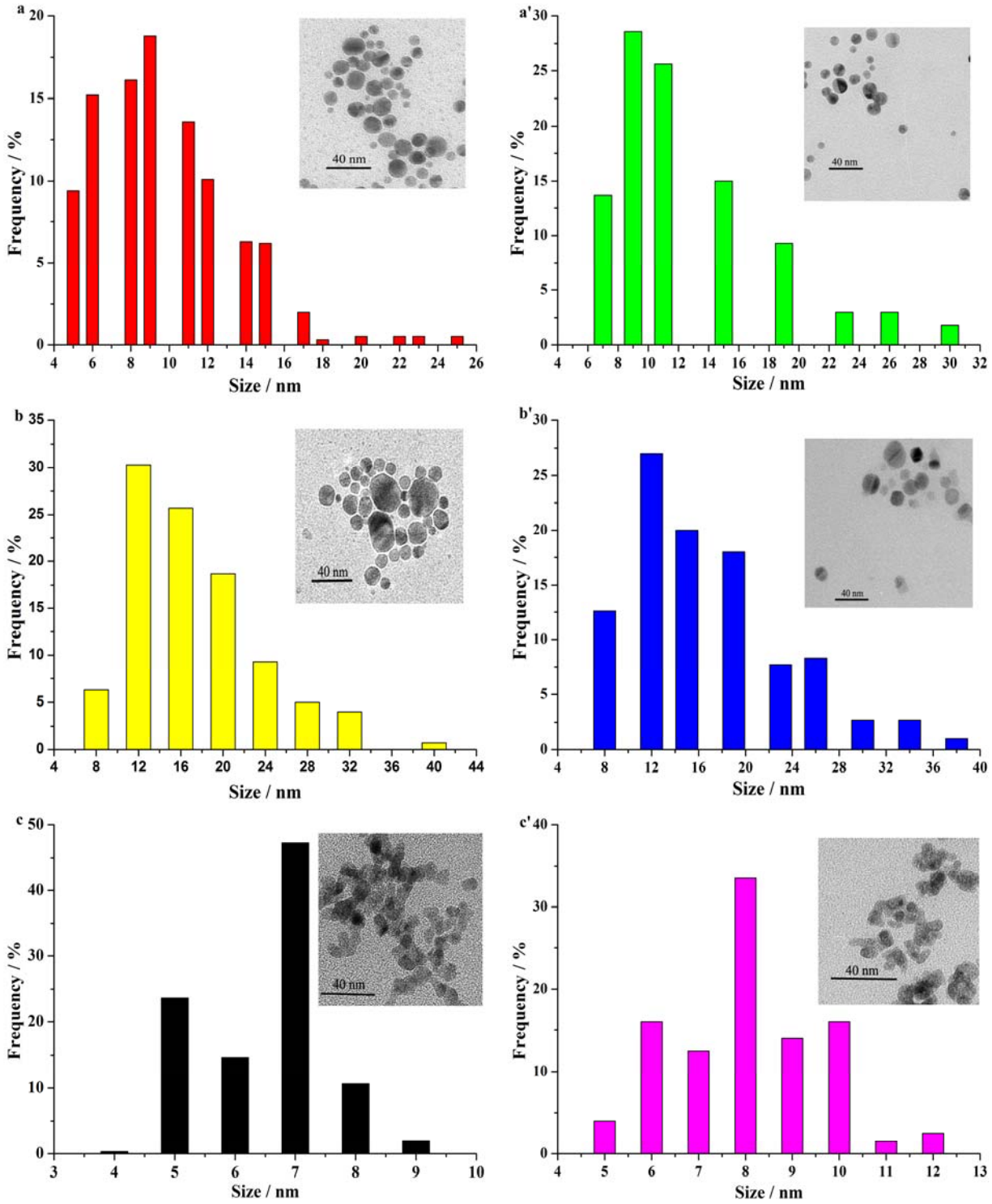

Figure 20. Size distribution of the NPs before (a, b, and c) and after (a', b' and c') the separation and extraction. Inset: TEM images of original and extracted samples. a and a') Au-NPs, b and b') Ag-NPs, and c and c') Pd-NPs

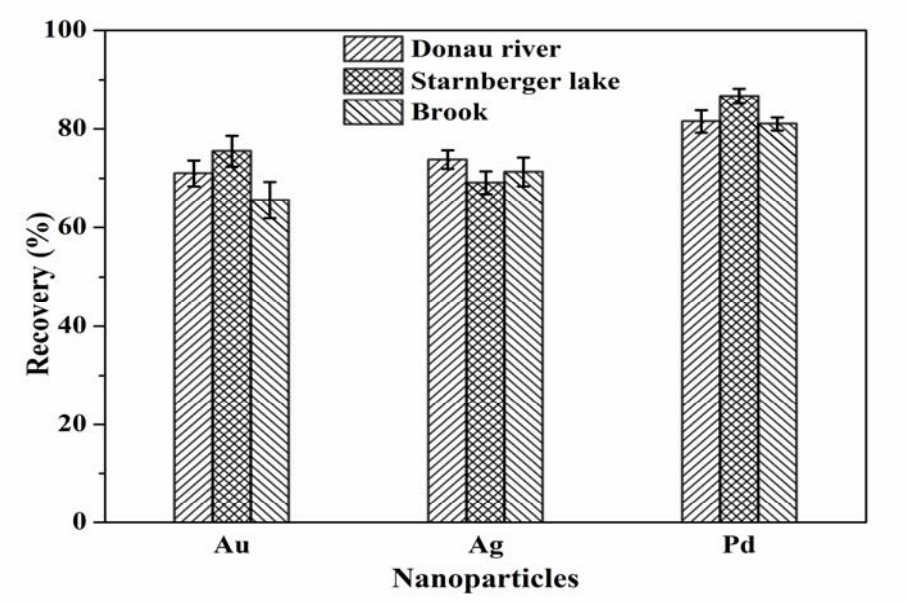

Figure 21. Recovery of NMNPs spiked in environmental water by the proposed method. The spiked concentrations of Au-NPs, Ag-NPs and Pd-NPs are 90, 80 and 130 ng/L, respectively

5 Quantification of Nanoscale Silver Particles Removal and Release from Municipal Wastewater Treatment Plants

5.1 Solid(IRN-78)-Liquid Extraction of Ag_2S-NPs from Water

As is the case for most other ENPs like TiO_2-NPs [44,45], the majority of Ag-NPs in consumer products will be likely released into sewer systems [43,46,47]. Municipal WWTPs therefore act as the 'gateways' controlling release of ENPs from domestic and/or industrial sources to aquatic environment via treated effluent which is discharged into surface waters. Numerous studies have shown that Ag-NPs entering wastewater treatment process are mostly sulfidized, which gives rise to the occurrence of silver mainly as Ag_2S-NPs in WWTPs. For example, Kim et al. [148] discovered the presence of Ag_2S-NPs in sewage sludge. In addition, based on batch bioreactors in laboratory, a general conclusion from previous investigations on Ag-NPs removal is that about 90% spiked Ag-NPs are efficiently removed from wastewater by biological treatment, and accumulated in activated sludge or biosolids as a form of Ag_2S [46,148-152].

Although the solid(IRN-78)-liquid extraction method has been proven to selectively and efficiently extract the Ag-NPs from water (Chapter 4), the feasibility of extracting Ag_2S-NPs from water by the proposed method is still unclear. Consequently, we investigated whether and to what extent the proposed method extracts Ag_2S-NPs from water. On the basic of these results, we quantified the nanoscale silver particles (n-Ag-Ps including Ag-NPs and Ag_2S-NPs) in field-collected wastewater, and further determined the relative contribution of biological treatment to n-Ag-Ps removal compared to mechanical treatment. Finally, we estimated the daily n-Ag-Ps load entering water environment through effluent discharge.

5.1.1 Optimization of the Extraction Procedure

Given the various extents of Ag-NPs sulfidation in environment [148,153], we prepared Ag_2S-NPs with four different ratios of Ag to S. As shown in Figure 22a, the sulfidation extent has no impact on the extraction efficiencies, indicating that the IER method can be applied to extract Ag_2S-NPs with varied ratios of Ag to S. In addition, we verified that the extraction time

clearly increased with higher initial concentrations of Ag_2S-NPs (Figure 22b). For Ag_2S-NPs concentrations below 10 μg/L, the extraction efficiency reached the maximum (～100%) within 4h and then levelled off, which is in good agreement with the case of Ag-NPs in our previous study [154]. Hence, the extraction time of 4h was selected in the present study.

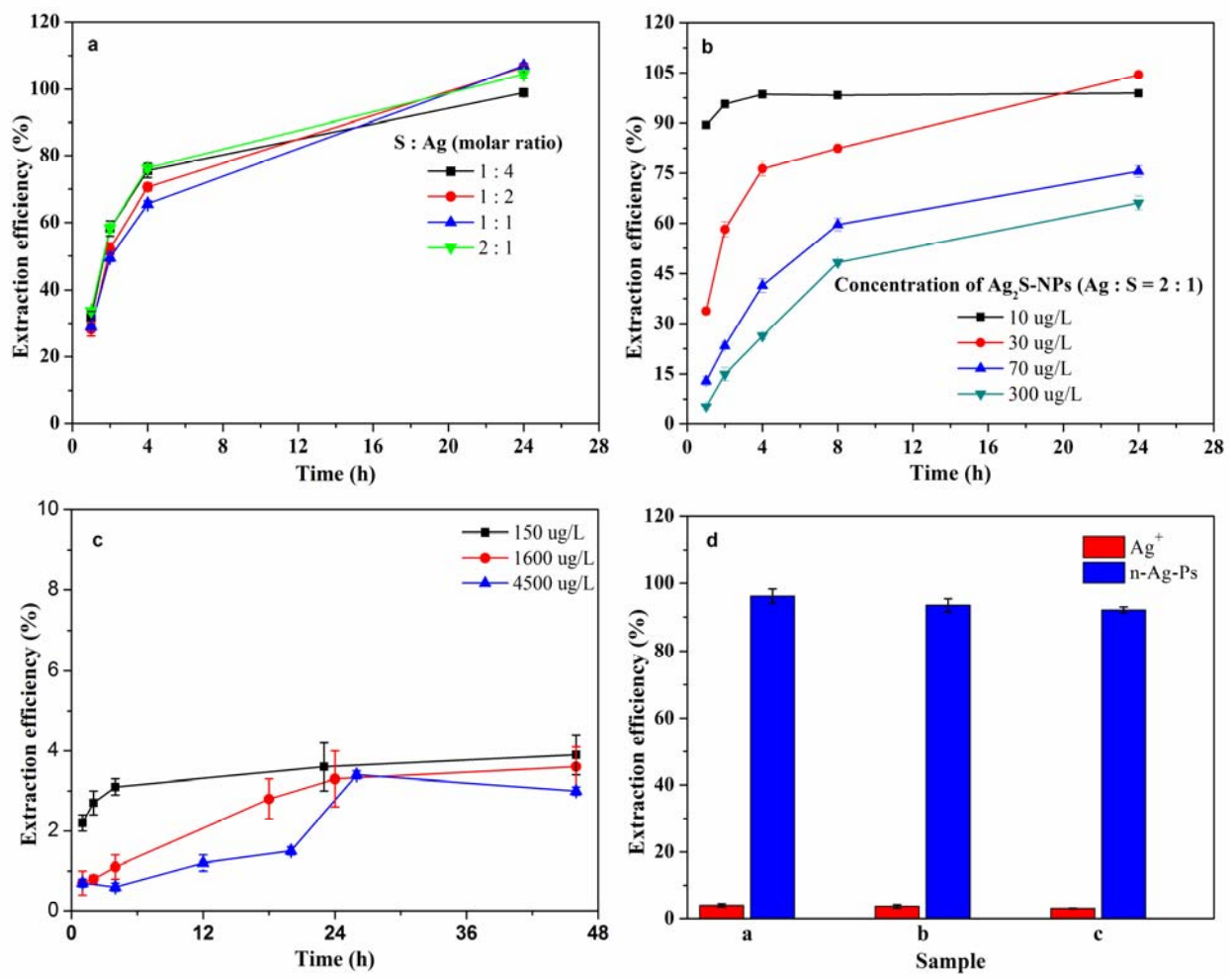

Figure 22. Optimization of the solid(IRN-78)-liquid method for n-Ag-Ps extraction. a) The effect of the S to Ag ratio on the extraction of Ag_2S-NPs (concentration: 30 μg/L). b) Effect of Ag_2S-NPs concentration on the extraction efficiency. c) Extraction of Ag ions as a function of time by the solid(IRN-78)-liquid method. d) Selective extraction of n-Ag-Ps versus Ag^+ using solid(IRN-78)-liquid method

5.1.2 Selective Extraction of Ag_2S-NPs versus Ag^+ ions

Due to the release of Ag^+ from Ag-NPs [35,155], environmental samples with Ag-NPs always contain Ag^+ ions. Furthermore, given the matrix associated Ag^+ in environmental samples might be extracted and falsely counted as Ag-NPs, the effect of coexisting Ag^+ on the determination of

Ag-NPs in water samples is especially worth mentioning. As shown in Figure 22c, it shows that only less than 4% of the adsorbed Ag^+ is extracted by 8:92 formic acid/methanol solution even after 46 h gentle shaking. On the contrary, the extraction efficiencies of the Ag-NPs can reach 92.1-96.2% (Figure 22d). The results imply that this method has the potential for selective extraction of n-Ag-NPs versus silver ions in water samples.

However, it should be noted that high content of Ag^+ in samples still can interfere with the analysis of n-Ag-Ps. In other words, when the Ag^+ concentration is tens- or hundreds-fold of the n-Ag-Ps concentration, the Ag^+ has an important impact on the quantification of n-Ag-Ps. This is because when the Ag^+ concentration is much higher than that of the n-Ag-Ps in samples, the absolute Ag^+ amount extracted is much higher than that of n-Ag-Ps even though the extraction efficiency of Ag^+ (< 4%) was much lower than that of n-Ag-Ps (> 92.1%). For example, a tested sample containing 150 μg/L Ag-NPs, 150 μg/L Ag_2S-NPs and 4500 μg/L of Ag^+, the extraction efficiency of 92.1% n-Ag-Ps corresponds to a extracted amount of 276.3 μg/L, and meanwhile the extraction efficiency of 4% Ag^+ corresponds to a extracted amount of 180 μg/L of Ag^+ which would be falsely counted as n-Ag-Ps in the following GFAAS analysis, so it would give rise to an enormously increased n-Ag-Ps in the sample.

Although high content of Ag^+ significantly interferes with the analysis of n-Ag-Ps, for most environmental samples, the coexisting Ag^+ concentration is low and has negligible effects on the quantification of n-Ag-Ps. To the best of our knowledge, the fraction of Ag^+ is less than 0.1% of the total mass of silver in all environmental water matrices [157]. Furthermore, two recent studies operated by Liu et al. [158] and Kittler et al. [159] found that the release of Ag^+ from Ag-NPs in water was dependent on the sample pH, temperature and NPs surface coating, and the final degree of dissolution in most cases did not exceed 70% of the weight of particles. Therefore, for most real samples, it is expected that the ratio of total Ag^+ to total n-Ag-Ps should be below 2 and the coexisting Ag^+ has negligible effects on the analysis of n-Ag-Ps in real samples.

5.2 Analysis of Silver in Wastewater Influents

Normally, Ag^+ and Ag-NPs commonly coexist, given the release of Ag^+ from Ag-NPs and the transformation of Ag^+ into Ag-NPs in the environment [35,155,160]. As shown in Table 11, the concentrations of n-Ag-Ps range from 0.06 to 1.50 μg/L which account for 13.3 to 49.2% of the

total silver, and meanwhile the majority of the influent samples contained indeed Ag^+; the concentration of Ag^+ ranged from 0.03 to 0.21 μg/L which account for between 6.0 and 58.3% of the total silver. Additionally, we also found that the ratio of total Ag^+ to total n-Ag-Ps were below 2, which was in good agreement with the previous studies [156,159]. Therefore, the effect of coexisting Ag^+ on the analysis of n-Ag-Ps in the wastewater influent is negligible.

Table 11. Determined concentrations of n-Ag-Ps and total silver with and without filtration, and the calculated concentration of free Ag^+, as well as the ratio of free Ag^+ to n-Ag-Ps in the nine field-collected wastewater influent samples

Sample	Silver concentration (μg/L)		n-Ag-Ps concentration (μg/L)	Calculated free Ag^+ (μg/L) [a]	Percent of free Ag^+ in the total silver (%)	Ratio of Ag^+ to n-Ag-Ps
	unfiltered	filtrated				
Mun	3.05 ± 0.13	1.30 ± 0.10	1.50 ± 0.05	- [b]	-	-
Gar	0.35 ± 0.04	0.31 ± 0.02	0.11 ± 0.00	0.20 ± 0.02	58.25 ± 9.03	1.82 ± 0.16
Reg	0.45 ± 0.04	0.22 ± 0.04	0.16 ± 0.01	0.06 ± 0.03	12.89 ± 7.41	0.35 ± 0.16
Aug	0.76 ± 0.03	0.33 ± 0.04	0.37 ± 0.03	-	-	-
Lan	0.41 ± 0.04	0.23 ± 0.05	0.15 ± 0.01	0.08 ± 0.04	18.24 ± 9.59	0.51 ± 0.27
Ulm	0.37 ± 0.07	0.18 ± 0.04	0.15 ± 0.03	0.06 ± 0.05	8.75 ± 10.23	0.28 ± 0.37
Ing	0.32 ± 0.02	0.30 ± 0.06	0.12 ± 0.00	0.18 ± 0.06	55.60 ± 22.63	1.47 ± 0.50
Fre	0.52 ± 0.04	0.22 ± 0.04	0.19 ± 0.01	0.03 ± 0.03	6.04 ± 6.00	0.16 ± 0.15
Moo	0.45 ± 0.05	0.27 ± 0.04	0.06 ± 0.01	0.21 ± 0.03	47.14 ± 12.35	3.51 ± 0.32

[a] Calculted by equation: total silver concentration (filtrated) - n-Ag-Ps concentration. [b] The value is negative.

As it can be seen in Table 11, the influent samples exhibit similar levels of total silver, with the exception of the sample named Mun, which is also found for the n-Ag-Ps. The population was presumed to influence both the total silver and n-Ag-Ps concentrations, since n-Ag-Ps are used in many personal care and household products. However, we found that the population did not show any significant association with both of total silver and n-Ag-Ps concentrations ($p > 0.05$), which indicated that these personal care and household products were not the unique sources. In other words, the sample named Mun had elevated total silver and n-Ag-Ps concentrations that

were statistically different from other samples ($p < 0.05$), perhaps due to an extra industrial source discharged into the plant.

Table 11 compares total silver concentrations in filtered and unfiltered influents. In general, total silver concentrations in filtered samples are lower than those in unfiltered samples. In the present study, the concentrations of total silver in the unfiltered influent were in a range from 0.32 to 3.05 μg/L, which is much lower than the influent samples in the USA [161]. Additionally, the concentrations of total silver in the filtered influent ranged from 0.18 to 1.30 μg/L, accounting for in a range from 43% to 93% of total silver concentration in unfiltered influents. The same phenomenon was observed when the semi-treated samples were analyzed (Table 12). The difference between total silver levels in filtered and unfiltered samples may be attributed to the relatively high levels of suspended organic matter [162,163]. The portion of silver associated with suspended organic matter is of a size larger than the pore size or silver formed aggregates bigger than 0.45 μm in size under organic matter abundant conditions.

Table 12. Determined concentrations of total silver with and without filtration and n-Ag-Ps, and the calculated concentration of free Ag^+, as well as the ratio of free Ag^+ to n-Ag-Ps in the nine field-collected wastewater semi-treatment samples

Sample	Total silver concentration (μg/L)		n-Ag-Ps concentration (μg/L)	Calculated free Ag^+ (μg/L) [a]	Ratio of Ag^+ to n-Ag-Ps
	Unfiltered	Filtrated			
Mun	1.82 ± 0.06	1.21 ± 0.09	1.15 ± 0.05	0.06 ± 0.09	0.06 ± 0.07
Gar	0.29 ± 0.04	0.28 ± 0.04	0.12 ± 0.01	0.16 ± 0.03	1.35 ± 0.10
Reg	0.36 ± 0.02	0.19 ± 0.01	0.07 ± 0.01	0.12 ± 0.01	1.82 ± 0.39
Aug	0.34 ± 0.06	0.15 ± 0.03	0.03 ± 0.01	0.12 ± 0.02	4.28 ± 0.75
Lan	0.30 ± 0.02	0.12 ± 0.02	0.07 ± 0.01	0.05 ± 0.02	0.73 ± 0.29
Ulm	0.31 ± 0.07	0.16 ± 0.02	0.15 ± 0.03	0.01 ± 0.01	0.08 ± 0.08
Ing	0.19 ± 0.02	0.18 ± 0.02	0.03 ± 0.00	0.25 ± 0.02	8.44 ± 0.70
Fre	0.47 ± 0.07	0.18 ± 0.02	0.18 ± 0.01	0.01 ± 0.02	0.06 ± 0.10
Moo	0.32 ± 0.07	0.23 ± 0.01	0.06 ± 0.01	0.17 ± 0.02	2.91 ± 0.77

[a] Calculted by equation: total silver concentration (filtrated) - n-Ag-Ps concentration.

5.3 Role of Mechanical Treatment in n-Ag-Ps Removal

As can be seen from Figure 23a, mechanical treatment plays an important role in removal of silver in general and n-Ag-Ps. Samples collected from nine diverse WWTPs in Germany exhibited varying extents of total silver and n-Ag-Ps removal by the mechanical treatment. We found that the concentration of total silver decreased in a range from 0.05 to 1.24 μg/L, corresponding to the decrease of n-Ag-Ps between 0.01 and 0.35 μg/L. This could be attributed to the occurrence of silver (ions and NPs) partly attached to larger particles like suspended organic matter. Obviously, large sized silver (e.g., μm level) and/or ions as well as small sized silver adsorbed/coated by suspended organic matter are removed efficiently by the mechanical treatment. Among the nine WWTPs, the Aug and Ing were the best performing WWTPs in terms of n-Ag-Ps removal by mechanical treatment and Gar, Ulm, Fre, and Moo were worst performing, indicating that different WWTPs can have very different n-Ag-Ps removal efficiencies by mechanical treatment. The type of mechanical device used in every WWTP and source of n-Ag-Ps, may be associated with this result.

5.4 Quantification of n-Ag-Ps in Municipal WWTPs Effluents

In general, after the mechanical treatment, the wastewater is subjected to the biological treatment, where microbes remove N and P in sequence. The majority of previous research has indicated that about 90% of spiked Ag-NPs are efficiently removed by biological treatment [46,161]. In this present study, the remaining n-Ag-Ps in the semi-treated wastewater were removed in a range of 72.3 - 99.3% (Figure 23b). In other words, the average removal efficiency for the nine samples was 92.4% which was in good agreement with the previous studies [46,161].

Totally, the effluent samples collected from different cities exhibited similar n-Ag-Ps removal trends through the wastewater treatment processes including the mechanical and biological treatments; at least approximately 95% of the n-Ag-Ps that entered municipal WWTPs were removed from wastewater (Figure 23c).

Given the extremely low concentration of n-Ag-Ps in environmental samples, systematic error risks would be high. Hence, two independent measurement methods namely

solid(IRN-78)-liquid extraction and cloud point extraction (CPE) were applied in the present study to confirm the real concentration of n-Ag-Ps in effluent samples. As shown in Table 13, the concentrations of n-Ag-Ps in the field-collected effluents range from 2.2 to 9.4 ng/L using solid(IRN-78)-liquid extraction method, which is in good agreement with the results obtained by using CPE method. Obviously, the concentrations of n-Ag-Ps in effluent are far lower than the values required by US EPA (2009) whose secondary maximum contaminant level is 0.1 mg/L for silver in drinking water [164]. Additionally, these effluent concentrations were at the much lower end of normal detection capabilities, and it is even below the limit of detection (LOD: 6 ng/L) of method reported by Liu et al., [138,139] so it is essential to extract and pre-concentrate the n-Ag-Ps before measurement.

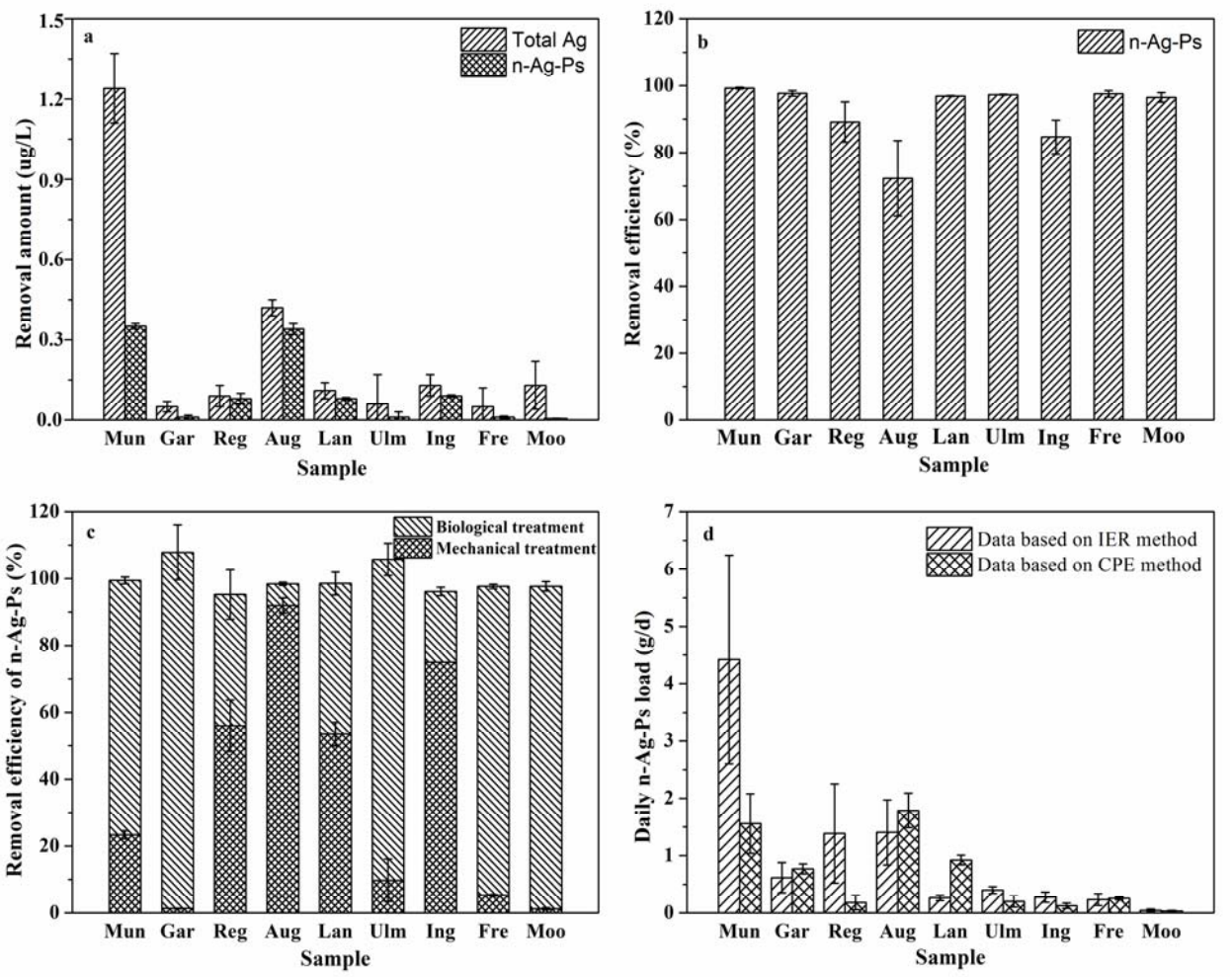

Figure 23. a) Removal of the total Ag and n-Ag-Ps respectively by the mechanical treatment. b) Removal efficiency of n-Ag-Ps by biological treatment. c) The relative contribution of mechanical treatment to the n-Ag-Ps removal compared to biological treatment. d) Daily n-Ag-Ps load entering the water environment by effluent discharge

In general, wastewater effluent is discharged primarily into surface waters (rivers, lakes, oceans) and represents a significant potential point source for pollutants into the environment. In the present study, the daily n-Ag-Ps load entering the water environment through effluent discharge as estimated for each of the nine municipal WWTPs is summarized in Figure 23d. Among the nine WWTPs, we found that even the highest daily n-Ag-Ps load was 4.4 g/d, indicating the WWTP is not a potential point source.

Table 13. Quantification of n-Ag-Ps in the effluent of municipal WWTPs

Method	Concentration of n-Ag-Ps (ng/L)																					
	Mun			Gar			Reg			Aug			Lan			Ulm			Ing			Fre			Moo		
Solid (IRN-78)	8.5	±	3.5	2.8	±	1.2	7.7	±	4.8	9.4	±	3.8	2.2	±	0.4	4.0	±	0.6	4.6	±	1.5	4.5	±	2.0	2.2	±	1.2
CPE	3.0	±	1.0	3.5	±	0.4	1.0	±	0.7	12.0	±	2.0	7.7	±	0.7	2.0	±	1.0	2.1	±	0.8	4.9	±	0.5	1.7	±	0.5

5.5 Conclusions

To the best of our knowledge, this study is the first to investigate whether and to what extent mechanical treatment plays a role in the n-Ag-Ps removal in real municipal WWTPs, and to further quantify n-Ag-Ps in the effluents. Both the mechanical and biological treatments can remove the n-Ag-Ps from wastewater. Totally, more than 95% of the n-Ag-Ps that entered municipal WWTPs are removed through the wastewater treatment processes, which gives rise to extremely low concentrations of n-Ag-Ps in the effluents (e.g., some ng/L). However, the new challenge namely visual observation of n-Ag-Ps in effluents rose due to the extremely low n-Ag-Ps concentration. On the other hand, the removed n-Ag-Ps are likely to be accumulated in the wastewater biosolids which are usually used as agricultural land amendments, placed in landfills, or incinerated. The biosolids may represent a potential source for n-Ag-Ps release into the environment that is very different from WWTP liquid discharge. Hence, future investigation will have to further enlighten the biosolids releases and resulting ecosystem exposures.

6 Final Conclusions

In this thesis, different types of extraction and pre-concentration methods for NMNPs (e.g., Au-NPs, Ag-NPs and Pd-NPs) in aqueous samples were developed. The ligand-assisted liquid-liquid extraction method was firstly investigated to extract and pre-concentrate Au-NPs. Among the four ligands namely DDT, DDA, ODT and ODA, DDT was found the most efficient ligand for extraction of Au-NPs from water to n-hexane; approximately 98% Au-NPs could be extracted from water to n-hexane, and the extracted Au-NPs could preserve their size and shape which was demonstrated by TEM. In addition, the whole extraction process can be completed within only 1 min. However, this DDT-assisted liquid-liquid extraction method was not applicable to extract Au-NPs at low concentration (< 100 μg/L). Consequently, another kind of sample pre-treatment method, solid-liquid extraction, was tested.

Two solid-liquid extraction methods using RP-C18 and IRN-78 as adsorbent respectively were optimized to efficiently and selectively extract NMNPs. For the solid(RP-C18)-liquid extraction, an enrichment factor as high as 250 was obtained and recovery studies in model solutions (recoveries: 99.5 - 103.2%) as well as in real waters (recoveries: 68.4 - 99.4%) confirm the feasibility of this approach. Selectivity in regard to chemical species was given, since separation from ionic gold species was provided. The presence of other NPs, namely Ag-NPs and Pd-NPs, did not interfere the proposed procedure. Moreover, Ag-NPs and Pd-NPs were also separated from aqueous suspensions in high yields, which indicates a high potential for application of the method to other MNPs. Interferences occurring in presence of DOM up to a concentration of 3.4 mg/L can be overcome by pre-treatment with hydrogen peroxide, which does not affect the extraction procedure. In addition, preservation of size and shape of the Au-NPs after application of the method was proved by UV-vis and TEM analysis of the NPs suspension.

For the solid(IRN-78)-liquid extraction method, an enrichment factor of up to 232 with 95% recovery efficiency was obtained when the initial concentration of NMNPs was as low as 100 ng/L. Moreover, the DOM at a concentration of 2 mg/L in the initial NMNPs hydrosol has no effect on the separation and pre-concentration. Three environmental water samples were tested by spiking 90, 80 and 130 ng/L Au-NPs, Ag-NPs, and Pd-NPs, respectively, yielding good (> 65%) recoveries. On the other hand, TEM analysis confirmed that the size and shape of NMNPs

could be preserved by this extraction method. Moreover, this method could also efficiently extract the Ag_2S-NPs in water, which provides a great opportunity to quantify the n-Ag-Ps concentration in real environmental samples.

Consequently, this study further investigated the concentration of n-Ag-Ps in the effluents of WWTPs. It was found that more than 95% of the n-Ag-Ps that entered municipal WWTPs were removed through the wastewater treatment processes, which gives rise to extremely low concentrations of n-Ag-Ps in the effluents (e.g., some ng/L). However, the new challenge namely visual observation of n-Ag-Ps in effluents rose due to the extremely low n-Ag-Ps concentration. Further studies should be conducted to identify and visualize the extracted n-Ag-Ps. In addition, the removed n-Ag-Ps are likely to be accumulated in the wastewater biosolids which are usually used as agricultural land amendments, placed in landfills, or incinerated. The biosolids may represent a potential source for n-Ag-Ps release into the environment that is very different from WWTP liquid discharge. Hence, future investigation will have to further enlighten the biosolids releases and resulting ecosystem exposures. For example, the mobility of NMNPs in the subsurface such as aquifer should be investigated. On the other hand, given the marked effect of DOM on the extraction, future investigation would have to further enlighten the influence of different initial NPs' coatings and their stability under environmental conditions on the extraction and pre-concentration of NMNPs in environmental samples. Thereby the natural "coating" by in particular the DOM will have to be considered in more detail.

7 Appendix

7.1 Chemicals and Materials

All reagents were of analytical grade and used as received without further purification. Sodium borohydride ($NaBH_4$), $HAuCl_4$, $AgNO_3$, Na_2PdCl_4 and hydrogen peroxide (31% (v/v) H_2O_2) were purchased from Merck (Darmstadt, Germany). The 1-dodecanethiol (DDT), dodecyl amine (DDA), 1-octadecanethiol (ODT), octadecylamine (ODA); polyoxyethylene (20) sorbitan monolaurate (Tween 20), tetra-n-octylammonium bromide (TOAB), sodium hydroxide, sodium bicarbonate, sodium citrate dehydrate, sodium sulfide, sodium thiosulphate, sodium acetate, ethylenediaminetetraacetic acid (EDTA), acetic acid, nitric acid, hydrochloric acid, Triton X-114 (TX-114) and 25 mm syringe filter with 0.45 μm poles used in this study were purchased from VWR International (Leuven, Belgium). Mercaptosuccinic acid (MSA), 11-Mercaptoundecanoic acid (MUA), polyvinylpyrrolidone (PVP) 10, polyvinylpyrrolidone (PVP) 40 and toluidine blue O (TBO) were purchased from Sigma-Aldrich (Steinheim, Germany). The Amberlite IRN-78 (particle size 500 μm, matrix: styrene divinylbenzene copolymer, functional group: trimethylammonium) was supplied by Alfa Aesar (Karlsruhe, Germany). Commercial Au-NPs, size of 10, 20, 40 and 80 nm, were purchased from BBI (Cardiff, Wales). Humic acid (HA, Carl ROTH, Karlsruhe, Germany) was used in DOM containing model solutions. The RP-C18 (particle size 40-63 μm) was purchased from Macherey-Nagel (Düren, Germany). Organic solvents (chloroform, methanol, ethanol, formic acid, n-hexane, ethyl acetate) were of analytical grade. Ultra pure water (UPW) from a Direct-Qsystem (Millipore, Billerica, USA) with a resistivity of 18.2 MΩ/cm was used for preparation of all solutions. For all experiments, glassware was thoroughly cleaned in nitric acid steam or with aqua regia solution, rinsed 3-fold with UPW, and oven-dried overnight before use.

7.2 Instrumentation

The pH of samples was measured using a Qph 70 pH-meter (VWR International GmbH, Darmstadt, Germany). The ultrasonication was carried out in a Branson 1200 (47 kHz, 150 W) ultrasonic bath (Branson, Danbury, USA). UV-vis spectra were recorded between 300 and 700

nm using a Cary 50 Scan UV-vis spectrophotometer (Varian, Darmstadt, Germany). The total organic carbon (TOC) concentration was measured with an Elementar High TOC analyzer (Elementar, Hanau, Germany) after separation from inorganic carbon achieved by addition of hydrochloric acid. The element analysis of wastewater samples was conducted by total reflection x-ray fluorescence (TXRF, Atomika 8010 and Bruker S2 Picofox, Germany). The concentrations of Au, Ag and Pd before and after separation/pre-concentration were determined using a 4100ZL graphite furnace atomic absorption spectrometer (GFAAS, Perkin-Elmer, Überlingen, Germany), equipped with Zeeman-effect background correction, a transversally heated graphite atomizer (THGA) and an AS-71 auto-sampler. Calibration of GFAAS was typically performed in a concentration range from 2 to 100 µg/L by measurement of aqueous standard solutions prepared by dilution of commercially available stock standard solution (1000 mg/L in 2 M HCl or HNO_3, Merck, Darmstadt, Germany). Ultracentrifugation was operated in an optima Max-E ultracentrifuge (Beckman, CA, USA) using a TLA-45 rotor. The zeta potential of samples was determined with a Zeta Potential Analyzer (ZETASIZER Nano series, Germany). Transmission electron microscopy (TEM) images were taken on a JEOL JEM 2010 (Munich, Germany) operating at 120 kV. Scanning electron microscopy (SEM) was performed with JEOL JSM5900LV (Röntec, Germany) at 15 kV. Energy dispersive x-ray fluorescence (EDX) was carried out on a FEI Titan 80-300 (Eindhoven, The Netherlands) instrument operated at 300 kV. Fourier transform infrared (FTIR) spectra of samples were recorded on a Varian FTIR-670 spectrometer, using a GladiATR accessory with a diamond ATR element.

7.3 Preparation of Citrate-Stabilized Au-NPs in Water

The citrate-stabilized Au-NPs were prepared according to the method developed by Haiss et al. [132]. Therefore, an aqueous solution of $HAuCl_4$ (1 mL, 5 mmol/L) was added to a 0.02% sodium citrate solution (98 mL) under vigorous shaking to give a final concentration of 0.05 mmol/L $HAuCl_4$. After 10 min of mixing, 1 mL of a freshly prepared 2 mol/L $NaBH_4$ solution in 1% sodium citrate solution was added rapidly. This addition immediately induced a color change to wine red, indicating the formation of Au-NPs. The reaction was allowed to continue for 10 min under vigorous shaking. A full conversion of Au(III) into Au-NPs can be assumed due to the large stoichiometric excess of the reductant. Figure 24 shows a photograph of the prepared

Au-NPs hydrosol, and an exemplary TEM image (spheres of 5 to 25 nm) as well as the size distribution (with average diameter of 10.0 ± 0.6 nm) of the Au-NPs. The Au-NPs concentration in the aqueous phase was determined by GFAAS and the temperature program of GFAAS measurement can be found in Table 14. The Au-NPs stock suspension at 10.0 mg/L was stored at 4 °C.

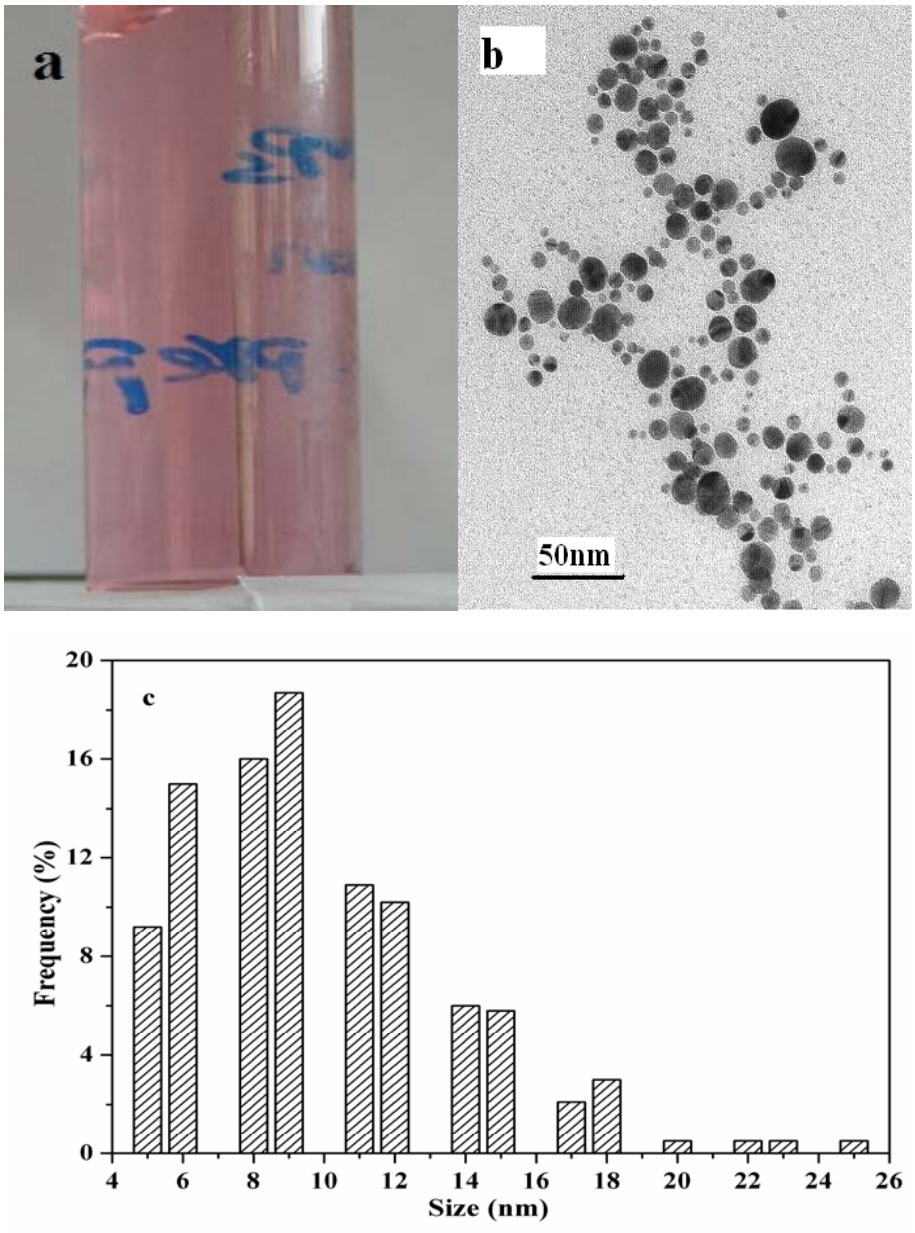

Figure 24. a) A photograph of the prepared citrate-stabilized Au-NPs hydrosol. b) TEM micrograph of the prepared citrate-stabilized Au-NPs, the scale bar corresponds to 50 nm. c) Size distribution of 650 of the prepared citrate-stabilized Au-NPs with average diameter of 10.0 ± 0.6 nm

Table 14. Graphite furnace temperature program for the measurement of gold in aqueous solution

Process	Temperature (°C)	Ramp time (s)	Hold time (s)	Argon flow rate (s)
Drying I	100	5	30	250
Drying II	140	15	20	250
Pyrolysis	800	10	20	250
Atomisation [a]	1800	0	5	0
Clean-out	2450	1	3	250

[a] Read step

7.4 Preparation of Citrate-Stabilized Ag-NPs in Water

The citrate-stabilized Ag-NPs were prepared by the method of Jana et al. [164] with minor modification. A 99 mL solution containing 0.06 % sodium citrate and 0.094 mmol/L $AgNO_3$ was prepared in UPW and stirred vigorously. As 1 mL of 2 mol/L $NaBH_4$ was added into the mixture, the solution turned to yellow, indicating formation of the Ag-NPs. The reaction was allowed to continue for 10 min under vigorous shaking. A full conversion of Ag(I) into Ag-NPs can be assumed due to the large stoichiometric excess of the reductant. Figure 25 shows a photograph of the prepared Ag-NPs hydrosol, and an exemplary TEM image (spheres of 8 to 40 nm) as well as the size distribution (with average diameter of 17.2 ± 0.5 nm) of the Ag-NPs. The Ag-NPs concentration in the aqueous phase was determined by GFAAS and the temperature program of GFAAS measurement can be found in the Table 15. The Ag-NPs stock suspension at 10.0 mg/L was stored at 4 °C.

Table 15. Graphite furnace temperature program for the measurement of silver in aqueous solution

Process	Temperature (°C)	Ramp time (s)	Hold time (s)	Argon flow rate (s)
Drying I	100	1	30	250
Drying II	130	15	30	250
Pyrolysis	800	10	20	250
Atomisation [a]	1700	0	5	0
Clean-out	2450	1	3	250

[a] Read step

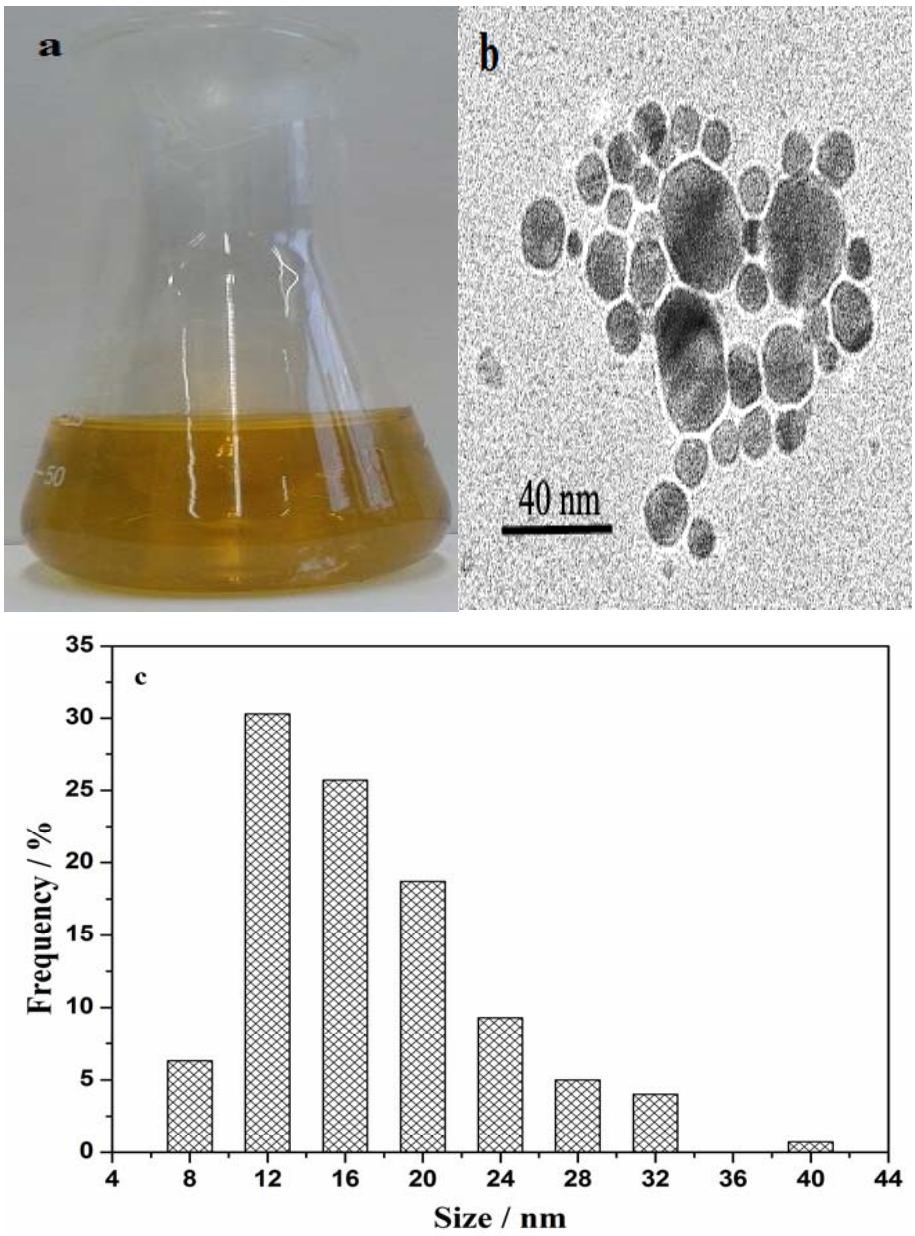

Figure 25. a) A photograph of the prepared citrate-stabilized Ag-NPs hydrosol. b) TEM micrograph of the prepared citrate-stabilized Ag-NPs, the scale bar corresponds to 40 nm. c) Size distribution of 350 of the prepared citrate-stabilized Ag-NPs with average diameter of 17.2 ± 0.5 nm

7.5 Preparation of Citrate-Stabilized Pd-NPs in Water

The citrate-stabilized palladium nanoparticles (Pd-NPs) were prepared according to the following method. A 99 mL solution containing 0.06 % sodium citrate and 0.094 mmol/L Na_2PdCl_4 was prepared in ultrapure water (UPW) and stirred vigorously. As 1 mL of 2 mol/L $NaBH_4$ was added into the mixture, the solution turned to black, indicating formation of the Pd-NPs. The reaction was allowed to continue for 10 min under vigorous shaking. A full conversion of Pd(II) into Pd-NPs can be assumed due to the large stoichiometric excess of the reductant. Figure 26 shows a photograph of the prepared Pd-NPs hydrosol, and an exemplary TEM image (spheres of 4 to 9 nm) as well as the size distribution (with average diameter of 6.5 ± 1.2 nm) of the Pd-NPs. The Pd-NPs concentration in the aqueous phase was determined by GFAAS and the temperature program of GFAAS measurement can be found in the Table 16. The Pd-NPs stock suspension at 10.0 mg/L was stored at 4 °C for later use.

Table 16. Graphite furnace temperature program for the measurement of palladium in aqueous solution

Process	Temperature (°C)	Ramp time (s)	Hold time (s)	Argon flow rate (s)
Drying I	100	5	40	250
Drying II	140	15	40	250
Pyrolysis	900	10	20	250
Atomisation [a]	2200	0	5	0
Clean-out	2450	1	3	250

[a] Read step

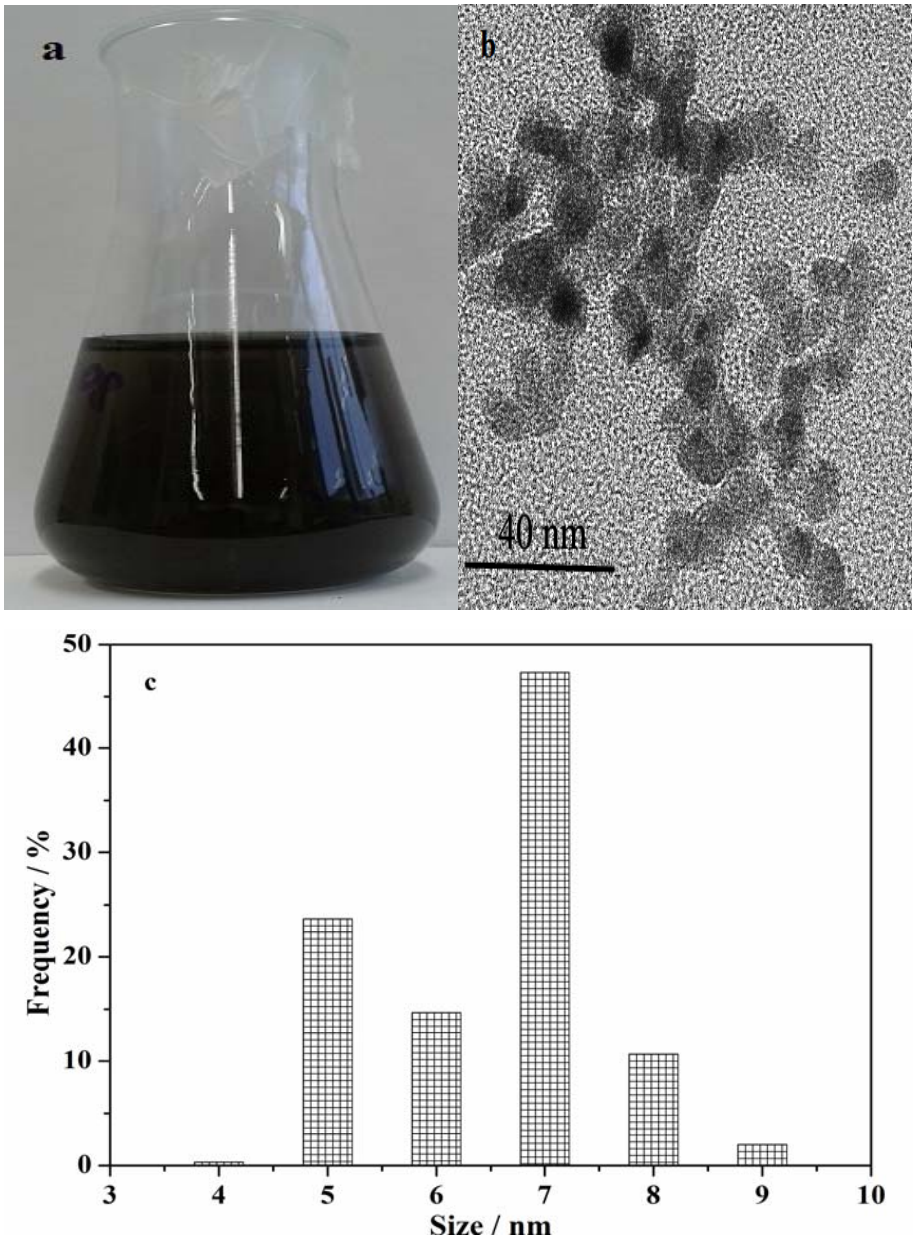

Figure 26. a) A photograph of the prepared citrate-stabilized Pd-NPs hydrosol. b) TEM micrograph of the prepared citrate-stabilized Pd-NPs, the scale bar corresponds to 40 nm. c) Size distribution of 280 of the prepared citrate-stabilized Pd-NPs with average diameter of 6.5 ± 1.2 nm

7.6 Preparation of Ag_2S-NPs in Water

Ag_2S-NPs were prepared according to the method of Choi et al. [165] with minor modifications. In the present study, Ag_2S-NPs with different ratios of Ag to S were prepared, namely 1:4, 1:2, 1:1, and 2:1. Different volumes (25, 50, 100 and 200 μL) of 0.01 mol/L Na_2S solution were added to 10 mL of freshly prepared Ag-NPs solutions (above-mentioned) and stirred vigorously for 3 h. Afterwards, the Ag_2S-NP suspensions were stored at 4 °C and were

used as stock solutions for the present study. The Ag_2S-NPs as well as Ag-NPs hydrosols were analyzed by UV-vis spectroscopy (Figure 27a) and TEM-EDX (Figure 27b, 27c and 27d). For example, the atomic ratio of Ag to S for the synthesized Ag_2S-NPs using 200 µL of 0.01mol/L Na_2S was measured by EDX at four sample positions to an average value of 2.08 ± 0.28. This is reasonably close to a ratio of 2.0 as expected for Ag_2S.

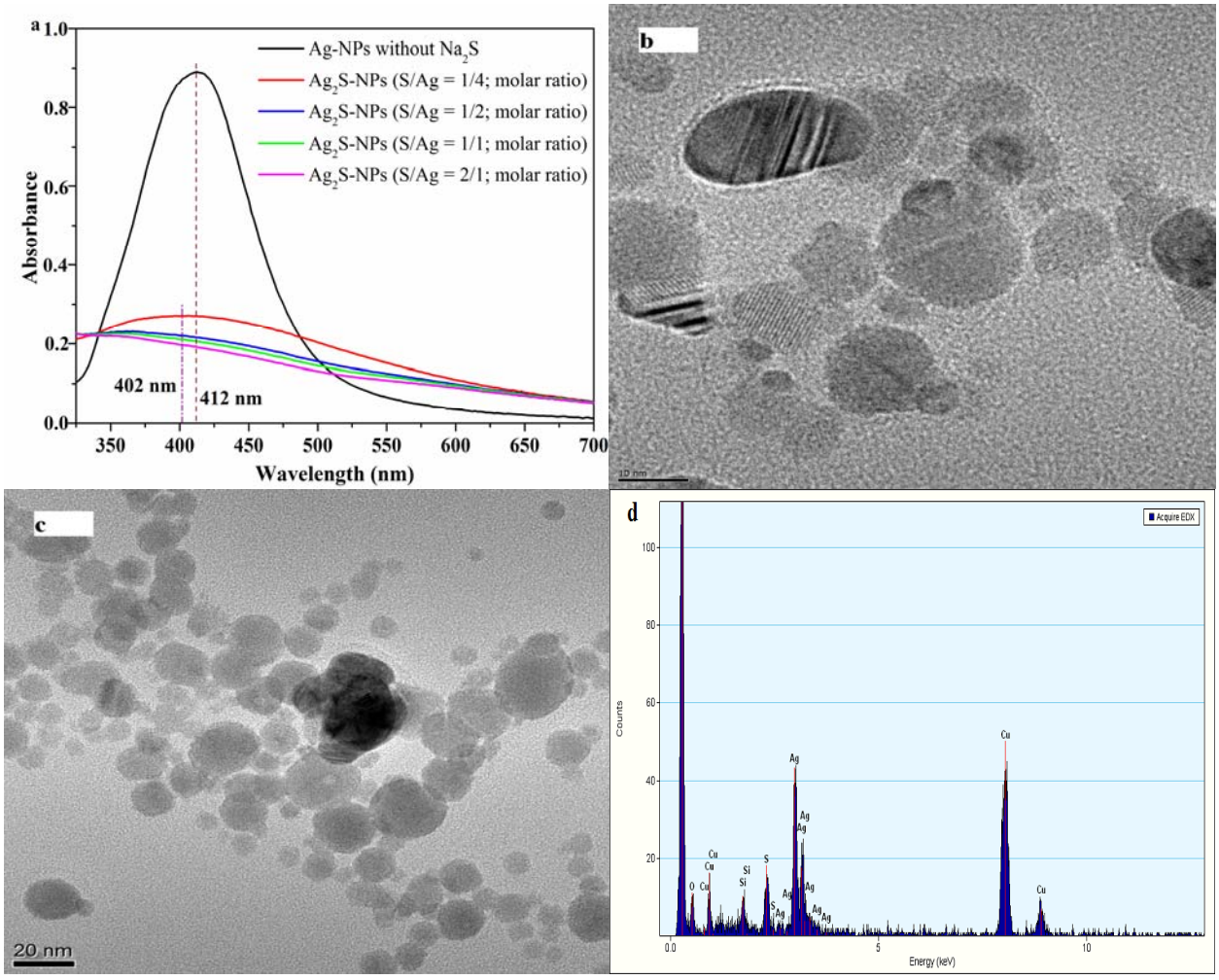

Figure 27. a) The UV-vis spectra of Ag-NPs and Ag_2S-NPs prepared in this study. b) TEM image of prepared Ag-NPs in this study, bar: 10 nm. c) TEM image of prepared Ag_2S-NPs (S/Ag = 1/2) in this study, bar: 20 nm. d) EDX of the prepared Ag_2S-NPs (S/Ag = 1/2) in this study

7.7 Preparation of Surfactant-Stabilized Au-NPs, Ag-NPs, and Pd-NPs in Water

The surfactant-stabilized Au-NPs, Ag-NPs, and Pd-NPs were prepared by the method of *Mahl et al.* [166] with minor modification. We added 15 mL of PVP10 (100 mmol/L), 15 mL of PVP40 (25 mmol/L), 3 mL of TOAB (10 mmol/L), or 3 mL of Tween 20 (90 mmol/L) respectively to 60 mL of citrate-stabilized Au-NPs, Ag-NPs, and Pd-NPs suspension (10 mg/L). The resulting mixtures were equilibrated at room temperature for at least 2 h before use.

7.8 Ligand-Assisted Liquid-Liquid Extraction of Au-NPs from Water

7.8.1 General Procedure of Ligand-Assisted Liquid-Liquid Extraction

In order to identify suitable ligands for ligand-assisted extraction of Au-NPs, liquid-liquid extraction study was performed with four different ligands, namely DDT, DDA, ODT, and ODA. For this purpose, 3 mL chloroform or n-hexane with different concentrations of above-mentioned ligands were added to 30 mL of Au-NPs hydrosol source. The biphasic system was shaken well for 30 s and then left for another 30 s. Subsequently, the mixture spontaneously separated into two layers. One layer was the n-hexane or chloroform phase now containing the ligand-Au-NPs complex compounds and the other layer was the Au-NPs depleted aqueous phase. The n-hexane or chloroform phase was collected and analyzed for Au concentration using a GFAAS spectrometer and NPs size distribution using a Cary 50 Scan UV-vis spectrophotometer and a TEM instrument operating at 120 kV. However, the proposed ligand-assisted liquid-liquid extraction is not applicable as a tool to separate and pre-concentrate of Au-NPs from environmental waters since the enrichment factors were not sufficient. Hence, the solid-liquid extraction procedure was developed as described in the following.

7.8.2 Transfer Efficiency and Transfer Index

To the best of our knowledge, in most of the literature reporting the phase transfer of NPs from an aqueous to an organic phase the transfer efficiency TE was calculated using equation 1

[112],

$$TE\ (\%) = \frac{100 \times (a - b)}{a} \qquad (1)$$

where a and b are the concentration of Au-NPs in the aqueous phase before and after phase transfer (μg/L).

However, these studies ignored one key point: although the TE, calculated according to the equation 1, is very high (～ 100%), the transferred NPs can either assemble at the interface between the aqueous and organic phase or disperse in the organic solvent or both. Consequently, in the present study, we used equation 2 named TI to evaluate the transfer efficiency of Au-NPs.

$$TI = \frac{c \times V_h}{(a - b) \times V_a} \qquad (2)$$

where a and b are the concentration of Au-NPs in the aqueous phase before and after phase transfer (μg/L), c is the concentration of Au-NPs in the organic phase (n-hexane) after the phase transfer, V_a is the volume of the Au-NPs containing aqueous solution (mL), and V_h is the volume of the organic phase (mL). Theoretically, the TI value should be close to 1, if the transferred Au-NPs are well dispersed in the organic phase.

7.9 Ligand-Assisted Solid-Liquid Extraction of NPs in Water

7.9.1 Ligand-Assisted Solid(RP-C18)-Liquid Extraction

7.9.1.1 General Procedure of Ligand-Assisted Solid(RP-C18)-Liquid Extraction

Separation and pre-concentration of MNPs like Au-NPs was conducted according to Figure 9a. First, Au-NPs were loaded onto RP-C18 material, and second the Au-NPs were extracted under ultrasonic condition into an organic solvent (chloroform) containing DDT. For this purpose, a column was packed with 0.25 g of RP-C18 in a glass tube with a porous glass frit (volume: 6 mL; inner diameter: 8 mm). This RP-C18 column was conditioned with 10 mL of methanol and successively rinsed three times with 10 mL of UPW. Then a volume of 10 to 500 mL of the Au-NPs hydrosol source was passed through the column at a constant flow rate of 3 mL/min. Subsequently, with the same flow rate, the column was rinsed with 10 mL of UPW and in a next

step dried by application of vacuum. Afterwards, the dry Au-NPs-loaded RP-C18 material was transferred to 10 mL of an organic solvent containing DDT. The ligand-assisted re-extraction was conducted at about 0 °C (ice-water mixture) under ultrasonic treatment. The cooling during ultrasonication minimizes chloroform loss from evaporation and more importantly prevents agglomeration of the NPs which otherwise would occur due the heat produced from ultrasonication. After centrifugation at 2000 rpm for 3 min, the supernatant containing Au-NPs was collected and concentrated to 2 mL by evaporation under nitrogen.

7.9.1.2 Extraction Efficiency of NPs by the Proposed Method

Extraction efficiency for the 1st step was found to be about 100% in all experiments except for samples with a pH higher than 7.1, or a TOC concentration higher than 2 mg/L. This was checked by GFAAS measurement of Au in the run-off of the RP-C18 column, where typically no Au was found (detection limit 4 µg/L). Hence, the extraction efficiency of the two-step procedure is mainly depending on the efficiency of the 2nd step which is calculated by the following equation (3):

$$Extraction\ efficiency(\%) = \frac{100 \times C_e \times V_e}{(C_0 - C_f) \times V_{in}} \qquad (3)$$

where C_0 is the initial concentration of Au-NPs before loading onto RP-C18 (µg/L), C_f is the concentration of Au-NPs in run-off (µg/L), C_e is the concentration of Au-NPs in extraction liquid such as chloroform (µg/L), V_e is the volume of extraction liquid (mL), and V_{in} is the volume of Au-NPs hydrosol source (mL).

7.9.1.3 Optimization of Ligand-Assisted Solid(RP-C18)-Liquid Extraction

In order to optimise this extraction procedure for efficient pre-concentration of MNPs from the hydrosol source, parameters that affect the two-step extraction procedure of MNPs (e.g., Au-NPs) from aqueous phase into organic phase, such as the flow rate of the sample passing the column, the organic extractant, the nature and concentration of the ligand in the organic extractant, the ultrasonication time, the centrifugation speed, and the pH of the Au-NPs hydrosol source were studied. Table 17 gives an overview of the performed experiments.

Table 17. Variable parameters and resulting conditions for the variations of the general procedure for extraction of Au-NPs

Parameter	Tested variations	Fixed parameters
Flow rate of the sample passing the column (mL/min)	3, 6, 9	ultrasonication time: 3 h [DDT]: 5mmol/L pH: 4.5 citrate-coated Au-NPs prepared in our lab
Organic solvent	methanol, ethanol, chloroform, ethyl acetate, n-hexane, mixtures of ethanol and chloroform (1:3, 1:1, 3:1)	ultrasonication time: 3 h [DDT]: 10 mmol/L pH: 4.5 citrate-coated Au-NPs prepared in our lab
Concentration of DDT (mmol/L)	0, 0.2, 1.0, 5.0, 10.0, 50.0	organic solvent: chloroform ultrasonication time: 3 h pH: 4.5 citrate-coated Au-NPs prepared in our lab
Ultrasonication time (minutes)	0, 5, 15, 30, 60, 120, 180, 240, 300, 360	organic solvent: chloroform [DDT]: 5 mmol/L pH: 4.5 citrate-coated Au-NPs prepared in our lab
Speed of centrifugation (rounds per minute)	1500, 2000, 2500, 3000, 3500	organic solvent: chloroform ultrasonication time: 3 h [DDT]: 5 mmol/L citrate-coated Au-NPs prepared in our lab
pH of the sample [a]	2.5, 3.5, 4.5, 6.0, 7.1, 8.0, 9.0	organic solvent: chloroform ultrasonication time: 3 h [DDT]: 5 mmol/L citrate-coated Au-NPs prepared in our lab
Coating of Au-NPs prepared in our lab	Citrate, MSA, MUA, TOAB, Tween 20	organic solvent: chloroform ultrasonication time: 3 h [DDT]: 5 mmol/L

		pH: 4.5 organic solvent: chloroform ultrasonication time: 3 h
Size of Au-NPs (nm)	10, 20, 40, 80	[DDT]: 5 mmol/L pH: 4.5

[a] pH adjustment was achieved by stepwise addition of HCl or NaOH solution (0.5 mol/L), respectively.

7.9.1.4 Effect of Dissolved Organic Matter in Au-NPs Hydrosol Source

Model solutions with DOM and Au-NPs were prepared as follows: 0.1 g of humic acid (HA) was dissolved in 100 mL of UPW under stirring for 24 h in the dark. Then adequate aliquots of this solution were added to the Au-NPs hydrosol source obtaining the following concentrations of total organic carbon (TOC): 0, 0.50, 0.70, 1.70, 3.40, 5.25, 6.60, 8.40, and 16.20 mg/L. These solutions were filtered through a 0.45μm nylon membrane syringe filter and Au concentration was determined by GFAAS. Every model solution was then divided into two subsamples: One group of subsamples was directly used for the two-step extraction procedure. The other group of subsamples was pre-treated with 3% (v/v) H_2O_2 solution and stirred at 150 rpm for 24 h prior to two-step extraction. The gold concentration of the resulting organosols was again measured by GFAAS. Table 18 gives the results from the GFAAS measurements.

Moreover, the effect of pH on extraction of Au-NPs in presence of 2 mg/L DOM was investigated in this study. The pH of the Au-NPs model solution containing 2 mg/L DOM was adjusted to 2.0, 3.5, 5.0, 7.3, 8.3, and 9.3, respectively, by addition of HCl (0.5 M) or NaOH (0.5 M) before extraction. Then the extraction and pre-concentration was performed analogue to the above-described general two-step extraction procedure.

Table 18. Concentration of Au-NPs before and after pretreatment with 3% H_2O_2 and filtration [a]

Concentration of humic acid (TOC, mg/L)	Concentration of Au (μg/L)			Au-NPs recovery (%)	
	Initially in the aqueous sample	In the resulting organosol			
		Without sample pretreatment	After sample pretreatment with 3% H_2O_2	Without pretreatment	After pretreatment with 3% H_2O_2
0.70	2837.0 ± 60.0	2123.1 ± 130.7	2693.3 ± 128.4	75.1 ± 3.0	94.9 ± 2.5
1.70	2427.0 ± 67.0	1776.1 ± 122.8	2287.6 ± 137.6	73.2 ± 3.2	94.2 ± 3.1
3.40	2820.0 ± 48.0	2042.4 ± 71.1	2613.0 ± 188.8	72.4 ± 1.3	92.6 ± 5.1
8.40	2508.0 ± 82.5	1071.6 ± 88.5	2049.4 ± 96.0	42.7 ± 2.1	81.7 ± 1.1
16.20	2302.0 ± 78.0	837.3 ± 60.1	1646.5 ± 80.4	36.3 ± 1.4	71.5 ± 1.0

[a] Given uncertainties represent ± one standard deviation with n=3, P=95%.

7.9.2 Ligand-Assisted Solid(IRN-78)-Liquid Extraction

7.9.2.1 General Procedure of Ligand-Assisted Solid(IRN-78)-Liquid Extraction

Separation and pre-concentration of MNPs was conducted according to the Figure 15. First, the freshly prepared MNPs like Au-NPs were modified by MSA; a mixture of 5 mL 0.01 mol/L MSA and a volume of 45 to 995 mL prepared MNPs solution was shaken (200 rpm) for 3 h at room temperature. Then, the MSA-modified MNPs colloidal solution (pH: 8.0 ± 0.5 by 0.5 mol/L NaOH) was, by means of peristaltic pump, passed through a glass tube with an internal diameter of 20 mm and a length of 9 cm tightly packed (packing length, 2 cm) with 4.5 g of Amberlite IRN-78 nuclear grade ion exchange resin (particle size 500 μm). The influent rate was controlled between 1.5 and 2.5 mL/min. Afterwards, the NPs-loaded resin was rinsed with 50 mL methanol and then transferred to 25 mL mixture of formic acid and methanol. The cleavage reaction was conducted using gentle shaking (250 rpm) for different time (2-88 h; it depends on the initial concentration of MNPs) at room temperature. After settling for 30 min the supernatant containing NPs was collected and concentrated to 2 or 5 mL by evaporation under nitrogen.

7.9.2.2 Extraction Efficiency of NPs by the Proposed Method

Calculating the separation and recovery efficiencies follows equations 4 and 5.

$$Separation\ efficiency\ (\%) = \frac{100 \times (C_i - C_f)}{C_i} \qquad (4)$$

After the cleavage step, the recovery of NPs was calculated as

$$\text{Recovery}\ (\%) = \frac{100 \times C_c \times V_c}{(C_i - C_f) \times V_i} \qquad (5)$$

where C_i is the concentration of MNPs in the initial suspension (μg/L), C_f is the concentration of MNPs in the filtrate (μg/L), C_c is the concentration of concentrated MNPs suspension (μg/L), V_c is the volume of concentrated suspension (mL), and V_i is the volume of NPs hydrosol source (mL).

7.9.2.3 Analysis of Surface Carboxyl Groups via TBO Dye Adsorption Assay in IRN-78 Method

The carboxyl groups of MSA on the surface of MNPs were analysed by the TBO colorimetric method according to Sano et al. [167] with following modifications. Carboxyl groups on the surface of extracted MNPs were complexed with 0.5 mmol/L Toluidine Blue O of pH 10 at room temperature overnight. Non-complexed dye was removed with 0.1 mmol/L NaOH and desorption of dye molecules complexed to the carboxyl groups on the surface of extracted NPs was conducted with 50% acetic acid solution. Absorbance was recorded by UV-vis spectroscopy.

7.10 Separation of n-Ag-Ps by Cloud Point Extraction

The extraction was improved and performed on the basis of a method reported by Liu et al. [138,139]. In brief, 40 mL of aqueous sample was mixed with 1.0 mL of saturated ethylenediaminetetraacetic acid (EDTA) solution, 400 μL of 1 M sodium acetate, 100 μL of 1.25 mol/L acetic acid, and 1 mL of 10 % (w/w) TX-114 in a 50 mL tapered polypropylene sample tube. The mixture was incubated at 40 °C for at least 60 minutes and then centrifuged for 5 minutes at 3000 rpm to enhance phase separation. Afterwards the sample was cooled in an ice bath for 5 minutes. The aqueous supernatant was removed by decanting. The remaining

surfactant-rich phase containing the n-Ag-Ps was dissolved in either 100 µL (for effluent samples) or 1.0 mL (for influent samples) of ethanol and forwarded to GFAAS measurement. Details of GFAAS measurement can be found in the Table 19. Calibration was performed using n-Ag-P solutions of known concentration that were subjected to the complete extraction procedure and measured the same way as the environmental samples. Using this method limits of detection (LOD) for n-Ag-Ps of 0.7 (for effluent samples) and 12.9 ng/L (for influent samples) were achieved for WWTP samples.

Table 19. Graphite furnace temperature program for the measurement of silver in TX-114-rich samples dissolved in ethanol after CPE

Process	Temperature (°C)	Ramp time (s)	Hold time (s)	Argon flow rate (s)
Drying I	80	5	20	250
Drying II	130	10	20	250
Pyrolysis	600	20	20	250
Cooling	300	1	5	250
Atomisation [a]	1800	0	5	0
Clean-out	2450	1	3	250

[a] Read step

7.11 Water Samples Collection

7.11.1 Water Samples for RP-C18 and IRN-78 Methods

The drinking water (public tap water) was collected directly from a tap in our lab. River, lake, and brook water samples were collected manually in the surrounding area of Munich, Germany. Briefly, river water was taken from the river Isar in Munich. Lake water was collected from the Starnberger See at Possenhofen. Brook water was collected on the campus of Technical University of Munich, Garching. Furthermore, a sample from the effluent of the wastewater treatment plant (WWTP) Gut Marienhof, Eching was taken. All samples were collected in glass containers, which were rinsed threefold with the sample before they were filled up to volume and

stored at 4 °C until use. Real samples were investigated after filtration through 0.45 µm as well as unfiltered. Some characteristics of samples are shown in Table 20.

Table 20. Characteristics of real samples

Sample	pH	Ca	Zn	Cu
			(mg/L)	
Tap water filtrated	7.49 ± 0.03	57.39 ± 0.32	1.45 ± 0.02	0.018 ± 0.002
Tap water unfiltered	7.50 ± 0.03	58.48 ± 5.81	1.49 ± 0.02	0.022 ± 0.000
River water filtrated	8.03 ± 0.02	56.22 ± 0.32	n.d.	n.d.
River water unfiltered	8.01 ± 0.03	54.91 ± 0.40	n.d.	n.d.
Lake water filtrated	8.05 ± 0.01	40.88 ± 0.32	n.d.	n.d.
Lake water unfiltered	8.04 ± 0.02	40.66 ± 0.13	n.d.	0.002 ± 0.001
Brook water filtrated	8.22 ± 0.02	53.71 ± 1.86	n.d.	n.d.
Brook water unfiltered	8.21 ± 0.01	52.24 ± 0.21	n.d.	n.d.
WWTP Effluent filtrated	6.72 ± 0.02	77.87 ± 0.05	0.02 ± 0.00	n.d.
WWTP Effluent unfiltered	6.70 ± 0.02	82.98 ± 0.95	0.01 ± 0.00	n.d.

Remarks: Given uncertainties represent ± one standard deviation with n=3, P=95%;

n.d.: Concentration was below detection limit (< 1 µg/L);

Total organic carbon was below detection limit in all samples, i.e.< 1 mg/L;

Particulate matter content was less than 1 mg/L in all samples.

7.11.2 Water Samples from Wastewater Treatment Plants

The field-collected wastewater effluent samples were from nine municipal WWTPs located in eight German cities, between March and October 2012. According to the treatment capacity, the nine WWTPs were classified into three groups: large (> 200 kt/d), middle (100 - 200 kt/d) and small (< 100 kt/d). All WWTPs except one named Moo employ the same treatment processes: first, mechanical treatment; second, biological treatment including nitrification, denitrification and phosphorus removal, because major WWTPs in Germany have been operated this way since 1989 [168]. For the WWTP named Moo, the mechanical treatment is replaced by mixing the influent with one branch of run-off without precipitation from biological treatment pools.

Detailed information on the WWTP samples is shown in Table 21.

Table 21. Basic information and characteristics of samples from nine municipal WWTPs in Germany

Sample	Capacity (kt/d)	Inhabit (k)	Influent		Semi-treated		Effluent	
			pH	TOC (mg/L)	pH	TOC (mg/L)	pH	TOC (mg/L)
Mun	520	1500 [a]	7.17	36.8 ± 3.7	7.27	25.9 ± 5.1	7.58	<1
Gar	220		7.27	17.2 ± 2.9	7.19	15.7 ± 2.1	6.70	<1
Reg	180	400	7.57	23.4 ± 3.6	7.67	13.0 ± 6.2	7.35	<1
Aug	149.5	375	7.78	14.2 ± 3.6	7.15	11.7 ± 1.7	7.03	<1
Lan	120	260	8.06	31.2 ± 5.6	7.55	19.0 ± 2.9	7.48	<1
Ulm	100	200	7.20	36.5 ± 2.6	7.11	27.8 ± 3.6	6.97	5.2 ± 0.3
Ing	60	275	7.51	53.0 ± 1.8	7.42	61.4 ± 7.2	7.81	<1
Fre	51.8	110	6.95	223.1 ± 19.1	7.11	125.7 ± 6.8	6.98	<1
Moo	18.9	40	7.39	15.6 ± 2.9	7.52	12.2 ± 1.9	7.25	<1

[a] The WWTPs named Mun and Gar serve one city whose population is 1.5 million.

8 Literature

[1] T. Hyeon, Chem. Commun. 2003, 927.

[2] X. Xu, Y. Li, Y. Gong, P. Zhang, H. Li, Y. Wang, J. Am. Chem. Soc. 2012, 134, 16987.

[3] M. C. Roco, W. S. Bainbridge, Societal Implications of Nanoscience and Nanotechnology. NSET, 2001.

[4] P. Miralles, T. L. Church, A. T. Harris, Environ. Sci. Technol. 2008, 42, 5828.

[5] The Royal Society & The Royal Academy of Engineering. Nanoscience and Nanotechnologies: Opportunities and Uncertainties; The Royal Society, Science Policy Section: London, 2004.

[6] B. Nowack, T. D. Bucheli, Environ. Pollut. 2007, 150, 5.

[7] J. Kao, P. Bai, V. P. Chuang, Z. Jiang, P. Ercius, T. Xu, Nano Lett. 2012, 12, 2610.

[8] N. Chandrasekharan, P. V. Kamat, Nano Lett. 2001, 1, 67.

[9] Y. Kim, R. C. Johnson, J. T. Hupp, Nano Lett. 2001, 1, 465.

[10] G. Raschke, S. Kowarik, T. Franzl, C. Sönnichsen, T. A. Klar, J. Feldmann, A. Nichtl, K. Kürzinger, Nano Lett. 2003, 3, 935.

[11] A. Yu, Z. Liang, J. Cho, F. Caruso, Nano Lett. 2003, 3, 1203.

[12] S. Lin, Y. Cheng, Y. Bobcombe, K. L. Jones, J. Liu, M. R. Wiesner, Environ. Sci. Technol. 2011, 45, 5209.

[13] H. Lee, S. Yeo, S. Jeong, J. Mater. Sci. 2003, 38, 2199.

[14] P. Jain, T. Pradeep, Biotechnol. Bioeng. 2005, 90, 59.

[15] M. Bosetti, A. Masse, E. Tobin, M. Cannas, Biomaterials 2002, 23, 887.

[16] W. Chou, D. Yu, M. Yang, Polym. Adv. Technol. 2005, 16, 600.

[17] A. McFarland, R. Van Duyne, Nano Lett. 2003, 3, 1057.

[18] H. Lee, K. Chou, K. Huang, Nanotechnology 2005, 16, 2436.

[19] Y. Shiraishi, N. Toshima, J. Mol. Catal. A : Chem. 1999, 141, 187.

[20] Nanotechnology Consumer Product Inventory, http://www.nanotechproject.org/inventories/consumer/analysis_draft/.

[21] D. E. Meyer, M. A. Curran, M. A. Gonzalez, Environ. Sci. Technol. 2009, 43, 1256.

[22] E. Ruiz-Hernandez, A. Baeza, M. Vallet-Regi, ACS Nano 2011, 5, 1259.

[23] X. Hong, Z. Wang, W. Cai, F. Lu, J. Zhang, Y. Yang, N. Ma, Y. Liu, Chem. Mater, 2005, 17, 1548.

[24] I. R. Pala, S. L. Brock, ACS Appl. Mater, Interfaces 2012, 4, 2160.

[25] B. M. Simonet, M. Valcarcel, Anal. Bioanal. Chem. 2009, 393, 17.

[26] N. S. Wigginton, K. L. Haus, M. F. Hochella, Jr, J. Environ. Monit. 2007, 9, 1306.

[27] M. Villalobos, J. Bargar, G. Sposito, Elements 2005, 1, 223.

[28] M. Villalobos, J. Bargar, G. Sposito, Environ. Sci. Technol. 2005, 39, 569.

[29] D. A. Bazylinski, R. B. Frankel, Nat. Rev. Microbiol. 2004, 2, 217.

[30] C. S. Chan, G. De Stasio, S. A. Welch, M. Girasole, B. H. Frazer, M. V. Nesterova, S. Fakra, J. F. Banfield, Science 2004, 303, 1656.

[31] C. Buzea, I. I. P. Blandino, K. Robbie, Biointerphases 2007, 2, MR17.

[32] S. R. Gislason, T. Hassenkam, S. Nedel, N. Bovet, E. S. Eiriksdottir, H. A. Alfredsson, C. P. Hem, Z. I. Balogh, K. Dideriksen, N. Oskarsson, B. Sigfusson, G. Larsen, S. L. S. Stipp, Proc. Natl. Acad. Sci. USA 2011, 108, 7307.

[33] D. A. Taylor, Environ. Health. Perspect. 2002, 110, A80.

[34] Y. Yin, J. Liu, G. Jiang, ACS Nano 2012, 6, 7910.

[35] R. D. Glover, J. M. Miller, J. E. Hutchison, ACS Nano 2011, 5, 8950.

[36] F. Rogers, P. Arnott, B. Zielinska, J. Sagebiel, K. E. Kelly, D. Wagner, J. S. Lighty, A. F. Sarofim, J. Air Waste Manag. Assoc. 2005, 55, 583.

[37] W. S. Seames, A. Fernandez, J. O. Wendt, Environ. Sci. Technol. 2002, 36, 2772.

[38] W. P. Linak, C. A. Miller, J. O. Wendt, J. Waste Manag. Assoc. 2000, 50, 1532.

[39] S. M. Ponder, J. G. Darab, J. Bucher, D. Caulder, I. Craig, L. Davis, N. Edelstein, W. Lukens, H. Nitsche, L. F. Rao, D. K. Shuh, T. E. Mallouk, Chem. Mater. 2001, 13, 479.

[40] H. C. Choi, S. Kundaria, D. Wang, A. Javey, Q. Wang, M. Rolandi, H. Dai, Nano Lett. 2003, 3, 157.

[41] R. Kaegi, B. Sinnet, S. Zuleeg, H. Hagendorfer, E. Mueller, R. Vonbank, M. Boller, M. Burkhardt, Environ. Pollut. 2010, 158, 2900.

[42] L. Hsu, H. Chein, J. Nanopart. Res. 2007, 9, 157.

[43] T. M. Benn, P. Westerhoff, Environ. Sci. Technol. 2008, 42, 4133.

[44] M. A. Kiser, P. Westerhoff, T. Benn, Y. Wang, J. Pérez-Rivera, K. Hristovski, Environ. Sci.

Technol. 2009, 43, 6757.

[45] L. Windler, C. Lorenz, N. von Goetz, K. Hungerbühler, M. Amberg, M. Heuberger, B. Nowack, Environ. Sci. Technol. 2012, 46, 8181.

[46] R. Kaegi, A. Voegelin, B. Sinnet, S. Zuleeg, H. Hagendorfer, M. Burkhardt, H. Siegrist, Environ. Sci. Technol. 2011, 45, 3902.

[47] L. Geranio, M. Heuberger, B. Nowack, Environ. Sci. Technol. 2009, 43, 8113.

[48] S. Novak, D. Drobne, J. Valant, P. Pelicon, J. Nanomater. 2012, 2012, 1.

[49] S. K. Poznyak, D. V. Talaapin, E. V. Shevchenko, H. Weller, Nano Lett. 2004, 4, 693.

[50] G. Markovich, C. P. Collier, S. E. Henrichs, F. Remacle, R. D. Levine, J. R. Heath, Acc. Chem. Res. 1999, 32, 415.

[51] N. C. Mueller, B. Nowack, Environ. Sci. Technol. 2008, 42, 4447.

[52] Y. Lin, C. Huang, H. Chang, Analyst 2011, 136, 863.

[53] A. Reyhanitabar, L. Alidokht, A. R. Khataee, S. Oustan, Eur. J. Soil Sci. 2012, 63, 724.

[54] T. P. McNicholas, K. Zhao, C. Yang, S. C. Hernandez, A. Mulchandani, N. V. Myung, M. A. Deshusses, J. Phys. Chem. C 2011, 115, 13927.

[55] M. Auffan, J. Rose, J. Bottero, G. V. Lowry, J. Jolivet, M. R. Wiesner, Nature Nanotech. 2009, 4, 634.

[56] M. R. Wiesner, G. V. Lowry, K. L. Jones, M. F. Hochella, Jr., R. T. Di Giulio, E. Casman, E. S. Bernhardt, Environ. Sci. Technol. 2009, 43, 6458.

[57] H. H. Lara, N. V. Ayala-Nunez, L. C. I. Turrent, C. R. Padilla, World J. Microbiol. Biotechnol. 2010, 26, 615.

[58] G. F. Webb, E. M. D'Agata, P. Magal, S. Ruan, Proc. Natl. Acad. Sci. USA 2005, 102, 13343.

[59] R. Brayner, R. Ferrari-Iliou, N. Brivois, S. Djediat, M. F. Benedetti, F. Fievet, Nano Lett. 2006, 6, 866.

[60] T. B. Henry, F. M. Menn, J. T. Fleming, J. Wilgus, R. N. Compton, G. S: Sayler, Environ. Health Perspec. 2007, 115, 1059.

[61] J. D. Fortner, D. Y. Lyon, C. M. Sayes. A. M. Boyd, J. C. Falkner, E. M. Hotze, L. B. Alemany, Y. J. Tao, W. Guo, K. D. Ausman, V. L. Colvin, J. B. Huges, Environ. Sci. Technol. 2005, 39, 4307.

[62] D. Y. Lyon, L. K. Adams, J. C. Falkner, P. J. J. Alvaraz, Environ. Sci. Technol. 2006, 40, 4360.

[63] M. K. Rai, S. D. Deshmukh, A. P. Ingle, A. K. Gade, J. Appl. Microbiol. 2012, 112, 841.

[64] Z. Huang, X. Zheng, D. Yan, G. Yin, X. Liao, Y. Kang, Y. Yao, D. Huang, B. Hao, Langmuir 2008, 24, 4140.

[65] A. M. Saliba, R. Nishi, B. Raymond, E. A. Marques, U. G. Lopes, L. Touqui, M. C. Plotkowski, Microbes Infect. 2006, 8, 450.

[66] L. M. Pasquini, S. M. Hashmi, T. J. Sommer, M. Elimelech, J. B. Zimmerman, Environ. Sci. Technol. 2012, 46, 6297.

[67] Z. Xiu, Q. Zhang, H. L. Puppala, V. L. Colvin, P. J. J. Alvarez, Nano Lett. 2012, 12, 4271.

[68] C. O. Dimkpa, J. E. McLean, D. W. Britt, A. J. Anderson, Nanotoxicology 2012, 6, 635.

[69] Q. Zeng, B. Liao, L. Zhang, X. Zhou, H. Tang, Chemosphere 2006, 63, 860.

[70] J. M. Unrine, S. E. Hunyadi, O. V. Tsyusko, W. Rao, W. A. Shoults, P. M. Bertsch, Environ. Sci. Technol. 2010, 44, 8308.

[71] D. H. Atha, H. Wang, E. J. Petersen, D. Cleveland, R. D. Holbrook, P. Jaruga, M. Dizdaroglu, B. Xing, B. C. Nelson, Environ. Sci. Technol. 2012, 46, 1819.

[72] C. Shen, Q. Zhang, J. Li, F. Bi, N. Yao, Am. J. Bot. 2010, 97, 1602.

[73] W. Lee, J. Kwak, Y. An, Chemosphere 2012, 86, 491.

[74] Y. S. El-Temsah, E. J. Joner, Environ. Toxicol. 2012, 27, 42.

[75] H. Zhu, J. Han, J. Q. Xiao, Y. Jin, J. Environ. Monit. 2008, 10, 713.

[76] D. L. Starnes, A. Jain, S. V. Sahi, Environ. Sci. Technol. 2010, 44, 7110.

[77] W. M. Lee, Y. J. An, H. Yoon, H. S. Kweon, Nanomater. Environ. 2008, 27, 1915.

[78] B. D. Johnston, T. M. Scown, J. Moger, S. A. Cumberland, M. Baalousha, K. Linge, R. V. AERLE, K. Jarvis, J. R. Lead, C. R. Tyler, Environ. Sci. Technol. 2010, 44, 1144.

[79] C. W. Hu, M. Li, Y. B. Cui, D. S. Li, J. Chen, L. Y. Yang, Soil Biol. Biochem. 2010, 42, 586.

[80] M. Golobic, A. Jemec, D. Drobne, T. Romih, K. Kasemets, A. Kahru, Environ. Sci. Technol. 2012, 46, 12112.

[81] J. L. Ferry, P. Craig, C. Hexel, P. Sisco, R. Frey, P. L. Pennington, M. H. Fulton, I. G. Scott, A. W. Decho, S. Kashiwada, C. J. Murphy, T. J. Shaw, Nat. Nanotechnol. 2009, 4, 441.

[82] M. J. C. van der Ploeg, J. M. Baveco, A. van der Hout, R. Bakker, I. M. C. M. Rietjens, N.

W. van den Brink, Environ. Pollut. 2011, 159, 198.

[83] L. Li, D. Zhou, W. J. G. M. Peijnenburg, C. A. M. van Gestel, S. Jin, Y. Wang, P. Wang, Environ. Int. 2011, 37, 1098.

[84] C. Sioutas, R. J. Delfino, M. Singh, Environ. Health Res. 2005, 113, 947.

[85] U.S. E.P.A. Health assessment for Diesel exhaust. 2002, Washington, dc

[86] D. Westerdahl, S. Fruin, T. Sax, P. M. Fine, C. Sioutas, Atmos. Environ. 2005, 39, 3597.

[87] E. G. Knox, J. Epidemiol. Community Health 2005, 59, 755.

[88] E. Garshick, M. B. Schenker, A. Mumoz, T. Segal, T. J. Smith, S. Woskiw, S. K. Hammond, F. E. Speizer, Am. J. Respir. Dis. 1988, 137, 820.

[89] A. Penn, G. Murphy, S. Barker, W. Henk, L. Penn, Environ. Health Persp. 2005, 113, 956.

[90] Z. Pan, W. Lee, L. Slutsky, R. A. Clark, N. Pernodet, M. H. Rafailovich, Small 2009, 5, 511.

[91] W. Liu, Y. Wu, C. Wang, H. C. Li, T. Wang, C. Y. Liao, L. Cui, Q. F. Zhou, B. Yan, G. B. Jiang, Nanotoxicology 2010, 4, 319.

[92] T. Cedervall, L. Hansson, M. Lard, B. Frohm, S. Linse, PLoS ONE 2012, 7, 32254.

[93] J. C. Trefry, J. L. Monahan, K. M. Weaver, A. J. Meyerhoefer, M. M. Markopolous, Z. S. Arnold, D. P. Wooley, I. E. Pavel, J. Am. Chem. Soc. 2010, 132, 10970.

[94] M. Roca, N. H. Pandya, S. Nath, A. J. Haes, Langmuir 2010, 26, 2035.

[95] J. P. Novak, C. Nickerson, S. Franzen, D. L. Feldheim, Anal. Chem. 2001, 73, 5758.

[96] A. M. Al-Somali, K. M. Krueger, J. C. Falkner, V. L. Volvin, Aanl. Chem. 2004, 76, 5903.

[97] G. -T. Wei, F. -K. Liu, C. R. C. Wang, Anal. Chem. 1999, 71, 2085.

[98] H. Hagendorfer, R. Kaegi, J. Traber, S. F. L. Mertens, R. Scherrers, C. Ludwig, A. Ulrich, Anal. Chim. Acta 2011, 706, 367.

[99] I. Römer, T. A. White, M. Baalousha, K. Chipman, M. R. Viant, J. R. Lead, J. Chromatogr. A 2011, 1218, 4226.

[100] K. L. Plathe, F. von der Kammer, M. Hassellöv, J. Moore, M. Murayama, T. Hofmann, M. F. Jr. Hochella, Environ. Chem. 2010, 7, 82.

[101] M. Hanauer, S. Pierrat, I. Zins, A. Lotz, C. Sönnichsen, Nano Lett. 2007, 7, 2881.

[102] C.Carrillo-Carrión, Y. Moliner-Martínez, B. M. Simonet, M. Válcarcel, Anal. Chem. 2011, 83, 2807.

[103] M. Baalousha, B. Stolpe, J. R. Lead, J. Chromatogr. A. 2011, 1218, 4078.

[104] B. Schmidt, K. Loeschner, N. Hadrup, A. Mortensen, J. J. Sloth, C. B. Koch, E. H. Larsen, Anal. Chem. 2011, 83, 2461.

[105] M. Hassellöv, J. W. Readman, J. F. Ranville, K. Tiede, Ecotoxicology 2008, 17, 344.

[106] V. Garbin, J. C. Crocker, K. J. Stebe, J. Colloid Interface Sci. 2012, 387, 1.

[107] O. P. Khatri, T. Ichii, K. Murase, M. Kanehara, T. Teranishi, H. Sugimura, J. Colloid Interface Sci. 2012, 382, 22.

[108] J.M. Campelo, D. Luna, R. Luque, J.M. Marinas, A.A. Romero, ChemsusChem 2009, 2, 18.

[109] D. Muir, E. Sverko, Anal. Bioanal. Chem. 2006, 386, 769.

[110] S. Chen, H. Yao, K. Kimura, Langmuir 2001, 17, 733.

[111] J. Yang, J. Y. Lee, H. Too, Analytica Chimica Acta 2007, 588, 34.

[112] J. Yang, E. H. Sargent, S. O. Kelley, J. Y. Ying, Nature Materials 2009, 8, 683.

[113] F. Ciesa, A. Plech, J. Colloid Interface Sci. 2010, 346, 1.

[114] H. J. Baik, S. Hong, S. Park, J. Colloid Interface Sci. 2011, 358, 317.

[115] M. J. Hollamby, J. Eastoe, Langmuir 2010, 26, 6989.

[116] J. Yang, J. Y. Lee, J. Y. Ying, Chem. Soc. Rev. 2011, 40, 1672.

[117] J. M. McMahon, S. R. Emory, Langmuir 2007, 23, 1414.

[118] S. Sekiguchi, K. Niikura, Y. Matsuo, K. Ijiro, Langmuir 2012, 28, 5503.

[119] K. S. Mayya, F. Caruso, Langmuir 2003, 19, 6987.

[120] K. Saha, S. S. Agasti, C. Kim, X. Li, V. M. Rotello, Chem. Rev. 2012, 112, 2739.

[121] C. Subramaniam, R. R. Tom, T. Pradeep, J. Nanopart. Res. 2005, 7, 209.

[122] D. V. Leff, L. Brandt, J. R. Heath, Langmuir 1996, 12, 4723.

[123] S. Zhang, G. Leem, L. Srisombat, T. Lee, J. Am. Chem. Soc. 2008, 130, 113.

[124] L. Li, K. Leopold, Anal. Chem. 2012, 84, 4340.

[125] X. N. Wang, S. P. Xu, J. Zhou, W. Q. Xu, J. Colloid Interface Sci. 2010, 348, 24.

[126] S. Underwood, P. Mulvaney, Langmuir 1994, 10, 3427.

[127] M. A. Caldwell, A. E. Albers, S. C. Levy, T. E. Pick, B. E. Cohen, B. A. Helms, D. J. Milliron, Chem Commun 2010, 47, 556.

[128] G. H. Woehrle, L. O. Brown, J. E. Hutchison, J. Am. Chem. Soc. 2005, 127, 2172.

[129] L. Li, M. L. Wang, S. C. Jiang, J. Colloid Interface Sci. 2012, 387, 146.

[130] X. Liu, F. Cheng, Y. Liu, W. Li, Y. Chen, H. Pan, H. Liu, J. Mater. Chem. 2010, 20, 278.

[131] Z. Chen, Z. Wang, J. Chen, S. Wang, Analyst 2012, 137, 3132.

[132] W. Haiss, N. T. K. Thanh, J. Aveyard, D. G. Fernig, Anal. Chem. 2007, 79, 4215.

[133] D. I. Gittins, F. Caruso, Angew. Chem. Int. Ed. 2001, 40, 3001.

[134] K. L. Kelly, E. Coronado, L. L. Zhao, G. C. Schatz, J. Phys. Chem. B 2003, 107, 668.

[135] T. Kim, C. H. Lee, S. W. Joo, K. Lee, J. Colloid Interface Sci. 2008, 318, 238.

[136] J. Yang, J. Y. Lee, T. C. Deivaraj, H. Too, J. Colloid Interface Sci. 2004, 277, 95.

[137] D. L. Plata, P. L. Ferguson, P. Westerhoff, Environ. Sci. Technol. 2012, 46, 12243.

[138] J. Liu, R. Liu, Y. Yin, G. Jiang, Chem. Commun. 2009, 1514.

[139] J. Liu, J. Chao, R. Liu, Z. Tan, Y. Yin, Y. Wu, G. Jiang, Anal. Chem. 2009, 81, 6496.

[140] M. A. Bryant, J. E. J. Pemberton, Am. Chem. Soc. 1991, 113, 8284.

[141] H. Wang, K. Schaefer, M. Moeller, J. Phys. Chem. C 2008, 112, 3175.

[142] S. J. Klaine, P. J. J. Alvarez, G. E. Batley, T. F. Fernandes, R. D. Handy, D. Y. Lyon, S. Mahendra, M. J. McLaughlin, J. R. Lead, Environ. Toxicol. Chem. 2008, 27, 1825.

[143] Y. Zhang, Y. -S. Chen, P. Westerhoff, J. Crittenden, Water Research 2009, 43, 4249.

[144] V. L. Pallem, H. A. Stretz, M. J. M. Wells, Environ. Sci. Technol. 2009, 43, 7531.

[145] K. Aslan, V. H. Perez-Luna, Langmuir 2002, 18, 6059.

[146] B. F. Silva, S. Pérez, P. Gardinalli, R. K. Singhal, A. A. Mozeto, D. Barceló, Trends Anal. Chem. 2011, 30, 528.

[147] D. Pornpattananangkul, S. Olson, S. Aryal, M. Sartor, C. M. Huang, K. Vecchio, L. F. Zhang, ACS Nano 2010, 4, 1935.

[148] B. Kim, C. Park, M. Murayama, M. F. Hochella, Environ. Sci. Technol. 2010, 44, 7509.

[149] J. Fabrega, S. R. Fawcett, J. C. Renshaw, J. R. Lead, Environ. Sci. Technol. 2009, 43, 7285.

[150] K. Tiede, A. B. A. Boxall, X. M. Wang, D. Gore, D. Tiede, M. Baxter, H. David, S. P. Tear, J. Lewis, J. Anal. At. Spectrom. 2010, 25, 1149.

[151] L. K. Limbach, R. Bereiter, E. Müller, R. Krebs, R. Gälli, W. J. Stark, Environ. Sci. Technol. 2008, 42, 5828.

[152] B. Nowack, Science 2010, 330, 1054.

[153] C. Levard, B. C. Reinsch, F. M. Michel, C. Oumahi, G. V. Lowry, G. E. J. Brown, Environ.

Sci. Technol. 2011, 45, 5260.

[154] L. Li, K. Leopold, M. Schuster, Chem. Commun. 2012, 48, 9165.

[155] J. Liu, D. A. Sonshine, S. Shervani, R. H. Hurt, ACS Nano 2010, 4, 6903.

[156] J. -B. Chao, S. -J. Yu, Y. -D. Feng, Z. -Q. Tan, R. Liu, Y. -G. Yin, Anal. Chem. 2011, 83, 6875.

[157] X. Jin, M. H. Li, J. W. Wang, C. Marambio-Jones, F. B. Peng, X. F. Huang, R. Damoiseaux, E. M. V. Hoek, Environ. Sci. Technol. 2010, 44, 7321.

[158] J. Y. Liu, R. H. Hurt, Environ. Sci. Technol. 2010, 44, 2169.

[159] S. Kittler, C. Greulich, J. Diendorf, M. Köller, M. Epple, Chem. Mater. 2012, 22, 4548.

[160] F. Maurer, I. Christl, M. Hoffmann, R. Kretzschmar, Environ. Sci. Technol. 2012, 46, 8808.

[161] M. M. Shafer, J. T. Overdier, D. E. Armstong, Environ. Toxicol. Chem. 1998, 17, 630.

[162] R. F. Domingos, N. Tufenkji, K. J. Wilkinson, Environ. Sci. Technol. 2009, 43, 1282.

[163] A. Petosa, D. P. Jaisi, I. R. Quevedo, M. Elimelech, N. Tufenkji, Environ. Sci. Technol. 2010, 44, 6532.

[164] US EPA. Secondary Drinking Water Regulations: Guidance for Nuisance Chemicals. EPA 816-F-10-079. Washington DC: 2009.

[164] N. R. Jana, L. Gearheart, C. J. Murphy, Chem. Commun. 2001, 617.

[165] O. Choi, T. E. Clevenger, B. Deng, R. Y. Surampalli, L. Jr., Ross, Z. Hu, Water Research 2009, 43, 1879.

[166] D. Mahl, C. Greulich, W. Meyer-Zaika, M. Köller, M. Epple, J. Mater. Chem. 2010, 20, 6176.

[167] S. Sano, K. Kato, Y. Ikada, Biomaterials 1993, 14, 817.

[168] H. Seeger, Eur. Water Manage. 1999, 2, 51.